



**Version No.:** 2.0

**Date submitted:** 6 July 2011

**Title:** ML238: An Antimalarial Small Molecule of a Unique Structural Class

**Authors:** Michel Weiwer<sup>1</sup>, Carol Mulrooney<sup>1</sup>, Daniela Massi<sup>1</sup>, Richard Heidebrecht<sup>1</sup>, Roger Wiegand<sup>6</sup>, Amanda K. Lukens<sup>6</sup>, Justin Dick<sup>6</sup>, Dyann Wirth<sup>6</sup>, Eric Ekland<sup>3</sup>, Chih-Chien Cheng<sup>2</sup>, Jean Zhao<sup>2</sup>, Jing Yuan<sup>4</sup>, Xin-Zhuan Su<sup>4</sup>, Ronald L. Johnson<sup>2</sup>, Rajarshi Guha<sup>2</sup>, Sivaraman Dandapani<sup>1</sup>, Benito Munoz<sup>1</sup>, Michelle Palmer<sup>1</sup>, Craig Thomas<sup>2</sup>, Christopher P. Austin<sup>2</sup>, David Fidock<sup>3</sup>, and Stuart L. Schreiber<sup>1,5</sup>

<sup>1</sup>The Broad Institute Probe Development Center, Cambridge, MA; <sup>2</sup>NIH Chemical Genomics Center, Bethesda, MD; <sup>3</sup>Columbia University, Department of Microbiology and Immunology, New York, NY; <sup>4</sup>National Institute of Allergy and Infectious Diseases, Bethesda, MD; <sup>5</sup>Howard Hughes Medical Institute, Chemistry & Chemical Biology, Harvard University, Cambridge, MA; <sup>6</sup>Harvard School of Public Health, Boston, MA.

Corresponding author: mweiwer@broadinstitute.org

**Assigned Assay Grant No.:** R21 NS059500

**Screening Center Name and PI:** NIH Chemical Genomics Center, Christopher Austin

**Chemistry Center Name and PI:** Broad Institute Probe Development Center, Stuart Schreiber

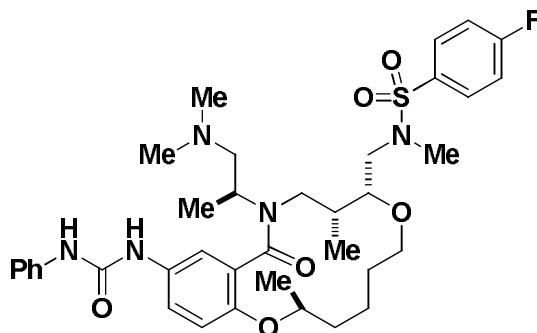
**Assay Submitter & Institution:** David Fidock, Columbia University

**PubChem Summary Bioassay Identifier (AID):** 488774

#### **Abstract:**

Malaria, the most devastating of the parasitic diseases, afflicts an estimated 300-500 million people worldwide and results in more than 800,000 deaths annually. Several parasites in the genus *Plasmodium* infect humans, but *Plasmodium falciparum* has the most significant lethality. Drug resistance has compromised the efficacy of existing drugs. New antimalarial agents, especially agents that work against new targets in *P. falciparum*, are needed. As part of efforts to identify novel inhibitors of *P. falciparum*, we initiated a quantitative high-throughput screening (qHTS) campaign against the 3D7 line of *P. falciparum*. The robust whole parasite viability assay was screened against the Molecular Libraries Small Molecule Repository (MLSMR) as well as the Diversity-Oriented Synthesis (DOS) informer I library (approximately 8,000 compounds), which is a subset of the Broad Institute DOS library. From these efforts, we have identified a unique and novel structural class of antimalarial compounds from the Broad Institute DOS Informer I library. The probe (ML238) displayed picomolar activity in the SBYR live/dead assay against 3D7 and Dd2 *P. falciparum*. This activity was recapitulated in the luciferase assay, albeit at single-digit nanomolar activity, while showing no apparent mammalian cell cytotoxicity. The probe is in a novel structural class in the antimalarial field with unknown mechanism of action; therefore, this probe will be highly useful to the malaria research community in identifying new targets or developing new drug classes.

### Probe Structure and Characteristics:



**ML238**

CID/ML No.	Target Name	IC <sub>50</sub> /EC <sub>50</sub> (nM) [SID, AID]	Anti-target Name(s)	IC <sub>50</sub> /EC <sub>50</sub> (nM) [SID, AID]	Fold Selective	Secondary Assay(s) Name: IC <sub>50</sub> /EC <sub>50</sub> (nM) [SID, AID]
49849912/ ML238	<i>Plasmodium falciparum</i> Dd2	13 [104179292, 504604]	Mammalian cell cytotoxicity	34,060 [104179292, 504602]	2620-fold	<i>Plasmodium falciparum</i> 3D7: 2 [104179292, 504599]

## Recommendations for scientific use of the probe:

Malaria, the most devastating of the parasitic diseases, afflicts an estimated 300-500 million people worldwide and results in more than 800,000 deaths annually. More than 85% of all malaria-related mortality is among children in sub-Saharan Africa. Drug resistance has compromised the efficacy of existing drugs, and new antimalarial agents, especially those that work against new targets in *Plasmodium falciparum*, are needed. This agent represents a novel structural class for small molecules with antimalarial properties and may possess promise as a novel antimalarial. Further, this chemotype may provide insight into new molecular target(s) for development of additional antimalarial agents.

## 1 Introduction

Malaria is a serious disease caused by parasites from the *Plasmodium* genus, which infects particular mosquitoes that feed on humans. This disease is often fatal and is common in poor areas of tropical and subtropical regions, such as Africa, Asia, and parts of the Americas. The disease results from the multiplication of malaria parasites within red blood cells (RBCs), causing symptoms that typically include fever and headache. In severe cases, symptoms may progress to coma and death. Malaria, particularly from *P. falciparum*, affects hundreds of millions of people worldwide and is responsible for almost a million deaths every year (1). Chloroquine and pyrimethamine-sulfadoxine (**Figure 1A**) have been used as the standard treatment for malaria throughout the 20th century because of their limited host toxicity, ease of use, low cost, and effective synthesis. But, their use progressively diminished due to the appearance and spread of resistance (2). Currently, the most effective strategy recommended by the World Health Organization (WHO) is artemisinin-based combination therapies (ACT; Artemether and Lumefantrine, **Figure 1B**) or simplified Fixed-Dose Combination (FDC; Artesunate and Amodiaquine, **Figure 1C**) to avoid the development of drug resistance against artemisinin-based therapies (3).

**Figure 1.** Antimalarial Drugs Recommended by the WHO

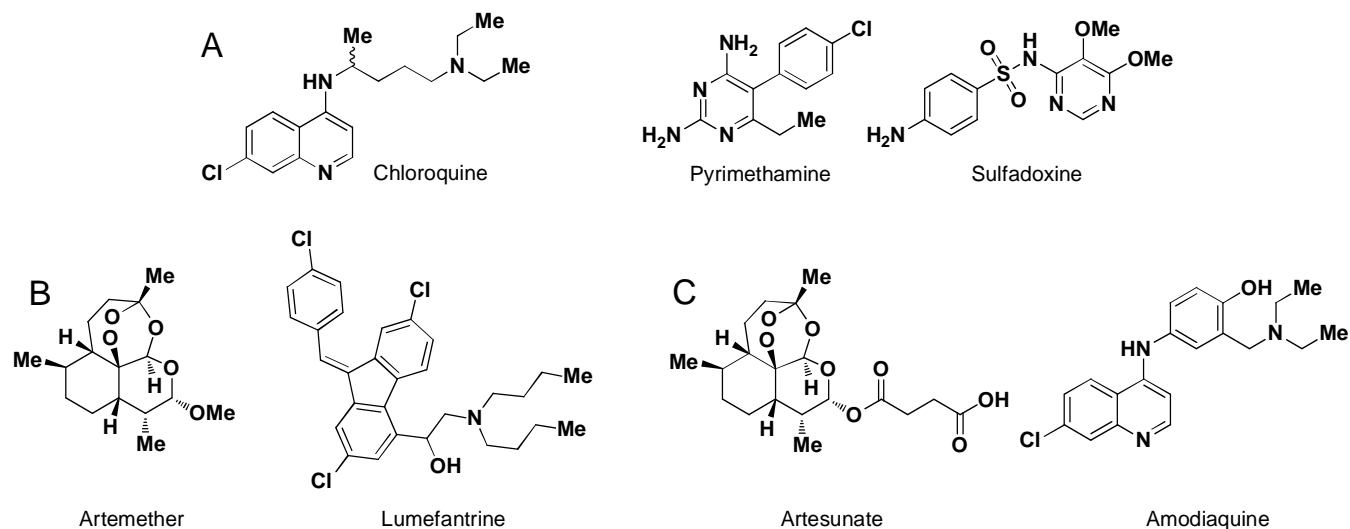


**Figure 1.** Antimalarial drugs recommended by WHO: Chloroquine and the combination Pyrimethamine-Sulfadoxine (A) are the drugs of choice but can be substituted by artemisinin-based treatments such as the combination Artemether-Lumefantrine (B) or Artesunate-Amodiaquine (C).

Recent studies suggest that resistance to the endoperoxide artemisinin family is emerging, particularly in southeast Asia; the main concern is not *if* but *when* will it spread (4, 5). Thus, the development of new drugs, which could be used against artemisinin-resistant malaria is critical. In this context, high-throughput screening (HTS) campaigns aimed at discovering new antimalarial probes is of great importance. Recently, Gamo et al. screened nearly 2 million compounds from GlaxoSmithKline's chemical library for inhibitors of *P. falciparum* and found more than 13,000 compounds showing inhibition of parasite growth by at least 80% at 2  $\mu$ M (6). More than 8,000 of these compounds showed potent activity against the multidrug resistant Dd2 line. Another recent study performed by Guiguemde et al. described the screening of more than 300,000 compounds using a phenotypic forward chemical genetic approach (7). This screening led to the identification of potent compounds against drug-resistant *P. falciparum* line. They further described a detailed profiling of 172 compounds and identified 19 new inhibitors of four validated drug targets and 15 novel binders among 61 malarial proteins.

There is a wide variety of structures that are and have been used as antimalarial drugs (8). **Table 1** presents a summary of currently used antimalarial drugs (9).



**Table 1.** Currently Used Antimalarial Drugs

Drug	Class	Target/Mode of Action	Major Problems
Chloroquine	4-aminoquinoline	Hemozoin formation	Resistance
Amodiaquine	4-aminoquinoline	Hemozoin formation	Resistance/toxicity
Quinine	Arylamino alcohol	unknown	Resistance/toxicity
Halofantrine	Arylamino alcohol	unknown	toxicity
Mefloquine	Arylamino alcohol	unknown	Resistance/toxicity
Lumefantrine	Arylamino alcohol	unknown	Resistance
Sulfadoxine/ pyrimethamine	Antifolate	Folate biosynthesis	Resistance
Artemether	Artemisinines	unknown	Emerging resistance
Artesunate	Artemisinines	unknown	Emerging resistance
Atovaquone/ Proguanil	Combination	Cytochrome bc <sub>1</sub> complex	Cytochrome bc <sub>1</sub> mutations
Doxycycline	Antibiotic	Ribosome	Combination with a faster acting drug
Clindamycin	Antibiotic	Ribosome	Combination with a faster acting drug
Primaquine	8-aminoquinoline	unknown	Hemolysis in G6PD deficient patients

Chloroquine (CID2719, **Figure 1A**) is a 4-aminoquinoline, fast-acting antimalarial drug and was introduced into clinical practice in 1947. It is used both for treatment and prevention of malaria. Amodiaquine is another 4-aminoquinoline, which is used against chloroquine-resistant *P. falciparum* (CRPF). Quinine (**Figure 2A**) was the first effective treatment for malaria caused by *P. falciparum*, appearing in therapeutics in the 17th century, when it was extracted from the bark of the cinchona tree. Several other arylamino alcohol antimalarial agents (such as Lumefantrine; **Figure 1B**) have been introduced to the clinic and are now commonly used in combination therapies with artemisinines. Antibiotics have also been shown to be potent antimalarial drugs (10). Doxycycline (**Figure 2D**) and Clindamycin (**Figure 2E**) are known as delayed death antimalarial drugs. They act in a delayed fashion and are only effective on the second generation of the parasite (typically after 4 days); thus, these drugs need to be used in combination with a fast-acting antimalarial drug.

**Figure 2.** Structures of Other Antimalarial Drugs Currently in Use

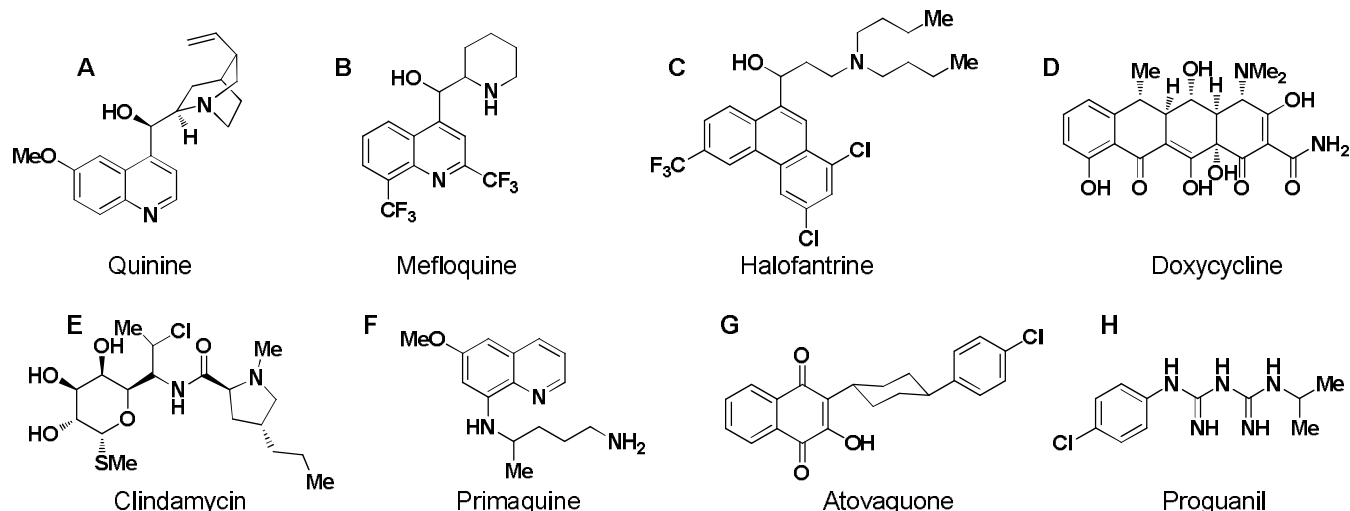


**Figure 2.** Structures of other antimalarial drugs currently in use: Doxycycline (D) and Clindamycin (E) are particularly important as they target the second generation of parasite in a so-called delayed death mechanism.

A large proportion of the antimalarial drugs currently undergoing clinical evaluation are combinations of known substances or new structures in the 4-aminoquinoline, 8-aminoquinoline, and artemisinin classes; thus, these combination therapies are very likely to lead to similar toxicity and resistance issues (9). Only three small molecules undergoing clinical evaluation are known to act against yet unexploited targets in malaria chemotherapy. Fosmidomycin (**Figure 3A**) is active against *P. falciparum* via inhibition of a new target enzyme, 1-deoxy-D-xylulose 5-phosphate reductoisomerase, involved in isoprenoid biosynthesis (11,12). T3 (SAR97267, **Figure 3B**) is a bisthiazolium salt that targets membrane biogenesis during intra-erythrocytic *P. falciparum* (13). One of the main drawbacks of these charged species is their low oral absorption and bioavailability. Thus, several prodrugs of T3 have been synthesized recently in order to overcome these barriers (14). Recently, spiroindolones have been described as potent antimalarial drugs with a new mode of action, and NITD609 (**Figure 3C**) has recently entered a phase I clinical trial (15). NITD609 works by inhibiting protein synthesis in *P. falciparum* and was optimized to address the metabolic liabilities of the lead compound, resulting in improved stability and exposure levels in animals. As a result, NITD609 is one of only a handful of molecules capable of completely curing mice infected with *P. berghei*, a model of blood-stage malaria.

**Figure 3.** Structure of Potential New Antimalarial Drugs

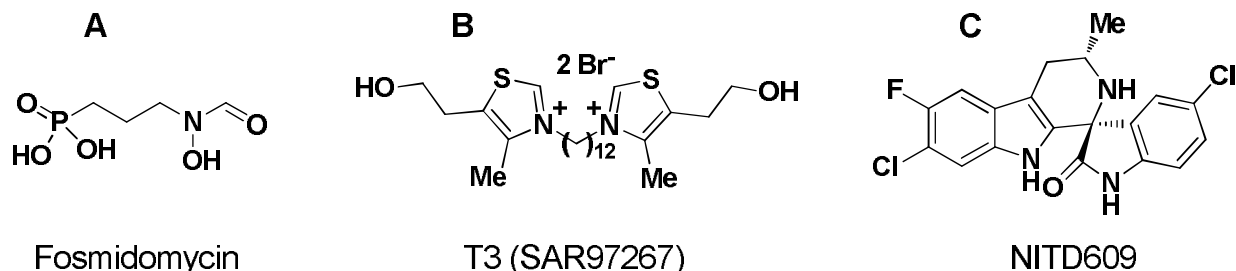


**Figure 3.** Fosmidomycin (A), T3 (B), and NITD609 (C) are known to act against yet unexploited targets in malaria chemotherapy and are currently undergoing clinical evaluation.

The discovery of new structural classes of antimalarial molecules with potential novel mode of action is greatly needed by the malaria research community to better understand the biology of the parasite and, thus, to better combat its deadly mechanisms.

## 2 Materials and Methods

### 2.1 Assays

A summary listing of completed assays and corresponding PubChem AID numbers is provided in **Appendix A** (Table A1). Refer to **Appendix B** for the detailed assay protocols.

#### Materials and Reagents:

##### *Plasmodium falciparum* Culture and Lines

*P. falciparum* cultures were grown at a 4% hematocrit in type AB blood obtained from anonymous donors (Interstate Blood Bank, Inc). The red blood cells (RBCs) were diluted in RPMI media (GIBCO) supplemented with 5 mg/ml Albumax (GIBCO), 50 µg/ml hypoxanthine (Sigma Aldrich), 2.4 mg/ml sodium bicarbonate (GIBCO), and 10 ng/ml gentamicin (GIBCO). Parasites were incubated at 37 °C in a humidified chamber (Billups-Rothenberg, Inc.), gassed with 5% CO<sub>2</sub>/5% O<sub>2</sub>/90% N<sub>2</sub>.

Two *P. falciparum* lines were used in these experiments: the chloroquine-sensitive 3D7 lines and the chloroquine-resistant Dd2 line. These parental lines were used for generating the firefly luciferase-expressing lines (3D7-HLH and Dd2-HLH). These lines were generated using the Bxb1 mycobacterial

integrase system. Briefly, Bxb1 catalyzed the recombination of an attP site, located on a plasmid containing a luciferase cassette (HLH), with an attB site that had previously been inserted into the *P. falciparum* cg6 gene. The luciferase cassette contained luciferase driven by an hrp3 promoter and followed by an hrp2 3' UTR. The lines contain two selectable markers (human dihydrofolate reductase [hDHFR] and blasticidin-s deaminase [BSD]) and are maintained in 2 nM WR99210 (Jacobus Pharmaceuticals) and 2.5 µg/ml blasticidin-S (Invitrogen). The hDHFR marker was used for integrating the attB site into the cg6 locus. The BSD gene was used for selecting parasites that had integrated the luciferase cassette into the attB site.

#### **2.1.1 Pilot *In vitro* *P. falciparum* Viability Assay (SYBR green) Performed at Harvard School of Public Health (HSPH)**

A SYBR green assay previously described (16) was modified for use in 384-well plates. The parasites were cultured in the presence of serial dilutions of test compounds in 40 µl of RPMI containing 4.16 mg/ml Albumax at a 1% hematocrit and an initial parasitemia of 1% in black Greiner GNF clear-bottom plates. Following a 72-hour incubation at 37 °C under 94% N<sub>2</sub>, 5% CO<sub>2</sub>, and 1% O<sub>2</sub>, SYBR green was added to a dilution of 1:10,000, and the plates were stored overnight (or until ready to be read) at -80 °C. The plates were centrifuged at 700 rpm prior to fluorescence measurement (EX 480 nm, EM 530 nm). In this assay, inhibition of parasite replication was reflected in a reduction in the fluorescence intensity of SYBR green bound to parasite DNA.

#### **2.1.2 Primary HTS Screen—Luciferase Drug Assays Performed at NCGC**

Luciferase assays were optimized to work in 30-µl culture volumes in clear-bottom, 384-well plates (Greiner Bio-one). A Precision-2000 microplate pipetting system (Bio Tek) was used to perform all of the liquid dispensing. The test compounds were diluted in the plate to 2X the desired concentration in 15 µl of RPMI culture media. The dispenser then added 15 µl of parasites at 2% hematocrit to each well (1% final hematocrit). The initial parasitemia was 0.2% for 48-hour assays and 0.1% for 96-hour assays. The test compounds were dissolved at 10 mM in DMSO. They were tested at ten 5-fold dilutions, ranging from 50 µM to 26 pM. For each experiment, the conditions were run in duplicate and the duplicates were averaged.

At the end of the assay, the parasites were frozen down. After thawing, each well received 15 µl of 3X Luciferin Lysis Buffer (15 mM DTT, 0.6 mM Coenzyme A, 0.45 mM ATP, 0.42 mg/ml luciferin, 10 mM

MgCl<sub>2</sub>, 10 mM Tris Base, 10 mM Tris HCl, 0.03% Triton X-100). After shaking and a 5-minute equilibration at 28 °C, the samples were read for 3 seconds each using the luminescence settings on a Victor3 (Wallac) microplate reader. Prism software (GraphPad Software, Inc.) was used to derive IC<sub>50</sub> values by nonlinear curve fitting.

### 2.1.3 Confirmatory *In vitro* *P. falciparum* Delayed Death Assay Performed at NCGC

Culture medium (4 µl) was dispensed into white, solid-bottom, 1536-well plates (Kalypsys) with a Multidrop Combi Dispenser (Thermo Scientific). Next, 23 µl of test and control compounds were pin-transferred into the assay plates (6.5 mM Azithromycin and 10mM Chloroquine; 1:2 dilution in duplicate). Using the Multidrop Combi, 4 µl/well *P. falciparum*-infected RBCs with 0.1% parasitemia for the 48-hour assay (at 37 °C, 5% CO<sub>2</sub>) and 0.05% parasitemia for the 96-hour assay (at 37 °C, 5% CO<sub>2</sub>) were dispensed. Following incubation, 2 µL/well of SteadyLite was added to the assay plates with the Multidrop Combi dispenser, and the plates were centrifuged at 1000 rpm for 30 seconds. The plates were read by a ViewLux (Perkin Elmer; 20 sec. exposure, 2x binning).

### 2.1.4 Secondary HepG2 Cell Viability Assay Performed at NCGC

The cells were plated at a density of 2000 cells /well /5 µL in 1536-well, white, tissue-culture treated plates with culture medium. Triplicate plates were prepared and incubated at 37 °C, 5% CO<sub>2</sub> for 5 hours. Next, 23 nl of compounds and positive control were transferred to the assay plates (Positive plate map: Row 1-30 = blank; Row 31 = 20 mM Tetraoctylammonium bromide in DMSO; Row 32 = DMSO). The plates were incubated at 37 °C, 5% CO<sub>2</sub> for 48 hours. Next, CellTiter-Glo reagent (5 µl) was added to each well, and the plates were incubated at room temperature for 30 minutes. Luminescence was measured using a ViewLux (1 second, 2X binning).

### **2.1.2 Tertiary Flow Cytometry Drug Assays Performed in the Fidock Lab**

For the flow cytometry-based validation screen, drug assays were conducted in flat-bottom, 96-well plates in a 200- $\mu$ l culture volume, with RBCs at a 1% hematocrit and starting parasitemias of 0.1%. Drug dilutions were set up as described for the luciferase assay. At the 48-hour and 96-hour time points, the cultures were suspended and 20  $\mu$ l of the culture was transferred to round-bottom, 96-well plates. The samples were stained with 40  $\mu$ l of 2.5X SYBR-green-1 (Invitrogen) and 150 nM MitoTracker Deep Red (Invitrogen) diluted in normal saline dextrose (0.9% NaCl, 5% dextrose) or in complete media. The infected erythrocytes were cultured with the stain for 40 minutes at 37 °C. The samples were washed by adding 100  $\mu$ l of saline dextrose and spinning the plate down for 1 minute at 400 x g in a swinging bucket centrifuge. The diluted stain was removed by flicking out the plate. The samples were resuspended in 100  $\mu$ l of saline dextrose containing 5% fetal calf serum and assayed on an Accuri C6 cytometer equipped with a Hypercyt microplate sampler, which was able to process a 96-well plate in about 15 minutes. Approximately 80,000 events were collected for 48-hour time points and 30,000 events for 96-hour time points.

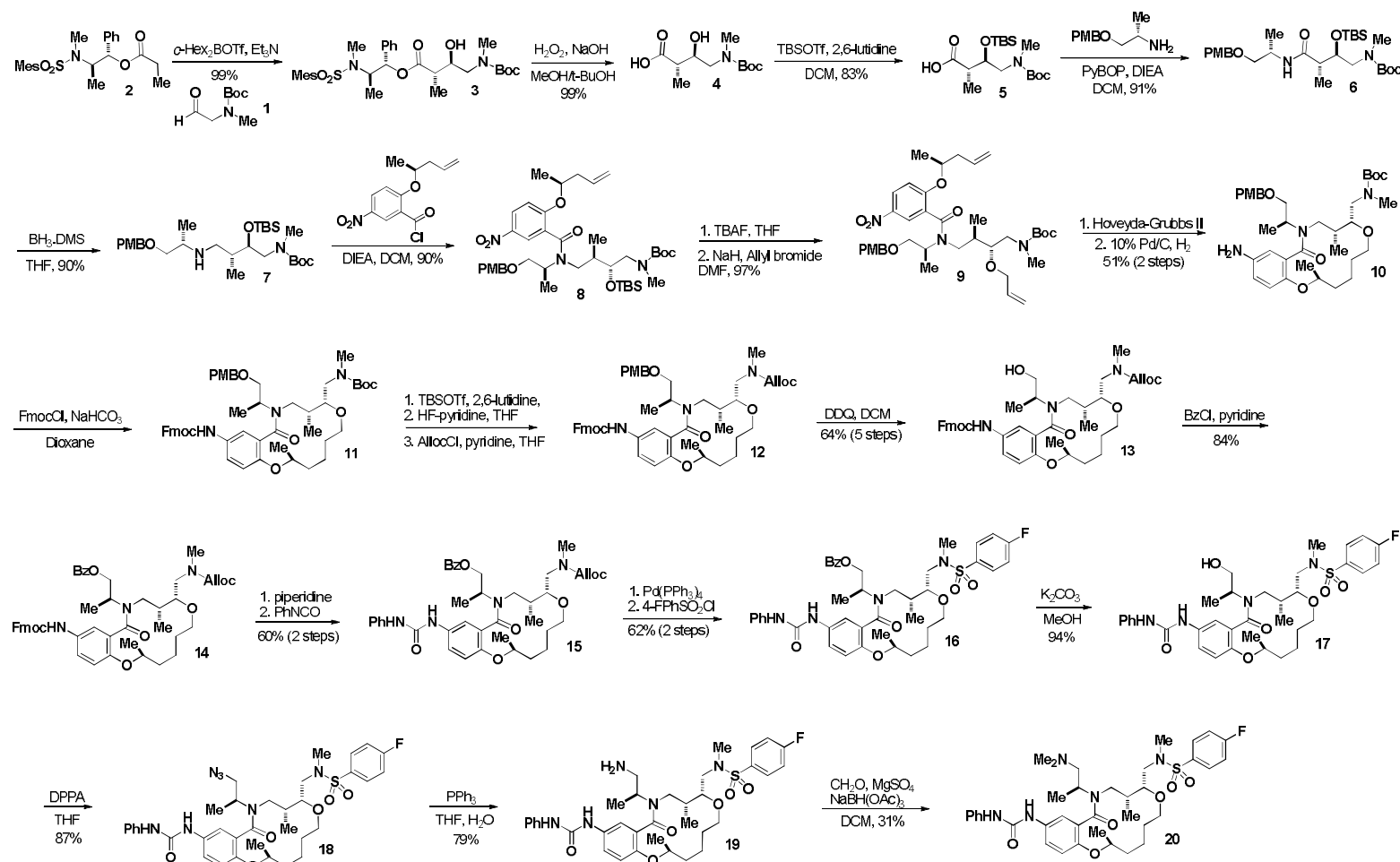
### **2.1.8 Tertiary Apicoplast Disruption Using a Whole Cell Imaging Assay Performed in the Fidock Lab**

ACP<sub>L</sub>-GFP parasites were cultured with compounds tested at approximately 2X their 96-hour EC<sub>50</sub> value to screen for inhibition of apicoplast elongation and segregation. Azithromycin was used as a positive control, while parasites treated with drug vehicle (medium containing 0.05 – 0.1% DMSO) served as a negative control. Assays began with synchronized ring stages, and parasites were harvested on day 4. Parasites were incubated with 1 mg/ml Hoechst 33342 nuclear stain and 20 nM Mitotracker-Red, washed, and deposited on poly-lysine coated slides. Images were taken on a Nikon Ti inverted microscope.



## 2.2 Probe Chemical Characterization

**Scheme 1. Synthesis of the Probe (ML238)**



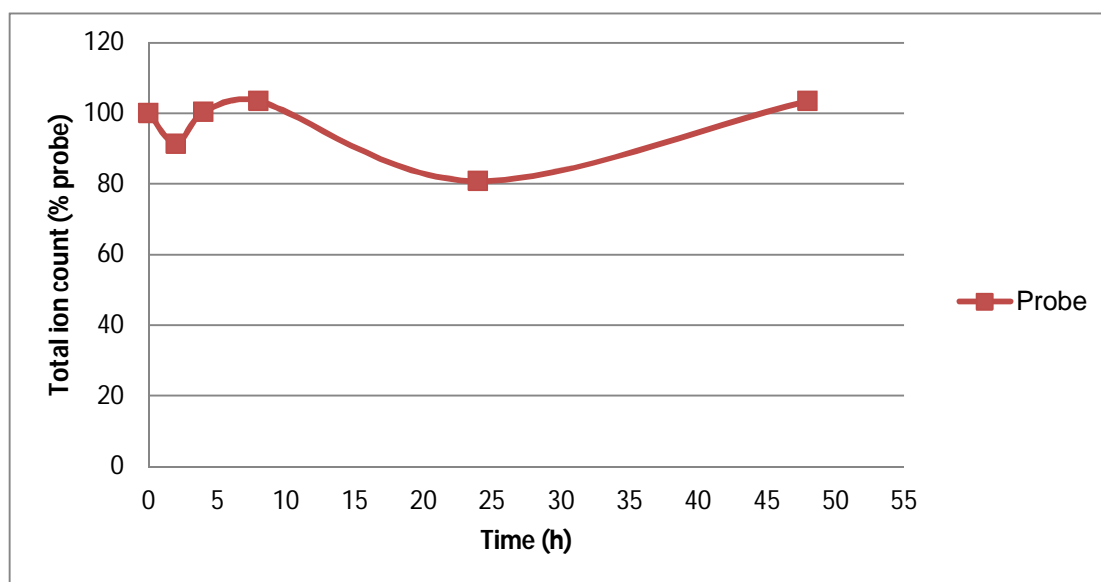


The probe (ML238) was synthesized as shown in **Scheme 1** using an aldol-based build/couple/pair strategy and full account of the synthesis of the macrocycle has already been reported by the DOS group at the Broad Institute (17). Full experimental details and characterization are provided in **Appendix C**.

The solubility of the probe (ML238) was measured at room temperature and was found to be 124.8  $\mu\text{M}$  in water but  $<1 \mu\text{M}$  in PBS.

The stability of the probe (ML238) in PBS (0.1% DMSO) was measured over 48 hours. We noticed that the concentration of the probe steadily increased over 48 hours to about 800% (data not shown). Since the solubility of the probe in PBS is low, we believe that the gradual increase in concentration is the direct result of more compound dissolving in PBS over time. In other words, when we performed the PBS stability assay under the recommended conditions, we measured the kinetic solubility of the probe in PBS and not its stability. Thus, we decided to increase the amount of DMSO so that the compound dissolves completely at the start of the stability assay and stays in solution during the course of the experiment. We tried 5%, 10% and 15% DMSO in PBS and followed stability of the probe over time. When 15% DMSO was used, the probe rapidly dissolved and remained completely soluble over 48 hours and the results from this experiment are shown in **Figure 4**. From these results, the probe seems to be stable in PBS since 100% is still present after 48 hours of incubation.

**Figure 4.** Stability Data for the Probe (ML238) in PBS (15% DMSO) Over 48 Hours



After preparation as described in Section 2.3, full characterization of the probe (ML238) was analyzed by UPLC,  $^1\text{H}$  and  $^{13}\text{C}$  NMR spectroscopy, and high-resolution LC mass spectrometry. The associated spectroscopic data is provided in **Appendix D**.

### 2.3 Probe Preparation

Full experimental details for preparation of the probe (ML238) are provided in **Appendix C**.

### 2.4 Additional Analytical Analysis

**Plasma Protein Binding.** Plasma protein binding was determined by equilibrium dialysis using the Rapid Equilibrium Dialysis (RED) device (Pierce Biotechnology, Rockford, IL) for both human and mouse plasma. Each compound was prepared in duplicate at 5  $\mu\text{M}$  in plasma (0.95% acetonitrile, 0.05% DMSO) and added to one side of the membrane (200  $\mu\text{l}$ ) with PBS pH 7.4 added to the other side (350  $\mu\text{L}$ ). Compounds were incubated at 37  $^\circ\text{C}$  for 5 hours in a 250-rpm orbital shaker. Following the incubation, the samples were analyzed by UPLC-MS (Waters, Milford, MA) with compounds detected by SIR detection on a single quadrupole mass spectrometer.

**Plasma Stability.** Plasma stability was determined at 37  $^\circ\text{C}$  for 5 hours in both human and mouse plasma. Each compound was prepared in duplicate at 5  $\mu\text{M}$  in plasma diluted 50/50 (v/v) with PBS pH 7.4 (0.95% acetonitrile, 0.05% DMSO). The compounds were incubated at 37  $^\circ\text{C}$  for 5 hours with a 250-rpm orbital shaker with time points taken at 0 hours and 5 hours. The samples were analyzed by UPLC-MS (Waters, Milford, MA) with compounds detected by SIR detection on a single quadrupole mass spectrometer.

## 3 Results

### Probe attributes:

- The probe should not be based on known antibiotics.
- $\text{IC}_{50} < 1 \mu\text{M}$  against Dd2 malarial cell line at 96 hours.
- Nontoxic to HepG2 cells for 72 hours at 10X  $\text{IC}_{50}$  against Dd2.

**Table 2. Compound Summary in PubChem**

IUPAC Chemical Name	<i>N</i> -(((2 <i>S</i> ,8 <i>R</i> ,9 <i>R</i> )-11-(( <i>S</i> )-1-(dimethylamino)propan-2-yl)-2,9-dimethyl-12-oxo-14-(3-phenylureido)-2,3,4,5,6,8,9,10,11,12-decahydrobenzo[ <i>b</i> ][1,9,5]dioxazacyclotetradecin-8-yl)methyl)-4-fluoro- <i>N</i> -methylbenzenesulfonamide
PubChem CID	49849912
Molecular Weight	711.88620 g/mol
Molecular Formula	C <sub>37</sub> H <sub>50</sub> FN <sub>5</sub> O <sub>6</sub> S
XlogP	5.32
H-Bond Donor	2
H-Bond Acceptor	7
Rotatable Bond Count	9
Exact Mass	711.34658
Topological Polar Surface Area	128.9

### 3.1 Summary of Screening Results

#### 3.1.1 NCGC Screen of the MLSMR Library

The delayed death qHTS screen was run at two time points corresponding to the 48-hour and 96-hour incubation periods. The median *Z'* across all the plates was 0.70 and 0.57 for the 48-hour and 96-hour time points, respectively. The signal-to-background values were 22 and 12 for the 48-hour and the 96-hour time points, respectively. Each plate had two controls: azithromycin (an antimalarial exhibiting the delayed death phenotype) and chloroquine (a classical “fast-acting” antimalarial). These controls were added as 16-point, 2-fold titrations (in duplicate) starting at 18.6  $\mu$ M for azithromycin and 28.7  $\mu$ M for chloroquine. The controls exhibited consistent potencies throughout the screen. In addition to the control titrations, wells containing fixed concentrations of azithromycin and chloroquine were used to normalize the 96-hour and 48-hour data, respectively. In total, 223,059 compounds were tested at both time points, at six concentrations ranging from 28.7  $\mu$ M to 1.84 nM.

Following the primary qHTS screen, the concentration-response curves were classified according to a heuristic scheme (18). This scheme allows us to distinguish active, inconclusive, and inactive compounds, based on efficacy and curve-fit parameters. Class 1 curves display a complete response with well-defined upper and lower asymptotes and an *R*<sup>2</sup> > 0.9. Class 2 curves are incomplete, having only one asymptote and an *R*<sup>2</sup> > 0.9. Class 3 curves show poor curve fits or have a single point of activity, and are considered as low confidence. Class 4 curves either have a curve fit below threshold

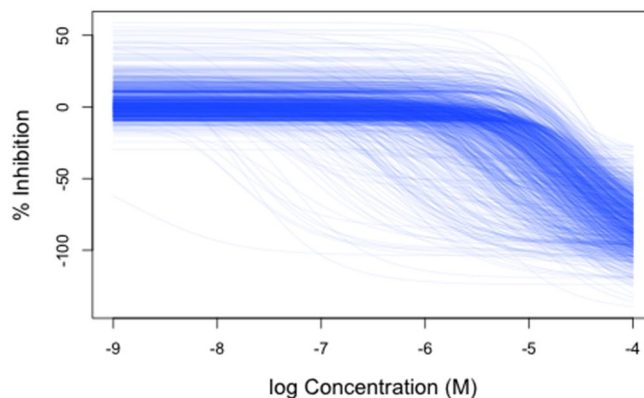
activity or lack one altogether, and these are considered inactive. Each class is further categorized into subclasses based on the efficacy of the response (18).

Using curve class and efficacy, we defined compounds as differentially active if they satisfied either of the following two criteria:

1. Inactive (Class 4) at the 48-hour time point but active (Class 1.1, 1.2, 2.1) with an efficacy greater than 60% at the 96-hour time point.
2. Active (Class 1.1, 1.2, 2.1) with efficacy greater than 60% at both time points, but with 5-fold lower  $IC_{50}$  at the 96-hour time point compared with the 48-hour time point.

From the 223,059 compounds screened, we used these constraints to identify 11,185 (0.53%) differential actives. Correspondingly, there were 121,502 (54.47%) inactive compounds (Class 4) at both time points. **Figure 5** represents an overlay of the concentration-response curves (at the 96-hour time point) for the 11,185 differentially active compounds.

**Figure 5.** Overlay of the Concentration-response Curves for the 11,185 Active Compounds at 96 Hours



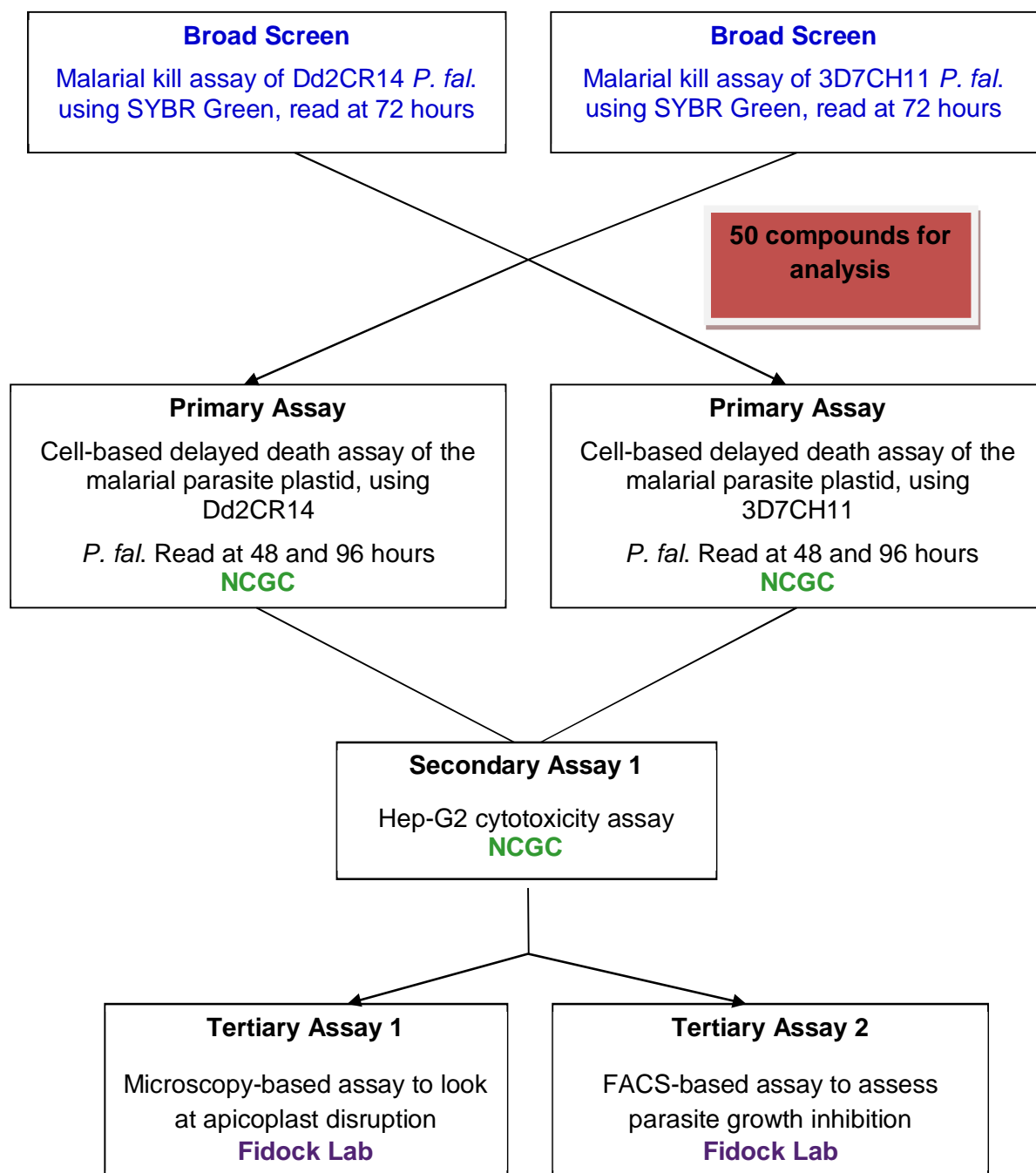
### 3.1.2 Broad Screen of the DOS Informer Set I

**Figure 6** displays the critical path for probe development.

A screen of an informer set of 8000 DOS compounds was performed in duplicate in the black Greiner GNF clear-bottom, 384-well plates (Greiner Bio-One Ltd.) using a SYBR dye detection method. Screening compounds were distributed into plates by a Labcyte Echo liquid handling system (Sunnyvale, CA). Parasites were synchronized at ring stage using the sorbitol method, before performing the assay. Next, 40  $\mu$ l of 1% parasitemia/1% hematocrit culture in RPMI containing 4.16 mg/ml Albumax was then robotically dispensed into wells, and the plates were briefly mixed and incubated for 72 hours in gas-controlled incubators. After incubation, 10  $\mu$ l of 10X SYBR Safe DNA Stain in Lysis buffer (Saponin 0.16%, Tris-HCl [pH 7.5] 20 mM, EDTA [disodium salt] 5 mM, Triton X-100 6% v/v) was added robotically to the wells. The plates were covered with aluminum seals, briefly centrifuged at 1000 rpm for 1 minute, mixed, and then incubated overnight at room temperature. The plates were then centrifuged and read from below in a Wallac EnVision plate reader using the routine parameters for SYBR detection (EX 480 nm, EM 530 nm). The SYBR assay in 384-well format performed favorably in the NIH Genomics validation criteria for 384-well plate assays are detailed in NCGC Assay Guidance Manual (19).  $Z'$  values were in the range of 0.65-0.75, with a signal-to-noise ratio of 1.8:2.5, and a standard deviation (SD) of control wells < 5%.

Primary hits were defined as compounds yielding a reduction in parasite growth of at least 90% in both duplicate assays. A total of 560 primary hits representing five scaffolds were identified and advanced through a four-point titration (1000, 303, 98, and 28 nM). One scaffold differentiated itself from the others, and this lead was confirmed via independent synthesis followed by iterative 12-point titrations. At the same time, untested derivatives of the lead and all of its stereoisomers were subject to full titration.

**Figure 6.** Critical Path for HTS of the DOS Informer Set and Probe Development



### 3.2 Dose Response Curves for Probe (ML238)

The dose-response curves for the probe (ML238) are presented in **Figure 7**.

**Figure 7.** Dose-Response Curves for the Probe (ML238)

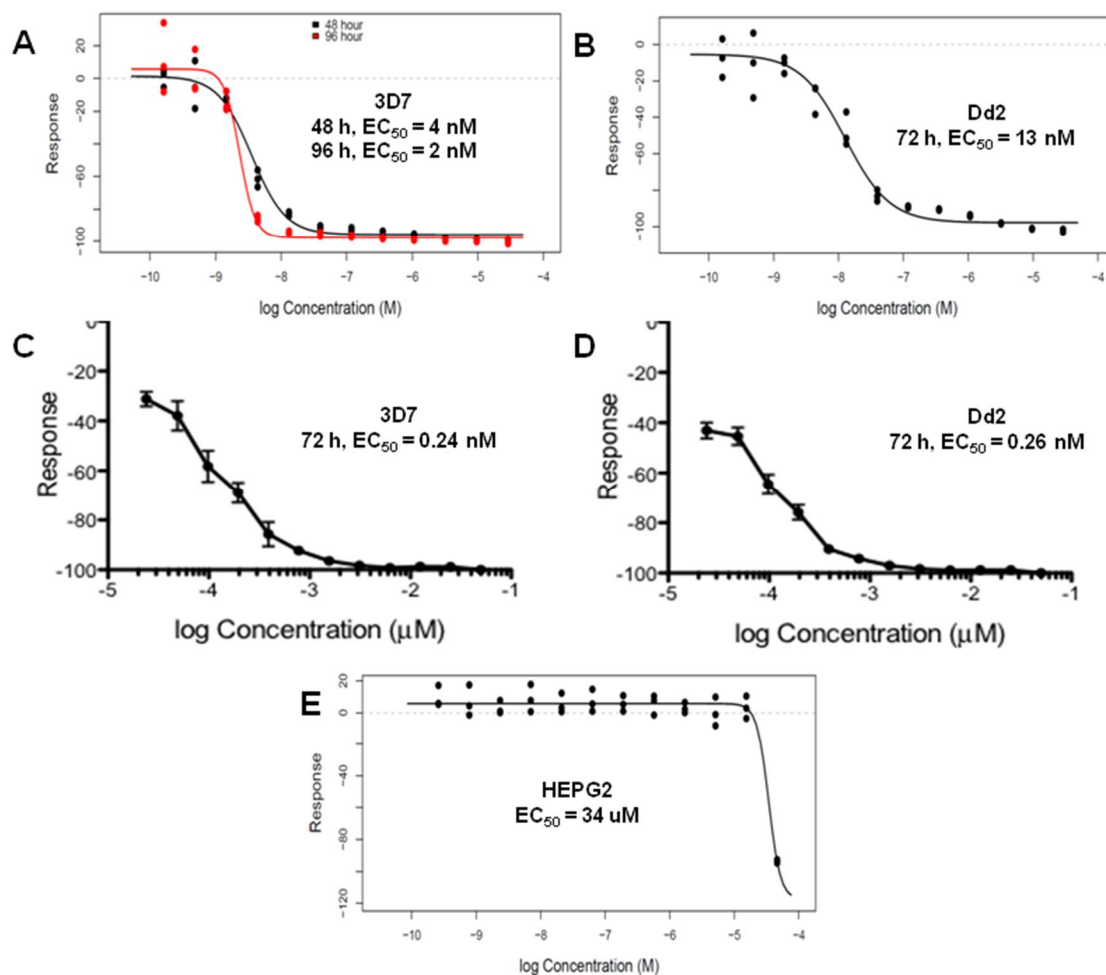


**Figure 7.** Dose-response curves for the probe (ML238) obtained using Luciferase assays against *P. falciparum* 3D7 (A) and Dd2 (B), and using a SYBR-green based assay in 3D7 (C) and Dd2 (D), low nanomolar to subnanomolar activity of the probe. The probe (ML238) only shows cytotoxicity in HEPG2 (E) at high micromolar, resulting in a large safety window.



The probe (ML238) displayed low nanomolar activities against both 3D7 and Dd2 lines of *P. falciparum*, when using a luciferase-based assay (**Figures 7A and 7B**, respectively). The probe displayed picomolar activities against both 3D7 and Dd2 lines of *P. falciparum*, when using a SYBR-green based assay (**Figures 7C and 7D**, respectively). The probe was found to have very low toxicity in a human cell line (HEPG2), with an EC<sub>50</sub> value of 34  $\mu$ M (**Figure 7E**).

### 3.3 Scaffold/Moiety Chemical Liabilities

The probe (ML238) has no functional group with known chemical reactivity that may lead to instability. Considering its structural complexity, it is also very unlikely to be promiscuous.

### 3.4 SAR Tables

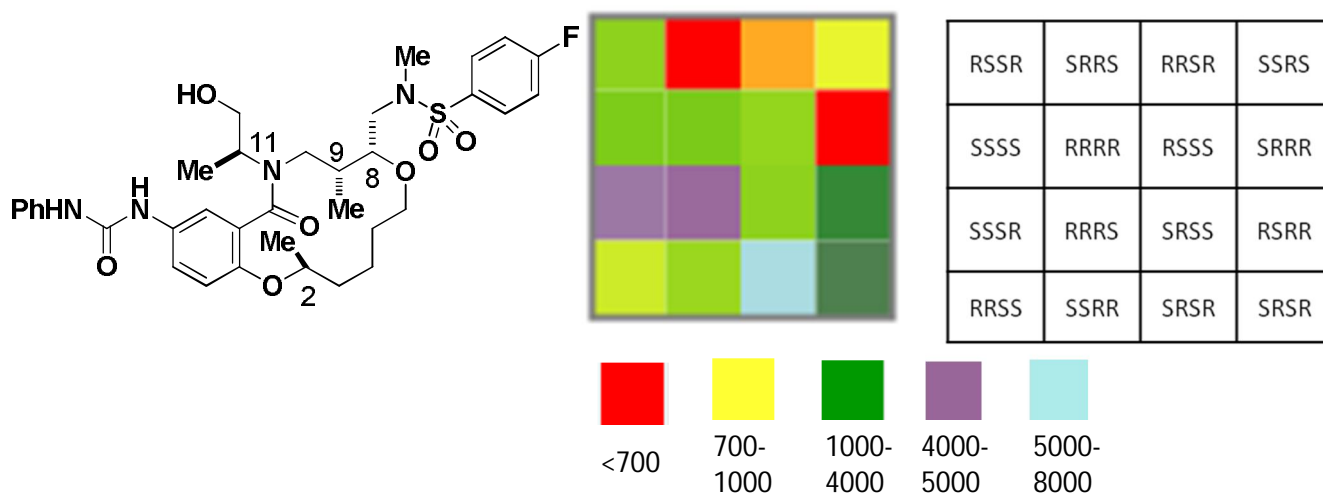
The Broad Institute has synthesized close to 100,000 complex small molecules through DOS for use in HTS. This DOS collection consists of a variety of different chemical skeletons, and they are generally rich in sp<sup>3</sup>-hybridized carbon atoms compared to members in the MLPCN library. A subset of the DOS library called the ‘informer set’ (approximately 8,000 compounds) was screened at the Broad Institute in the live/dead assay against both Dd2 and 3D7 malarial strains. This effort led to the identification of the hit compound (CID44487502, **Figure 8**).

A number of related analogs (based both on stereochemistry and building blocks) were then screened at the Broad Institute to identify SAR trends and to optimize activity. A vast majority of these analogs were also screened at NCGC, and the data from both institutions were remarkably close. We report data from NCGC in **Figure 8** and in **Tables 3-7**. In **Table 8**, we compare data from the Broad Institute, and NCGC for the probe (ML238) and a limited set of analogs to illustrate data reproducibility across institutions and assay platforms.

The informer set that was screened included all the stereoisomers of the hit compound and additional related analogs. The initial hit has four stereocenters; hence, there is a total of 16 possible stereoisomers. Results from all 16 stereoisomers are summarized in **Table 3**. The stereo-structure-activity relationship (SSAR) can be readily visualized from the SSAR heat map shown in **Figure 8**. Of the 16 stereoisomers, two stereoisomers demonstrated < 1  $\mu$ M activity against the resistant Dd2 cell line. These two compounds have the same configuration (S,R,R) on all three stereocenters (C2, C8, and C9, respectively) inside the macrocycle with different configurations at the exocyclic stereocenter

(C11). SRRR-1 was the most active isomer with 0.49  $\mu\text{M}$  activity (**Table 3**, entry 5); however, this isomer showed some toxicity in the HepG2 assay (4.26  $\mu\text{M}$ ). SRRS-1 (**Table 3**, entry 11) had very similar activity (0.66  $\mu\text{M}$ ) against Dd2 and was totally inactive in the HepG2 assay; hence, this stereoisomer was chosen for further studies.

**Figure 8.** Stereochemical SAR Heat Map of the HTS Hit Compound (CID44487502) in Dd2



Having identified the optimal stereoisomer, we focused on the SAR of the hit compound (CID44487502) around a) the urea, b) the sulfonamide, and c) the exocyclic primary alcohol. **Table 4** presents the SAR at the phenyl urea position. Replacing the phenyl urea with an aniline (**Table 4**, entry 2) led to a slight increase in potency in 3D7 *P. falciparum* but to a slight decrease in potency in Dd2 *P. falciparum*. Replacement of the phenyl urea by an isopropyl urea (**Table 4**, entry 3) led to a 3-fold decrease in activity. Using a 4-isoxazolyl urea (**Table 4**, entry 4) in place of the phenyl urea improved potency slightly. A more rigid mimic of the phenyl urea portion, a benzoxazol analog (**Table 4**, entry 5) was also synthesized, but led to a decrease in activity and an increase in toxicity.

SAR study at the phenyl urea portion did not lead to significant improvements in activity, thus, we turned our attention to the sulfonamide portion of the hit compound (**Table 5**). Moving the fluoro substituent on the phenyl sulfonamide portion from the *para*- (**Table 5**, entry 1) to the *meta*- position (**Table 5**, entry 2) or the *ortho*- position (**Table 5**, entry 3) had a great influence on the activity. The

*meta*-fluoro phenyl sulfonamide analog was found to be approximately 10-fold more potent than the hit compound but led to low micromolar toxicity in HEPG2. Introduction of a 3-pyridyl sulfonamide ring (**Table 5**, entry 4) in order to improve solubility led to a 15-fold decrease in activity. Replacing the *para*-fluoro substituent by a *para*-trifluoromethyl substituent (**Table 5**, entry 5) also led to a decrease in activity in both 3D7 and Dd2 *P. falciparum* lines. Next, we replaced the sulfonamide portion by carbamates (**Table 5**, entries 6-9) or amine (**Table 5**, entry 10), but these modifications did not improve potency.

We also studied SAR on the exocyclic substituents attached to the lactam nitrogen atom (**Table 6**). Removing the methyl at C-11 (**Table 6**, entry 2) led to a decrease in activity. Replacing the hydroxymethylene portion by a methyl group (**Table 6**, entry 3) led to a 10-fold increase in activity but also increased toxicity. Using the hydroxymethylene portion for further derivatization as esters (**Table 6**, entries 4-5) or ethers (**Table 6**, entries 6-10) led to more potent compounds, showing that this portion of the molecule could be exploited to improve activity through hydrophobic interactions. Particularly, the *tert*-butyl ether analog (**Table 6**, entry 6) was found to be the most potent compound, showing subnanomolar activity in the 3D7 strain after 96 hours. The *tert*-butyl dimethyl silyl analog (**Table 6**, entry 11) was also found to be very active with IC<sub>50</sub> values of 0.8 nM and 6 nM against 3D7 *P. falciparum* and Dd2 *P. falciparum*, respectively. In the *tert*-butyl dimethyl silyl series, the presence of the (*S*)-methyl group was found to be critical as removal (**Table 6**, entry 12) or inversion of its configuration (**Table 6**, entry 13) led to a high decrease in potency. In order to improve solubility of the molecule, we also introduced a dimethylamine group (**Table 6**, entry 14). Although this analog was not as potent as the *t*-butyl and TBDMS analogs, it still had low nanomolar potencies (2.4 nM in 3D7 and 13 nM in Dd2 after 96 hours) and was found to have good aqueous solubility (124.8  $\mu$ M in water and <1  $\mu$ M in PBS) and good plasma stability (98% in human and 83.1% in mouse). This compound was later designated as the probe (ML238). The azido analog (**Table 6**, entry 15), which was used as an intermediate in the synthesis of the dimethylamine analog, was also tested and found to be less active and less soluble than the dimethylamine analog.

**Table 7** presents several analogs synthesized by modifying multiple diversity sites. Maintaining the phenyl urea on the western portion of the molecule (R<sub>1</sub>) and the benzoyl ester on the lactam nitrogen side chain (R<sub>2</sub>), and replacing the 4-fluoro sulfonamide by different aliphatic carbamates (**Table 7**, entries 1-2) led to an approximate 10-fold decrease in activity. Using a phenyl urea as R<sub>1</sub>, a PMB-

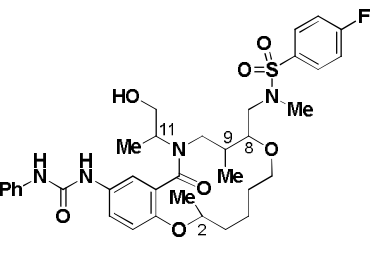
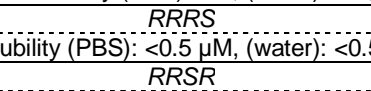
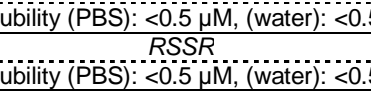
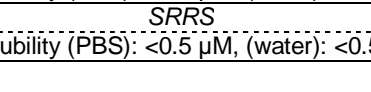

protected ether on the lactam nitrogen side chain and a *p*-methoxybenzylamine as R<sub>3</sub> (**Table 7**, entry 3) did not improve activity. Using a 4-isoxazolyl urea as R<sub>1</sub>, an isopropyl as R<sub>2</sub> and a *p*-fluorophenylsulfonamide as R<sub>3</sub> (**Table 7**, entry 4) led to a reasonably active analog along with low micromolar toxicity.

**Table E1** (shown in **Appendix E**) presents other analogs synthesized during the course of the SAR study. The macrocyclization step involves a ring closing metathesis that generally afforded a mixture of *E* and *Z* olefins. In most cases, the two diastereoisomers were not separable on silica gel and were subsequently hydrogenated. In the case of the SRRS stereoisomer, the two diastereoisomers were separable on silica gel, although it was impossible to assign the stereochemistry at the olefin position due to very complex NMR signals. Both stereoisomers (**Table E1**, entries 1-2) were tested but showed similar potencies.

**Table 8** presents a comparison of the data obtained at the NCGC (Luciferase Assay) with the original results obtained at the Broad Institute (SYBR Assay) for the probe (ML238) and nine analogs. Overall, a good correlation is observed between the two assays performed at different institutions. In the SYBR green-based, fluorescence assay (live/dead assay), the probe (ML238; **Table 8**, entry 1) showed picomolar activity against both 3D7 (0.24 nM) and Dd2 *P. falciparum* (0.26 nM), while showing low nanomolar activity in the luciferase-based assay. Another analog (**Table 8**, entry 5), possessing a PMB-protected ether in place of the dimethylamine substituent, also showed picomolar activity.

**Table F1** (shown in **Appendix F**) presents the data obtained by the Assay Provider for the probe (ML238) and five analogs against 3D7 and Dd2 lines using flow cytometry. In general, this data matches well with the data obtained by using other platforms (SYBR and luciferase).

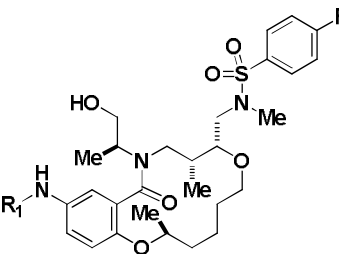
**Table 3.** Summary of Stereochemical SAR (SSAR) on the Hit Compound

Entry No.	CID	SID	Broad ID	Structure	Potency ( $\mu\text{M}$ ) Mean $\pm$ S.E.M.				Fold Selectivity HepG2/ Dd2
				Configuration (C2,C8,C9,C11)	3D7 48 h (n=1)	3D7 96 h (n=1)	Dd2 72 h (n=1)	HepG2 48 h (n=1)	
1	49849936	104179297	BRD-K02585972	 RRRR Solubility (PBS): ND, (water): ND; Purity: 80%	1.42	1.13	2.56	12.98	5.1
2	44487559	85794036	BRD-K79131428	 RRRS Solubility (PBS): <0.5 $\mu\text{M}$ , (water): <0.5 $\mu\text{M}$ ; Purity: 95%	2.63	1.79	5.11	IA	NA
3	44489738	85796329	BRD-K88059273	 RRSR Solubility (PBS): <0.5 $\mu\text{M}$ , (water): <0.5 $\mu\text{M}$ ; Purity: 95%	0.53	0.43	0.90	IA	NA
4	49849919	104179298	BRD-K92315747	 RSRR Solubility (PBS): ND, (water): ND; Purity: 100%	2.97	2.43	4.35	9.45	2.2
5	44483977	104179269	BRD-K81592585	 SRRR Solubility (PBS): ND, (water): ND; PPB (h): 99.0%, (m): 99.4%; PS (h): 92.5%, (m) 100%; Purity: 95%	0.13	0.077	0.49	4.26	8.7
6	44484569	85790999	BRD-K18794550	 RRSS Solubility (PBS): <0.5 $\mu\text{M}$ , (water): <0.5 $\mu\text{M}$ ; Purity: 98%	1.37	1.13	1.59	IA	NA
7	44483817	85790224	BRD-K66952385	 RSSR Solubility (PBS): <0.5 $\mu\text{M}$ , (water): <0.5 $\mu\text{M}$ ; Purity: 97%	1.17	0.99	2.34	IA	NA
8	44485781	85792233	BRD-K51454562	 SSRR Solubility (PBS): <0.5 $\mu\text{M}$ , (water): <0.5 $\mu\text{M}$ ; Purity: 98%	1.10	0.75	2.18	IA	NA
9	44486410	85792873	BRD-K51189903	 RSRS Solubility (PBS): <0.5 $\mu\text{M}$ , (water): <0.5 $\mu\text{M}$ ; Purity: 96%	1.86	1.55	4.51	0.02	0.004
10	44486991	85793461	BRD-K76042595	 SRSR Solubility (PBS): <0.5 $\mu\text{M}$ , (water): <0.5 $\mu\text{M}$ ; Purity: 95%	2.44	1.72	7.69	10.71	1.4
11	44487502	104179262	BRD-K91034707	 SRRS Solubility (PBS): <0.5 $\mu\text{M}$ , (water): <0.5 $\mu\text{M}$ ; Purity: 98%	0.21	0.16	0.66	IA	NA

Entry No.	CID	SID	Broad ID	Structure	Potency ( $\mu\text{M}$ ) Mean $\pm$ S.E.M.				Fold Selectivity HepG2/ Dd2
				Configuration (C2,C8,C9,C11)	3D7 48 h (n=1)	3D7 96 h (n=1)	Dd2 72 h (n=1)	HepG2 48 h (n=1)	
12	44487483	85793960	BRD-K89005359	SSSR	1.80	1.02	5.45	IA	NA
				Solubility (PBS): <0.5 $\mu\text{M}$ , (water): <0.5 $\mu\text{M}$ ; Purity: 95%					
13	44486382	85792845	BRD-K75296800	SSRS	0.77	0.71	1.27	IA	NA
				Solubility (PBS): <0.5 $\mu\text{M}$ , (water): <0.5 $\mu\text{M}$ ; Purity: 99%					
14	44488751	85795281	BRD-K60558220	SRSS	1.09	0.90	2.34	14.93	6.4
				Solubility (PBS): ND, (water): ND; Purity: 91%					
15	44487451	85793928	BRD-K59563627	RSSS	1.60	1.42	2.26	1.00	0.4
				Solubility (PBS): <0.5 $\mu\text{M}$ , (water): <0.5 $\mu\text{M}$ ; Purity: 97%					
16	44485115	85791559	BRD-K30523950	SSSS	1.09	0.43	2.52	IA	NA
				Solubility (PBS): ND, (water): ND; Purity: 86%					

IA = Inactive; (m) = mouse; NA = Not applicable; ND = Not determined; PPB (h) = Plasma protein binding in human; PS (h) = Plasma stability in human

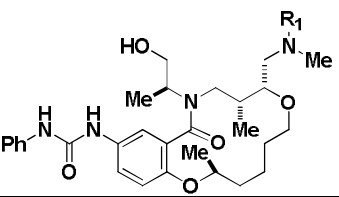
**Table 4.** Summary of SAR on the Urea Portion

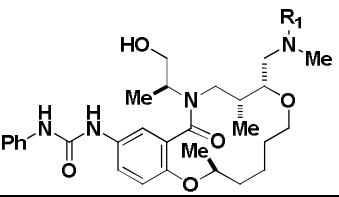
Entry No.	CID	SID	Broad ID	Structure	Potency ( $\mu\text{M}$ ) Mean $\pm$ S.E.M.				Fold Selectivity HepG2/ Dd2
				R <sub>1</sub>	3D7 48 h (n=1)	3D7 96 h (n=1)	Dd2 72 h (n=1)	HepG2 48 h (n=1)	
1	44487502	104179262	BRD-K91034707		0.21	0.16	0.66	IA	NA
Solubility (PBS): <0.5 $\mu\text{M}$ , (water): <0.5 $\mu\text{M}$ ; Purity: 98%									
2	49849922	104179270	BRD-K61455620	H	0.18	0.072	0.99	20.8	21.0
Solubility (PBS): ND, (water): ND; Purity: 98%									
3	49849920	104179295	BRD-K23239903		0.69	0.45	1.86	IA	NA
Solubility (PBS): 1.0 $\mu\text{M}$ , (water): 3.4 $\mu\text{M}$ ; Purity: 98%									
4	49843020	104179266	BRD-K05563014		0.14	0.083	0.63	IA	NA
Solubility (PBS): ND, (water): ND; PPB (h): 90.7%, (m): 88.2%; PS (h): 93.9%, (m) 97.2%; Purity: 96%									
5	49849904	104179278	BRD-K97304223		1.54	1.23	2.95	3.45	1.2
Solubility (PBS): <0.5 $\mu\text{M}$ , (water): <0.5 $\mu\text{M}$ ; Purity: 84%									

IA = Inactive; (m) = mouse; NA = Not applicable; ND = Not determined; PPB (h) = Plasma protein binding in human; PS (h) = Plasma stability in human



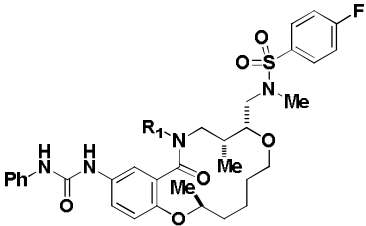
**Table 5.** Summary of SAR on the Sulfonamide Portion

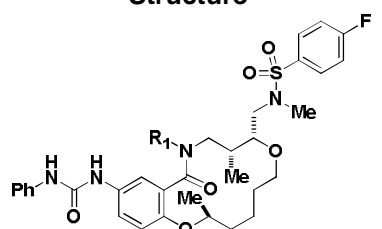
Entry No.	CID	SID	Broad ID	Structure	Potency ( $\mu\text{M}$ ) Mean $\pm$ S.E.M.				Fold Selectivity HepG2/ Dd2
					3D7 48 h (n=1)	3D7 96 h (n=1)	Dd2 72 h (n=1)	HepG2 48 h (n=1)	
1	44487502	104179262	BRD-K91034707		0.21	0.16	0.66	IA	NA
Solubility (PBS): <0.5 $\mu\text{M}$ , (water): <0.5 $\mu\text{M}$ ; Purity: 98%									
2	49849918	104179257	BRD-K71027224		0.013	0.008	0.059	0.96	16.3
Solubility (PBS): <0.5 $\mu\text{M}$ , (water): <0.5 $\mu\text{M}$ ; Purity: 95%									
3	49849913	104179267	BRD-K59844958		0.81	0.58	2.26	IA	NA
Solubility (PBS): <0.5 $\mu\text{M}$ , (water): <0.5 $\mu\text{M}$ ; Purity: 97%									
4	49849924	104179268	BRD-K40437294		3.47	2.83	4.85	IA	NA
Solubility (PBS): ND, (water): ND; Purity: 95%									
5	49849929	104179258	BRD-K57246549		0.97	0.94	1.44	19.2	27.6
Solubility (PBS): <0.5 $\mu\text{M}$ , (water): <0.5 $\mu\text{M}$ ; Purity: 94%									

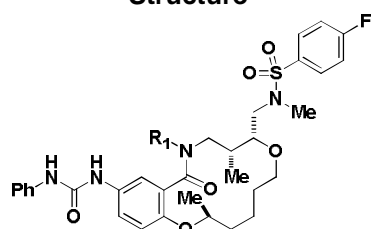
Entry No.	CID	SID	Broad ID	Structure	Potency ( $\mu$ M) Mean $\pm$ S.E.M.				Fold Selectivity HepG2/ Dd2
				 R <sub>1</sub>	3D7 48 h (n=1)	3D7 96 h (n=1)	Dd2 72 h (n=1)	HepG2 48 h (n=1)	
6	49849917	104179272	BRD-K08398610		0.44	0.27	1.32	IA	NA
Solubility (PBS): <0.5 $\mu$ M, (water): <0.5 $\mu$ M; Purity: 88%									
7	49849932	104179275	BRD-K06180729		16.0	18.6	19.41	3.37	0.2
Solubility (PBS): ND, (water): ND; PPB (h): 87.5%, (m): 94.3%; PS (h): 100%, (m) 99.0%; Purity: 98%									
8	49849914	104179284	BRD-K51799542		0.99	0.83	2.25	IA	NA
Solubility (PBS): <0.5 $\mu$ M, (water): <0.5 $\mu$ M; Purity: 94%									
9	49849908	104179274	BRD-K99647730		4.40	2.02	8.96	IA	NA
Solubility (PBS): <0.5 $\mu$ M, (water): <0.5 $\mu$ M; Purity: 98%									
10	49843214	104179265	BRD-K25147450		1.13	0.83	1.87	IA	NA
Solubility (PBS): ND, (water): ND; Purity: 93%									

IA = Inactive; (m) = mouse; NA = Not applicable; ND = Not determined; PPB (h) = Plasma protein binding in human; PS (h) = Plasma stability in human

**Table 6.** Summary of SAR on the Exocyclic Substituents of the Lactam Nitrogen Atom

Entry No.	CID	SID	Broad ID	Structure	Potency ( $\mu\text{M}$ ) Mean $\pm$ S.E.M.				Fold Selectivity  HepG2/ Dd2
					3D7 48 h (n=1)	3D7 96 h (n=1)	Dd2 72 h (n=1)	HepG2 48 h (n=1)	
1	44487502	104179262	BRD-K91034707		0.21	0.16	0.66	IA	NA
				Solubility (PBS): <0.5 $\mu\text{M}$ , (water): <0.5 $\mu\text{M}$ ; Purity: 98%					
2	49849923	104179282	BRD-K76448995		0.36	0.27	2.74	IA	NA
				Solubility (PBS): <0.5 $\mu\text{M}$ , (water): <0.5 $\mu\text{M}$ ; Purity: 97%					
3	49849935	104179271	BRD-K74880585		0.028	0.023	0.086	11.17	130
				Solubility (PBS): <0.5 $\mu\text{M}$ , (water): <0.5 $\mu\text{M}$ ; PPB (h): 99.8%, (m): 99.3%; PS (h): 100%, (m) 88.0%; Purity: 99%					
4	49849915	104179276	BRD-K89015850		0.069	0.055	0.19	IA	NA
				Solubility (PBS): ND, (water): ND; Purity: 93%					
5	49849931	104179288	BRD-K91442916		0.013	0.006	0.057	2.73	47.9
				Solubility (PBS): ND, (water): ND; PPB (h): 96.4%, (m): 90.8%; PS (h): 98.1%, (m) 61.6%; Purity: 98%					

Entry No.	CID	SID	Broad ID	Structure	Potency ( $\mu\text{M}$ ) Mean $\pm$ S.E.M.				Fold Selectivity HepG2/ Dd2
				 R <sub>1</sub>	3D7 48 h (n=1)	3D7 96 h (n=1)	Dd2 72 h (n=1)	HepG2 48 h (n=1)	
6	49849930	104179296	BRD-K22860098		0.002	0.0008	0.004	5.49	1373
Solubility (PBS): <0.5 $\mu\text{M}$ , (water): <0.5 $\mu\text{M}$ ; PPB (h): 97.7%, (m): 95.6%; PS (h): 97.8%, (m) 97.7%; Purity: 99%									
7	49849909	104179286	BRD-K95212245		0.004	0.003	0.014	IA	NA
Solubility (PBS): ND, (water): ND; PPB (h): 100%, (m): 100%; PS (h): 100%, (m) 100%; Purity: 100%									
8	49849903	104179259	BRD-K69927069		0.11	0.083	0.26	1.33	5.1
Solubility (PBS): <0.5 $\mu\text{M}$ , (water): <0.5 $\mu\text{M}$ ; Purity: 100%									
9	49849928	104179294	BRD-K22114431		0.013	0.009	0.032	7.91	247
Solubility (PBS): <0.5 $\mu\text{M}$ , (water): <0.5 $\mu\text{M}$ ; Purity: 99%									
10	49849921	104179293	BRD-K56802845		0.013	0.011	0.040	9.24	231
Solubility (PBS): <0.5 $\mu\text{M}$ , (water): <0.5 $\mu\text{M}$ ; PPB (h): 99.1%, (m): 99.6%; PS (h): 100%, (m) 100%; Purity: 98%									

Entry No.	CID	SID	Broad ID	Structure	Potency ( $\mu\text{M}$ ) Mean $\pm$ S.E.M.				Fold Selectivity HepG2/ Dd2
				 R <sub>1</sub>	3D7 48 h (n=1)	3D7 96 h (n=1)	Dd2 72 h (n=1)	HepG2 48 h (n=1)	
11	49849916	104179273	BRD-K72437079		0.001	0.0008	0.006	IA	NA
Solubility (PBS): <0.5 $\mu\text{M}$ , (water): <0.5 $\mu\text{M}$ ; PPB (h): 100%, (m): 100%; PS (h): 82.8%, (m) 91.4%; Purity: 100%									
12	49849934	104179283	BRD-K67472155		0.064	0.045	0.23	IA	NA
Solubility (PBS): <0.5 $\mu\text{M}$ , (water): <0.5 $\mu\text{M}$ ; Purity: 98%									
13	49849938	104179260	BRD-K61974895		0.23	0.17	0.61	IA	NA
Solubility (PBS): <0.5 $\mu\text{M}$ , (water): <0.5 $\mu\text{M}$ ; Purity: 100%									
14	49849912	104179292	BRD-K45399554		0.004	0.002	0.013	34.06	2620
Solubility (PBS): <0.5 $\mu\text{M}$ , (water): 124.8 $\mu\text{M}$ ; PPB (h): 99.1%, (m): 99.2%; PS (h): 98.0%, (m) 83.1%; Purity: 100%									
15	49849906	104179287	BRD-K67216671		0.021	0.003	0.069	IA	NA
Solubility (PBS): <0.5 $\mu\text{M}$ , (water): <0.5 $\mu\text{M}$ ; Purity: 99%									

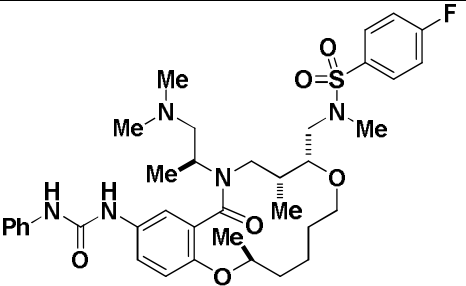
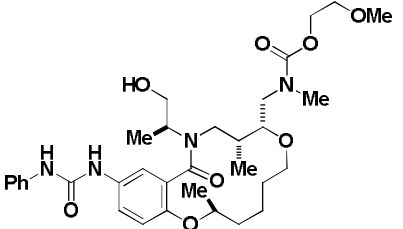
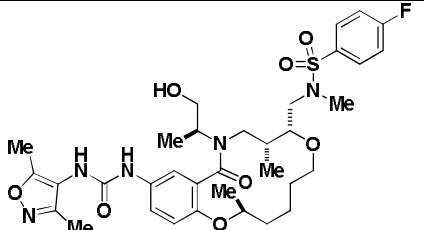
IA = Inactive; (m) = mouse; NA = Not applicable; ND = Not determined; PPB (h) = Plasma protein binding in human; PS (h) = Plasma stability in human

**Table 7.** SAR Study on Multiple Diversity Sites

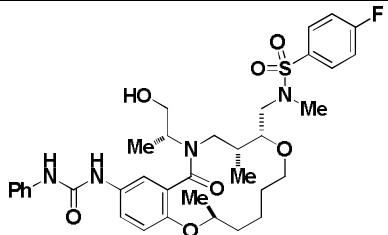
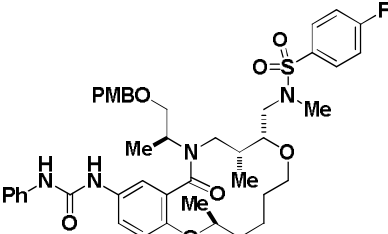
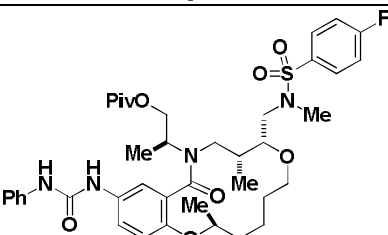
Entry No.	CID	SID	Broad ID	Structure			Potency ( $\mu\text{M}$ ) Mean $\pm$ S.E.M.				Fold Selectivity HepG2/ Dd2
				R <sub>1</sub>	R <sub>2</sub>	R <sub>3</sub>	3D7 48 h (n=1)	3D7 96 h (n=1)	Dd2 72 h (n=1)	HepG2 48 h (n=1)	
1	49849907	104179279	BRD-K25658764				0.47	0.37	0.99	IA	NA
				Solubility (PBS): ND, (water): ND; Purity: 91%							
2	49849911	104179277	BRD-K94338472				0.59	0.54	1.01	IA	NA
				Solubility (PBS): <0.5 $\mu\text{M}$ , (water): <0.5 $\mu\text{M}$ ; Purity: 100%							
3	49849925	104179291	BRD-K59375763				0.64	0.51	0.94	35.34	37.6
				Solubility (PBS): <0.5 $\mu\text{M}$ , (water): 38.8 $\mu\text{M}$ ; Purity: 99%							
4	49849905	104179289	BRD-K70297465				0.069	0.049	0.21	6.28	29.9
				Solubility (PBS): <0.5 $\mu\text{M}$ , (water): 165.6 $\mu\text{M}$ ; Purity: 98%							

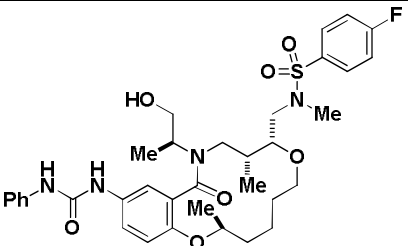
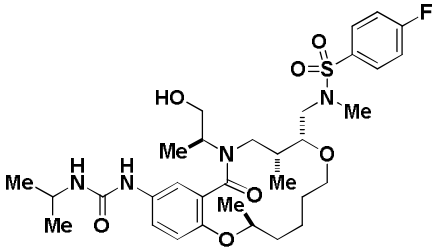
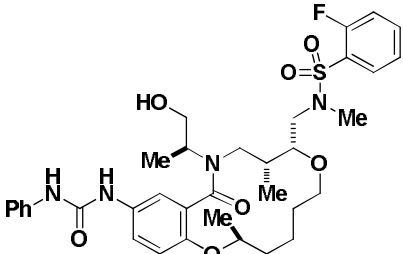
IA = Inactive; (m) = mouse; NA = Not applicable; ND = Not determined; PPB (h) = Plasma protein binding in human; PS (h) = Plasma stability in human

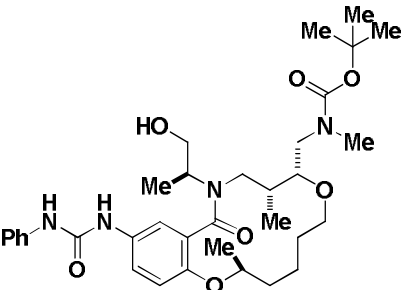
**Table 8.** Summary of Data Obtained in the SYBR Green-based Fluorescence Assay Versus the Luciferase Assay Against *P. falciparum*

Entry No.	CID	SID	Broad ID	Structure	Potency ( $\mu\text{M}$ ) Mean $\pm$ S.E.M.				
					SYBR Assay		Luciferase Assay		
					3D7 72 h (n=1)	Dd2 72 h (n=1)	3D7 96 h (n=1)	Dd2 72 h (n=1)	HepG2 48 h (n=1)
1	49849912	104179292	BRD-K45399554		0.0002	0.0003	0.002	0.013	34.06
2	49849932	104179275	BRD-K06180729		>5.0	>5.0	18.596	19.41	3.37
3	49843020	104179266	BRD-K05563014		0.70	0.57	0.083	0.63	IA



Entry No.	CID	SID	Broad ID	Structure	Potency ( $\mu\text{M}$ ) Mean $\pm$ S.E.M.				
					SYBR Assay		Luciferase Assay		
					3D7 72 h (n=1)	Dd2 72 h (n=1)	3D7 96 h (n=1)	Dd2 72 h (n=1)	HepG2 48 h (n=1)
4	44483977	104179269	BRD-K81592585		0.10	0.048	0.077	0.49	4.26
5	49849909	104179286	BRD-K95212245		0.0003	0.0002	0.003	0.014	IA
6	49849931	104179288	BRD-K91442916		0.005	0.008	0.006	0.057	2.73

Entry No.	CID	SID	Broad ID	Structure	Potency ( $\mu\text{M}$ ) Mean $\pm$ S.E.M.				
					SYBR Assay		Luciferase Assay		
					3D7 72 h (n=1)	Dd2 72 h (n=1)	3D7 96 h (n=1)	Dd2 72 h (n=1)	HepG2 48 h (n=1)
7	44487502	104179262	BRD-K91034707		0.15	0.11	0.16	0.66	IA
8	49849920	104179295	BRD-K23239903		0.71	0.77	0.45	1.86	IA
9	49849913	104179267	BRD-K59844958		0.92	1.57	0.58	2.26	IA

Entry No.	CID	SID	Broad ID	Structure	Potency ( $\mu\text{M}$ ) Mean $\pm$ S.E.M.				
					SYBR Assay		Luciferase Assay		
					3D7 72 h (n=1)	Dd2 72 h (n=1)	3D7 96 h (n=1)	Dd2 72 h (n=1)	HepG2 48 h (n=1)
10	49849914	104179284	BRD-K51799542		2.41	1.37	0.83	2.25	IA

IA=Inactive

**Figure 9** presents a visual summary of the SAR performed on the 14-membered ring scaffold. Stereochemistry, as well as three points of diversity were investigated and led to the identification of a subnanomolar antimalarial probe (ML238). This probe is developed from the DOS compound collection at the Broad Institute; hence, it is structurally unique compared to all the other compounds pursued by both academic institutions and pharmaceutical companies for malaria. This DOS-based probe possesses good water solubility and exhibits picomolar activity against 3D7 and the chloroquine-resistant Dd2 *P. falciparum*. Research efforts are currently underway to advance this probe (ML238) to subsequent stages of drug discovery.

**Figure 9.** Summary of SAR Performed on the Probe (ML238; 54 Synthetic Analogs)

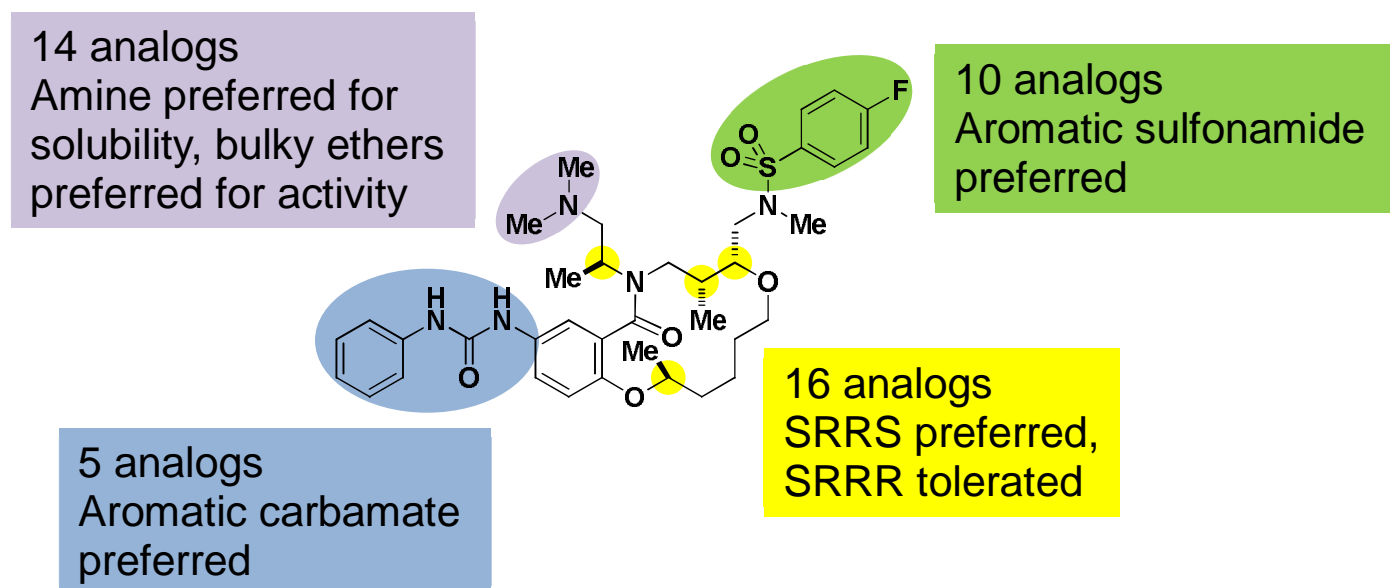


**Figure 9.** Summary of SAR studies showing that the SRRS stereoisomer series as well as aromatic groups at the urea and sulfonamide positions are preferred for activity, while amines are preferred at C-12, particularly for aqueous solubility.

The probe (ML238/MLS003448149) as well as five analogs (MLS003448150, MLS003448151, MLS003448152, MLS003448153, MLS003448154) have been submitted to the MLSMR collection.

### 3.5 Cellular Activity

In order to be a valuable tool, the probe (ML238) has to be noncytotoxic. Thus, its toxicity was assessed using HEPG2, a human liver carcinoma cell line. The probe showed an LC<sub>50</sub> value of 34.06

$\mu\text{M}$  in HEPG2, while showing subnanomolar  $\text{EC}_{50}$  values in both 3D7 and Dd2 lines of *P. falciparum*. This corresponds to a safety window greater than 30,000-fold. In addition, we have also screened the probe and several of its structural analogs for toxicity in kidney epithelial cells, dermal fibroblasts, lung epithelial cancer cells, and erythrocyte lysis. The data from these safety studies are presented in **Table G1 (Appendix G)**. The probe and all the analogs show excellent safety window.

### 3.6 Profiling Assays

The probe (ML238) was issued from the DOS effort of the Broad Institute. This probe is a novel structure and has not been reported previously in PubChem. We plan to perform off-target testing through a standard commercial panel (CEREP/Ricerca).

## 4 Discussion

### 4.1 Comparison to Existing Art and How the New Probe is an Improvement

Investigation into relevant prior art entailed searching the following databases: SciFinder, Reaxys, PubChem, PubMed, US Patent and Trademark Office (USPTO) PatFT and AppFT, and World Intellectual Property Organization (WIPO) databases. The search terms applied and hit statistics are provided below in **Table 9**. Abstracts were obtained for all references returned and were analyzed for relevance to the current project. The searches were performed on, and are current as of, March 2, 2011.

**Table 9.** Search Strings and Databases Employed in the Prior Art Search

Search String	Database	Hits Found
"Delayed death antimalarial"	Sci Finder	4
"antimalarial AND apicoplast"	Sci Finder	84
"Delayed death antimalarial"	Reaxys	3
"antimalarial AND apicoplast"	Reaxys	5
"Delayed death AND antimalarial"	USPTO PatFT	0
"antimalarial AND apicoplast"	USPTO PatFT	2
"Delayed death antimalarial"	USPTO AppFT	0
"antimalarial AND apicoplast"	USPTO AppFT	6
"Delayed death antimalarial"	PubChem Bioassay	107
"antimalarial AND apicoplast"	PubChem Bioassay	147
"Delayed death antimalarial"	PubMed	71
"antimalarial AND apicoplast"	PubMed	5

In the field of antimalarial drugs, all classes of compounds, from the 4-aminoquinoline and arylamino alcohol to the more recently developed artemisinins, have or are in the process of suffering development of resistance in various malaria lines. The discovery of new structural classes of antimalarial drugs, acting on different targets or different stages of the malaria parasite development, is of great interest. The probe (ML238) is derived from the Broad Institute DOS chemistry effort; thus, its structure is in a completely new class. The probe shows subnanomolar  $IC_{50}$  values in 3D7 and the chloroquine-resistant Dd2 strain of *P. falciparum* constituting an improvement over existing antimalarial drugs, which typically show low nanomolar  $IC_{50}$  values (20). In our hands, Atovaquone was found to have an  $IC_{50}$  of  $0.089 \pm 0.030$  nM in 3D7 and  $0.097 \pm 0.046$  nM in Dd2. Chloroquine was found to have an  $IC_{50}$  of  $13.0 \pm 12.0$  nM in 3D7 and  $252 \pm 119$  nM in Dd2. Thus, ML238 is more potent than chloroquine and compares with atovaquone.

## 4.2 Mechanism of Action Studies

### 4.2.1 Assessing Apicoplast Disruption Using a Whole Cell Imaging Assay

Delayed death inhibitors specifically target the parasite apicoplast; an organelle of cyanobacterial origin that employs prokaryotic-derived transcription and translation machinery (21). During asexual blood-stage development, this organelle adopts an elongated and branched structure as the parasite matures into its trophozoite form, then segregates into individual organelles that parse with the individual

daughter merozoites prior to their release from the infected erythrocyte. To verify if the compounds do interfere with the apicoplast, we used a whole-cell imaging screen with a recombinant parasite line that has GFP-labeled apicoplasts. This line, ACP<sub>L</sub>-GFP, has already been developed and benefits from chromosomal integration of the GFP fusion, producing excellent signal homogeneity. Antibiotics (such as zithromycin and doxycycline) that are known to interfere with the apicoplast have been observed to disrupt the morphology of the apicoplast in this GFP-expressing line (see **Figure 10**) (22).

For this imaging screen, ACP<sub>L</sub>-GFP parasites were cultured with compounds tested at approximately 2X their EC<sub>50</sub> value at 96 hours to screen for inhibition of apicoplast elongation and segregation. Azithromycin was used as a positive control, while parasites treated with drug vehicle (medium containing 0.05 – 0.1% DMSO) served as a negative control. Assays began with synchronized ring stages, and the parasites were harvested on Day 4. The parasites were incubated with 1 mg/ml Hoechst 33342 nuclear stain, and 20 nM Mitotracker-Red, washed, and deposited on poly-lysine coated slides. Images were taken on a Nikon Ti inverted microscope.



**Figure 10.** Effect of Compound Treatment on Apicoplast Morphology

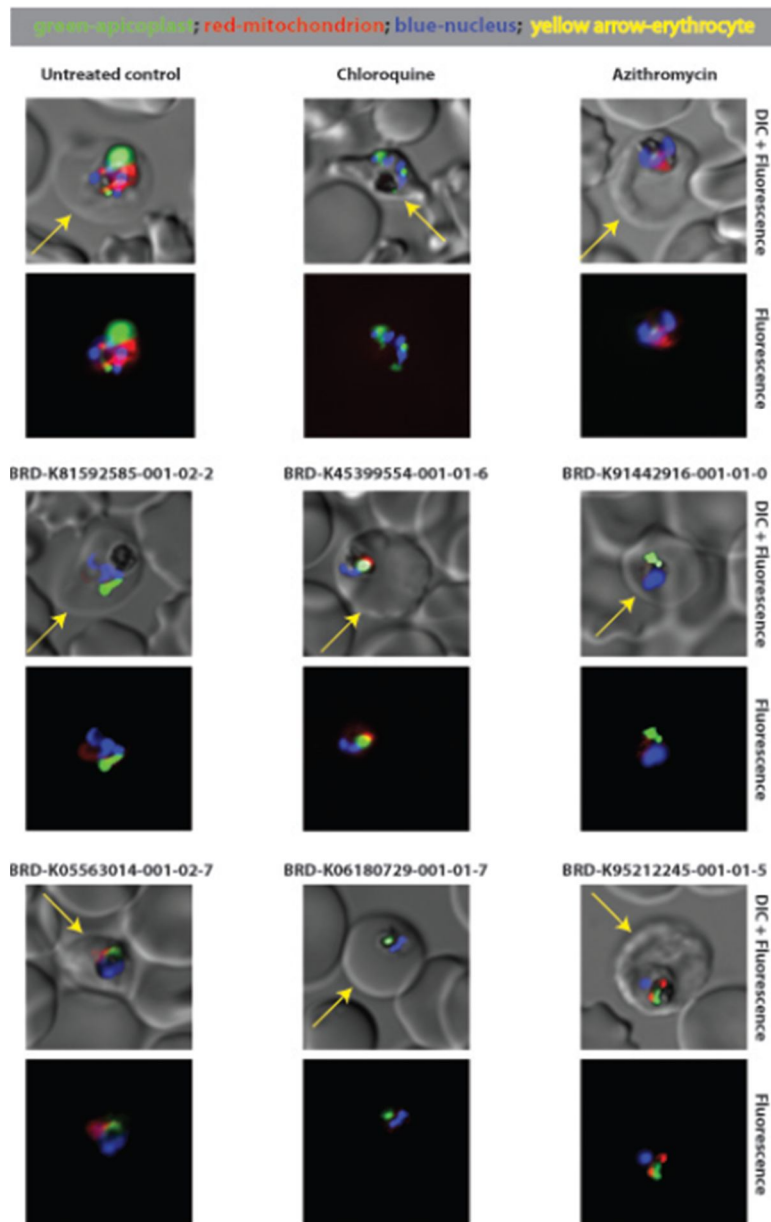


**Figure 10.** Parasites expressing GFP targeted to the apicoplast, 3D7 ACP<sub>L</sub>-GFP, were treated with the indicated compounds in 200  $\mu$ L of culture media at a 1% hematocrit. At 96 hours, 30  $\mu$ L of culture was harvested and stained with Hoechst (1  $\mu$ g/ml) and MitoTracker Red (20 nM) for 30 minutes at 37  $^{\circ}$ C. Stained parasites were imaged on a Nikon Ti inverted microscope with a 100X objective. The nuclei appear blue, mitochondria appear red, and the apicoplast appears green. The periphery of the infected erythrocyte is indicated with a yellow arrow. Drug concentrations: chloroquine, 16 nM; azithromycin, 80 nM; BRD-K81592585-001-02-2, 400 nM; BRD-K45399554-001-01-6, 0.64 nM; BRD-K91442916-001-01-0, 16 nM; BRD-K05563014-001-02-7, 400 nM; BRD-K06180729-001-01-7, 50  $\mu$ M; BRD-K95212245-001-01-5, 0.64 nM.

The untreated parasites exhibit bright staining for all three markers. Chloroquine is a fast-acting drug that inhibits heme detoxification in the parasite digestive vacuole. Chloroquine-treated parasites exhibit small, but intact apicoplast structures. The mitochondria are metabolically inactive and do not stain. Azithromycin is a delayed death-inducing drug that inhibits the apicoplast encoded 50s ribosomal subunit. The apicoplast has been disrupted in azithromycin treated-parasites, although many still display intact mitochondria. None of the experimental compounds including the probe (ML238) appeared to disrupt the apicoplast. The apicoplast morphology resembles the phenotype seen with chloroquine treatment; it is much smaller than in the untreated parasites but still present. Mitochondrial staining was generally diminished, though not entirely absent, in parasites treated with the probe (ML238) and some of its analogs.

As of now, the mode of action of the probe (ML238) is still unknown. But its structure, very different from known antimalarial drugs and probes, suggests that its mode of action could involve a new target. In this context, target identification will help understanding the mechanism of action of the probe and will be a priority in the near future.

#### **4.3 Planned Future Studies**

Research efforts are currently underway at the Broad Institute to advance this probe (ML238) to subsequent stages of drug discovery including target identification, drug metabolism and pharmacokinetic (DMPK) optimization, and animal studies.

## 5. References

- (1) Snow RW, Guerra CA, Noor AM, Myint HY, Hay SI. The global distribution of clinical episodes of *Plasmodium falciparum* malaria. *Nature*. 2005 Mar 10;434(7030):214-7. PubMed PMID: 15759000
- (2) Fidock DA. Drug discovery: priming the antimalarial pipeline. *Nature*. 2010 May 20;465(7296):297-8. PubMed PMID: 20485420
- (3) Wikipedia contributors. Malaria [Internet]. Wikipedia, The Free Encyclopedia; Available at: <http://en.wikipedia.org/wiki/Malaria>. Accessed 05 April 2011.
- (4) White NJ. Qinghaosu (artemisinin): the price of success. *Science*. 2008 Apr 18;320(5874):330-4. PubMed PMID: 18420924
- (5) Dondorp AM, Yeung S, White L, Nguon C, Day NP, Socheat D, von Seidlein L. Artemisinin resistance: current status and scenarios for containment. *Nat Rev Microbiol*. 2010 Apr;8(4):272-80. Epub 2010 Mar 8. PubMed PMID: 20208550
- (6) Gamo FJ, Sanz LM, Vidal J, de Cozar C, Alvarez E, Lavandera JL, Vanderwall DE, Green DV, Kumar V, Hasan S, et al. Thousands of chemical starting points for antimalarial lead identification. *Nature*. 2010 May 20;465(7296):305-10. PubMed PMID: 20485427
- (7) Guiguemde WA, Shelat AA, Bouck D, Duffy S, Crowther GJ, Davis PH, Smithson DC, Connelly M, Clark J, Zhu F, Jiménez-Díaz MB, et al. Chemical genetics of *Plasmodium falciparum*. *Nature*. 2010 May 20;465(7296):311-5. PubMed PMID: 20485428; PMCID: PMC2874979
- (8) Robert A, Benoit-Vical F, Dechy-Cabaret O, Meunier B. From classical antimalarial drugs to new compounds based on the mechanism of action of artemisinin. *Pure Appl. Chem*. 2001; 73(7), 1173-88.
- (9) Schlitzer M, Ortmann R. Feeding the antimalarial pipeline. *ChemMedChem*. 2010 Nov 8;5(11):1837-40. PubMed PMID: 20922746
- (10) Pradel G, Schlitzer M. Antibiotics in malaria therapy and their effect on the parasite apicoplast, *Curr Mol Med*. 2010 Apr;10(3):335-49. PubMed PMID: 20331433
- (11) Lell B, Ruangweera R, Wiesner J, Missinou MA, Schindler A, Baranek T, Hintz M, Hutchinson D, Jomaa H, Kremsner PG. Fosmidomycin, a novel chemotherapeutic agent for malaria. *Antimicrob Agents Chemother*. 2003 Feb;47(2):735-8. PubMed PMID: 12543685; PMCID: PMC151759
- (12) Steinbacher S, Kaiser J, Eisenreich W, Huber R, Bacher A, Rohdich F. Structural basis of fosmidomycin action revealed by the complex with 2-C-methyl-D-erythritol 4-phosphate synthase (IspC). Implications for the catalytic mechanism and anti-malaria drug development. *J Biol Chem*. 2003 May 16;278(20):18401-7. Epub 2003 Mar 5. PubMed PMID: 12621040
- (13) Nicolas O, Margout D, Taudon N, Wein S, Calas M, Vial HJ, Bressolle FM. Pharmacological properties of a new antimalarial bithiazolium salt, T3, and a corresponding Prodrug, TE3. *Antimicrob Agents Chemother*. 2005 Sep;49(9):3631-9. PubMed PMID: 16127032; PMCID: PMC1195427
- (14) Caldarelli SA, Duckert JF, Wein S, Calas M, Périgaud C, Vial H, Peyrottes S. Synthesis and evaluation of bis-thiazolium salts as potential antimalarial drugs. *ChemMedChem*. 2010 Jul 5;5(7):1102-9. PubMed PMID: 20540062
- (15) Rottmann M, McNamara C, Yeung BK, Lee MC, Zou B, Russell B, Seitz P, Plouffe DM, Dharia NV, Tan J, et al. Spiroindolones, a potent compound class for the treatment of malaria. *Science*. 2010 Sep 3;329(5996):1175-80. PubMed PMID: 20813948; PMCID: PMC3050001
- (16) Plouffe D, Brinker A, McNamara C, Henson K, Kato N, Kuhen K, Nagle A, Adrián F, Matzen JT, Anderson P, et al. In silico activity profiling reveals the mechanism of action of antimalarials discovered in a high-throughput

screen. *Proc Natl Acad Sci U S A.* 2008 Jul 1;105(26):9059-64. Epub 2008 Jun 25. PubMed PMID: 18579783; PMCID: PMC2440361

(17) Marcaurelle LA, Comer E, Dandapani S, Duvall JR, Gerard B, Kesavan S, Lee MD 4th, Liu H, Lowe JT, Marie JC, et al. An aldol-based build/couple/pair strategy for the synthesis of medium- and large-sized rings: discovery of macrocyclic histone deacetylase inhibitors. *J Am Chem Soc.* 2010 Dec 1;132(47):16962-76. Epub 2010 Nov 10. PubMed PMID: 21067169; PMCID: PMC3004530

(18) Inglese J, Auld DS, Jadhav A, Johnson RL, Simeonov A, Yasgar A, Zheng W, Austin CP. Quantitative high-throughput screening: a titration-based approach that efficiently identifies biological activities in large chemical libraries. *Proc Natl Acad Sci U S A.* 2006 Aug 1;103(31):11473-8. Epub 2006 Jul 24. PubMed PMID: 16864780; PMCID: PMC1518803

(19) Eli Lilly and Company and the National Institutes of Health Chemical Genomics Center. Assay Guidance Manual. NCGC High Throughput Screening Assay Guidance Criteria 2008. Available at: <http://www.ncgc.nih.gov/guidance/index.html>. Access Date: 31 March 2011.

(20) Mu J, Myers RA, Jiang H, Liu S, Ricklefs S, Waisberg M, Chotivanich K, Wilairatana P, Krudsood S, White NJ, et al. *Plasmodium falciparum* genome-wide scans for positive selection, recombination hot spots and resistance to antimalarial drugs. *Nat Genet.* 2010 Mar;42(3):268-71. Epub 2010 Jan 31. PubMed PMID: 20101240; PMCID: PMC2828519

(21) Lim L, McFadden GI. The evolution, metabolism and functions of the apicoplast, *Philos Trans R Soc Lond B Biol Sci.* 2010 Mar 12;365(1541):749-63. PubMed PMID: 20124342; PMCID: PMC2817234

(22) Dahl EL, Rosenthal PJ. Multiple antibiotics exert delayed effects against the *Plasmodium falciparum* apicoplast. *Antimicrob Agents Chemother.* 2007 Oct;51(10):3485-90. Epub 2007 Aug 13. PubMed PMID: 17698630; PMCID: PMC2043295

(23) Kato S, Harada H, Morie TM. *J Chem Soc Perkin Trans.* 1997;3219-25.

## Appendix A: Assay Summary Table

**Table A1.** Summary of Completed Assays and AIDs

PubChem AID Nos.	Type	Target	Concentration Range ( $\mu\text{M}$ )	Samples Tested
488774	Summary	NA	NA	NA
488752	Confirmatory 48-h time point	Malarial parasite plastid	28.7 $\mu\text{M}$ – 0.00184 $\mu\text{M}$	1280
488745	Confirmatory 96-h time point	Malarial parasite plastid	28.7 $\mu\text{M}$ – 0.00184 $\mu\text{M}$	1280
504608	Confirmatory 48hr time point (3D7)	Malarial parasite plastid	28.7 $\mu\text{M}$ – 0.00184 $\mu\text{M}$	54
504599	Confirmatory 96hr time point (3D7)	Malarial parasite plastid	28.7 $\mu\text{M}$ – 0.00184 $\mu\text{M}$	54
504602	Cell viability (HepG2)	HepG2 toxicity	28.7 $\mu\text{M}$ – 0.00184 $\mu\text{M}$	54
504604	Confirmatory (DD2)	Malarial parasite plastid	28.7 $\mu\text{M}$ – 0.00184 $\mu\text{M}$	54
504631	Confirmatory (DD2)	Malarial parasite plastid	0.625 $\mu\text{M}$ – 2.44 $\times 10^{-5}$ $\mu\text{M}$	10
504633	Confirmatory (3D7)	Malarial parasite plastid	0.625 $\mu\text{M}$ – 2.44 $\times 10^{-5}$ $\mu\text{M}$	10
504658	Confirmatory FACS 48-h time point	Malarial parasite plastid	100 nM – 0.045 nM	54
504659	Confirmatory FACS 96-h time point	Malarial parasite plastid	100 nM – 0.045 nM	54
504661	Apicoplast disruption	Malarial apicoplast	400 nM – 3.2 nM	54

## Appendix B: Detailed Assay Protocols

### Cell-based Assay with Luciferase Reporter

#### *For the 48-hour time point*

1. Dispense 4  $\mu$ L of culture medium (RPMI 1640 with 0.5% w/v Albumax (GIBCO), 24 mM sodium bicarbonate and 10  $\mu$ g/mL gentamycin) by a Multi-drop Combi into white, solid, 1536-well plates (Grenier).
2. Next, add 23 nL compound by a pin tool.
3. Dispense 4  $\mu$ L of infected erythrocytes (2% hematocrit, 0.1% parasitemia final concentration) in the culture medium.
4. Incubate the plates for 48 hours at 37 °C in 5% CO<sub>2</sub>.
5. Add 2  $\mu$ L of luciferase detection reagent and detect luminescence by a ViewLux (PerkinElmer) reader.

#### *For the 96-hour time point*

1. Dispense 4  $\mu$ L of culture medium (RPMI 1640 with 0.5% w/v Albumax (GIBCO), 24 mM sodium bicarbonate and 10  $\mu$ g/mL gentamycin) by a Multi-drop Combi into white, solid, 1536-well plates (Grenier)
2. Add 23 nL compound by a pin tool.
3. Dispense 4  $\mu$ L of infected erythrocytes (2% hematocrit, 0.1% parasitemia final concentration) in the culture medium.
4. Incubate the plates for 96 hours at 37 °C in 5% CO<sub>2</sub>.
5. Add 2  $\mu$ L of luciferase detection reagent and detect luminescence by a ViewLux (PerkinElmer) reader

### Primary HTS Screen Luciferase Drug Assays

1. Optimize luciferase assays to work in 30- $\mu$ L culture volumes in clear-bottom, 384-well plates (Greiner Bio-one).
2. Use a Precision-2000 microplate pipetting system (Bio Tek) to perform all of the liquid dispensing in the 384-well plates.
3. Dilute the test compounds in the plate to 2X the desired concentration in 15  $\mu$ L of RPMI culture media.
4. Add 15  $\mu$ L of parasites at 2% hematocrit to each well (1% final hematocrit). The initial parasitemia was 0.2% for 48-hour assays and 0.1% for 96-hour assays.
5. Dissolve the test compounds at 10 mM in DMSO and test at ten 5-fold dilutions, ranging from 50  $\mu$ M to 26 pM. Run the conditions in duplicate and average the duplicates.
6. At the end of the assay, freeze down the parasites.
7. After thawing, dispense 15  $\mu$ L of 3X Luciferin Lysis Buffer (15 mM DTT, 0.6 mM Coenzyme A, 0.45 mM ATP, 0.42 mg/ml luciferin, 10 mM MgCl<sub>2</sub>, 10 mM Tris Base, 10 mM Tris HCl, 0.03% Triton X-100) into each well.
8. After shaking and a 5-minute equilibration at 28 °C, read the samples for 3 seconds each using the luminescence settings on a Victor3 (Wallac) microplate reader.



## Flow Cytometry Drug Assays

1. For the flow cytometry-based validation screen, conduct the drug assays in flat-bottom, 96-well plates in a 200  $\mu$ l culture volume, with RBCs at a 1% hematocrit and starting parasitemias of 0.1%.
2. Set up drug dilutions as described for the luciferase assay. At 48-hour and 96-hour time points, suspend the cultures and transfer 20  $\mu$ l of the culture to round-bottom, 96-well plates.
3. Stain the samples with 40  $\mu$ l of 2.5X SYBR-green-1 (Invitrogen) and 150 nM MitoTracker Deep Red (Invitrogen) diluted in normal saline dextrose (0.9% NaCl, 5% dextrose) or in complete media.
4. Culture the infected erythrocytes with the stain for 40 minutes at 37 °C.
5. Wash the samples by adding 100  $\mu$ l of saline dextrose and spinning the plate down for 1 minute at 400 x g in a swing bucket centrifuge.
6. Remove the diluted stain by flicking out the plate. Resuspend the samples in 100  $\mu$ l of saline dextrose containing 5% fetal calf serum and assayed on an Accuri C6 cytometer equipped with a Hypercyt microplate sampler (process a 96-well plate in about 15 minutes).

### Primary *In vitro* *P. falciparum* Delayed Death Assay (AID 504608, AID 504599)

1. Dispense culture medium (4  $\mu$ l) into white, solid-bottom, Kalypsys plates with a Multidrop Combi Dispenser (Thermo Scientific).
2. Next, pin-transfer 23  $\mu$ l of compounds and positive control into the assay plates. (6.5 mM Azithromycin and 10mM Chloroquine; 1:2 dilution in duplicate).
3. Using the Multidrop Combi, dispense 4  $\mu$ l *P. falciparum*-infected RBCs with 0.1% parasitemia for the 48-hour assay (at 37 °C, 5% CO<sub>2</sub>) and 0.05% parasitemia for the 96-hour assay (at 37 °C, 5% CO<sub>2</sub>).
4. Add 2  $\mu$ l of SteadyLite into the assay plates with the Multidrop Combi dispenser, and centrifuge the plates at 1000 rpm for 30 seconds.
5. Read the plates by ViewLux: Excitation filter wheel A. 20 sec. exposure, 2x binning, slow.

### Secondary *In vitro* *P. falciparum* Viability Assay (SYBR green) Ran at HSPH

1. Modify a SYBR green assay as previously described by Plouffe et al.(16) for use in 384-well plates.
2. Culture parasites in the presence of serial dilutions of test compounds in 40  $\mu$ l of RPMI containing 4.16 mg/ml Albumax at a 1% hematocrit and an initial parasitemia of 1% in black Greiner GNF clear-bottom plates.
3. Following a 72-hour incubation at 37 °C under 94% N<sub>2</sub>, 5% CO<sub>2</sub>, and 1%O<sub>2</sub>, add SYBR green to a dilution of 1:10,000, and store the plates overnight (or until ready to be read) at -80 °C.
4. Centrifuge the plates at 700 rpm prior to fluorescence measurement (EX 480 nm, EM 530 nM).

### Secondary *In vitro* *P. falciparum* Viability Assay (SYBR green) Ran at NCGC (AID 504604)

1. Dispense the culture medium (3  $\mu$ l) into black, clear-bottom plates (Aurora) with a Multidrop Combi dispenser (Thermo Scientific).
2. Next, pin-transfer 23  $\mu$ l of compounds and positive control into the assay plates (control: 1 mM Artemisinin; 1:2 dilution in duplicate).
3. Using the Multidrop Combi, dispense *P. falciparum*-infected RBCs (0.3% parasitemia, 2.5% hematocrit final concentration).
4. Incubate the plates for 72 hours at 37 °C, 5% CO<sub>2</sub>.
5. Using the Multidrop Combi, dispense 2  $\mu$ l 10X SYBR Green lysis buffer (20 M Tris-HCl, 10 mM EDTA, 0.16% saponin (w/v), 1.6% Triton-X (v/v), 10 x SYBR Green I supplied as 10,000X final concentration by Invitrogen) into the assay plates, and store the plates at room temperature, overnight in the dark.
6. Read the plates with EnVision (Perkin Elmer) setup: fluorescence intensity at 485 nM excitation; 535 nM emission wavelengths.



## Secondary Cell Viability Assay in HepG2 (passage16)

### *Cell grown conditions:*

Supplement Eagle's Minimum Essential Medium (Catalog no.30-2003; ATCC) with 10% Hyclone FBS (Catalog no. SH30071-03; Invitrogen) and 1% Penn-Strep (Catalog no. 15140; GIBCO, 10,000 units/ml-10,000 µg/ml).

### *Procedures:*

1. To passage the cells, briefly rinse the cell monolayer twice with 1X Dulbecco's Phosphate Buffered Saline (DPBS, Catalog no.14190; GIBCO) and prewarm at 37 °C with 0.05% Trypsin-EDTA solution for 5 to 7 minutes.
2. Once the cell layer is dispersed (5-7 minutes at 37 °C), deactivate the solution Trypsin by adding equal volume of complete growth medium with 10% FBS.
3. To avoid clumping, do not agitate the cells by shaking the flask while waiting for the cells to detach.
4. Split the cells 1:4 every 3 days or 1:8 every 6 days. Incubate the cultures at 37 °C in humidified atmosphere with 5% CO<sub>2</sub>.

### **Materials/reagents/instrument:**

1. DMSO
2. 20 mM Tetraoctylammonium bromide (Sigma Catalog no.14866-33-2)
3. 1536-well, white, tissue culture plate (Greiner Catalog no.789175-F)
4. CellTiter-Glo reagent (Promega Catalog no.G7573)
5. ViewLux
6. PinTool
7. BioRAPTR

## Secondary HepG2 Cell Viability Assay (AID 504602)

1. Plate the cells at a density of 2000 cells/well/5 µL in 1536-well, white, tissue-culture treated plates with culture medium.
2. Prepare triplicate plates and incubate at 37 °C, 5% CO<sub>2</sub> for 5 hours.
3. Next, transfer 23 nl of compounds and positive control to the assay plates (Positive plate map: Row 1-30 = blank; Row 31 = 20 mM Tetraoctylammonium bromide in DMSO; Row 32 = DMSO).
4. Incubate the plates at 37 °C, 5% CO<sub>2</sub> for 48 hours.
5. Add CellTiter-Glo reagent (5 µl) to each well, and incubate the plates at room temperature for 30 minutes. Measure luminescence using ViewLux (1 second, slow, 2X).

### **Tertiary Apicoplast Disruption Using a Whole Cell Imaging Assay**

1. Culture ACP<sub>L</sub>-GFP parasites with compounds tested at approximately 2X their 96-hour EC<sub>50</sub> value to screen for inhibition of apicoplast elongation and segregation.
2. Use Azithromycin as a positive control, while parasites treated with drug vehicle (medium containing 0.05 – 0.1% DMSO) serve as a negative control.
3. Begin assays with synchronized ring stages, and harvest the parasites on Day 4.
4. Incubate the parasites with 1 mg/ml Hoechst 33342 nuclear stain and 20 nM Mitotracker-Red, wash, and deposit on poly-lysine coated slides.
5. Take images on a Nikon Ti inverted microscope.

## Appendix C: Experimental Details of the Synthesis of the Probe

**Preparation of *tert*-Butyl methyl(2-oxoethyl)carbamate (1):** A flame-dried, three-neck, 3-liter, round-bottom flask containing a mechanical stirrer (central port), internal temperature probe, and addition funnel was charged with oxalyl chloride (176 ml, 2.01 mol, 1.5 equiv) and dichloromethane (634 ml). The flask was cooled to -70 °C and dimethyl sulfoxide (286 ml, 4.02 mol, 3.0 equiv) was introduced at a rate that maintained an internal temperature below -65 °C. An initial exotherm was observed, and the temperature did rise. After addition of approximately 50 ml, the addition was slowed to allow the reaction to cool. This type of intermittent addition strategy was followed to prevent overheating. The addition proceeded over 2.5 hours. Then, the mixture was stirred for an additional 15 minutes, after which *t*-butyl 2-hydroxyethyl(methyl)carbamate (235 g, 1.34 mol, 1.0 equiv) in methylene chloride (CH<sub>2</sub>Cl<sub>2</sub>; 700 ml) was added over 1 hour, followed by slow addition of triethylamine (841 ml, 6.04 mol, 4.5 equiv) over 30 minutes. Both of these reactants were added at a rate that does not cause any increase in internal temperature. After addition of the alcohol solution the reaction was cloudy. Upon initial addition of triethylamine, the reaction became colorless/clear; however, at the end, the reaction was milky white. The reaction was monitored by thin-layer chromatography (TLC; Hex:EtOAc 1:1) until the reaction was deemed complete (2.5 hours additional, -70 °C). Saturated sodium bicarbonate solution (500 ml) was introduced to quench the reaction at -78 °C. The reaction was warmed to room temperature, and the phases were separated. The combined organics were washed with water (2 x 100 ml), dried over magnesium sulfate, and concentrated. Distillation (87-89 °C, 3 mm Hg) provided aldehyde **1** (22.2 g, 128 mmol) as a colorless oil, which matched all data reported by Kato et al. (23).

**Preparation of (2*S*,3*R*)-(1*S*,2*R*)-1-phenyl-2-(*N*,2,4,6-tetramethylphenylsulfonamido)propyl 4-((*tert*-butoxycarbonyl)(methyl)amino)-3-hydroxy-2-methylbutanoate (3):** An oven-dried, 3-liter, three-neck, round-bottom flask was equipped with a mechanical stirrer and temperature probe. Under a positive flow of nitrogen, the vessel was charged with (1*S*,2*R*)-1-phenyl-2-(*N*,2,4,6-tetramethylphenylsulfonamido)propyl propionate (109 g, 270 mmol) and CH<sub>2</sub>Cl<sub>2</sub> (932 ml). The reaction was cooled to -78 °C with constant agitation at which point triethylamine (Et<sub>3</sub>N; 112 ml, 810 mmol) was added dropwise, maintaining an internal reaction temperature no greater than -65 °C (approximately 10 minutes). After 15 minutes of additional stirring, a solution of dicyclohexylboron triflate (1.0 M in CH<sub>2</sub>Cl<sub>2</sub>, 176 g, 540 mmol) was added dropwise, maintaining an internal reaction temperature below -67 °C (approximately 30 minutes). The resulting yellow enolate reaction solution was stirred at -78 °C for an additional 2 hours. At this point *t*-butyl methyl(2-oxoethyl)carbamate **1** (68.1 ml, 405 mmol) was added dropwise at a rate so as to maintain an internal temperature below -67 °C (approximately 15 minutes). The reaction mixture was stirred at -78 °C for 2 hours and then was allowed to warm to 0 °C for 1 hour. The reaction was quenched by addition of methyl alcohol (MeOH; 1.09 L) and pH 7 buffer (130 ml). Then, aqueous hydrogen peroxide (35% by wt, 130 ml, 1.5 mol) was slowly added such that the internal reaction temperature did not exceed 20 °C. After the addition was complete, the mixture was allowed to warm to ambient temperature where it was stirred for 1 hour. The resultant slurry was then concentrated *in vacuo*, and the residue was partitioned between water (550 ml) and CH<sub>2</sub>Cl<sub>2</sub> (500 ml). The aqueous layer was extracted with CH<sub>2</sub>Cl<sub>2</sub> (4 x 300 ml), and the combined organic layers were washed with water (100 ml) followed by brine (100 ml). The organic layer was dried over anhydrous MgSO<sub>4</sub> and the solvent was removed *in vacuo* to yield 1-phenyl-2-(*N*,2,4,6-tetramethylphenylsulfonamido)propyl 4-((*tert*-butoxycarbonyl(methyl)amino)-3-hydroxy-2-methylbutanoate **3** (156 g, 99%) as a yellow oil, which was deemed sufficiently pure and carried forward without any further purification.

(*R,S,S,R*)-(+)-**3**: **TLC**:  $R_f$  = 0.34 (30% EtOAc in hexanes).  $[\alpha]_D^{20}$  +6.42 (*c* 1.0, CHCl<sub>3</sub>). **IR** (cm<sup>-1</sup>) 3446 (br), 2975, 2930, 1778, 1682, 1481, 1455, 1390, 1366, 1294, 1210, 1154, 1109, 1050, 1015, 990, 969, 925, 879, 763, 749, 703. **<sup>1</sup>H NMR** (500 MHz, CDCl<sub>3</sub>, 60 °C)  $\delta$  7.20 (d, *J* = 7.4, 2H), 7.05 (d, *J* = 7.5, 1H), 6.87 (s, 1H), 5.79 (d, *J* = 5.3, 1H), 4.07 (s, 1H), 3.90 (s, 1H), 3.30 (s, 2H), 2.90 (s, 3H), 2.78 (s, 3H), 2.68-2.56 (m, 1H), 2.45 (s, 6H), 2.29 (s, 3H), 1.45 (s, 9H), 1.31 (d, *J* = 6.8, 2H), 1.19 (d, *J* = 7.2, 1H). **<sup>13</sup>C NMR** (125 MHz, CDCl<sub>3</sub>, 60 °C)  $\delta$  173.8, 142.5, 140.6, 138.3, 132.9, 132.1, 128.6, 128.1, 126.5, 126.3, 80.2, 78.4, 73.1, 58.8, 55.9, 53.3, 47.3, 44.3, 36.3, 35.7, 28.6, 25.7, 24.2, 22.7, 20.9, 13.6, 12.3, 8.9. **HRMS (ESI)** calcd for C<sub>21</sub>H<sub>30</sub>N<sub>2</sub>O<sub>6</sub>Na [M + Na]<sup>+</sup>: 429.1996. Found: 429.2000.

**Preparation of (2*S*,3*R*)-4-((*tert*-butoxycarbonyl)(methyl)amino)-3-hydroxy-2-methylbutanoic acid (**4**)**: A 3-liter, three-neck, round-bottom flask was equipped with an overhead stirrer, an internal temperature probe, and an addition funnel. The vessel was charged with the crude 1-phenyl-2-(*N*,2,4,6-tetramethylphenylsulfonamido)propyl-4-((*tert*-butoxycarbonyl)(methyl)amino)-3-hydroxy-2-methylbutanoate (156.0 g, 270 mmol, 1.0 equiv) and 1:1 *t*-BuOH/MeOH (1700 ml) was added and cooled 0 °C. A solution of hydrogen peroxide (H<sub>2</sub>O<sub>2</sub>; 30% in water, 166 ml, 1623 mmol, 6.0 equiv) was added *via* addition funnel, followed by aqueous sodium hydroxide (NaOH; 1.0 M, 811 ml, 811 mmol, 3.0 equiv), which was added at such a rate that the internal temperature did not rise above 10 °C. The mixture was warmed to room temperature slowly and allowed to stir overnight. In the morning, organic solvents were removed *in vacuo*. The resulting aqueous layer was diluted with water (300 ml) and extracted with ethyl acetate (EtOAc; 4 x 200 ml) to remove the auxiliary. The resulting aqueous layer was then acidified with 6 M HCl to pH 4 and extracted with EtOAc (5 x 250 ml). The combined EtOAc extracts were dried (MgSO<sub>4</sub>), filtered and concentrated, to provide the desired product **4** as a yellow oil (66.0 g, 99%). While the crude product was carried on to the next step without further purification, an analytical sample was obtained by chromatography on silica gel. (*S,R*)-(+)-**4**: **TLC**:  $R_f$  = 0.34 (33% EtOAc in hexanes).  $[\alpha]_D^{20}$  +2.1 (*c* 1.0, CHCl<sub>3</sub>). **IR** (cm<sup>-1</sup>) 3446 (br), 2977, 2933, 1678, 1483, 1456, 1393, 1367, 1249, 1154, 1056, 874, 766. **<sup>1</sup>H NMR** (500 MHz, CDCl<sub>3</sub>, 60 °C)  $\delta$  3.99 (s, 1H), 3.91 (dd, *J* = 5.7, 11.4, 1H), 3.39 (m, 1H), 2.95 (s, 1.5H), 2.93 (s, 1.5H), 2.59 (dd, *J* = 6.2, 12.0, 1H), 1.48 (s, 4.5H), 1.47 (s, 4.5H), 1.28 (dd, *J* = 7.2, 3H). **<sup>13</sup>C NMR** (125 MHz, CDCl<sub>3</sub>, 60 °C)  $\delta$  181.1, 158.2, 81.0, 72.6, 53.4, 43.8, 36.2, 28.7, 15.0. **HRMS (ESI)** calcd for C<sub>11</sub>H<sub>21</sub>NO<sub>5</sub>Na [M + Na]<sup>+</sup>: 270.1312. Found: 270.1312.

**Preparation of (2*S*,3*R*)-4-((*tert*-butoxycarbonyl)(methyl)amino)-3-((*tert*-butyldimethylsilyl)oxy)-2-methylbutanoic acid (**5**)**: An oven dried, 5-liter, three-neck, round-bottom flask equipped with a magnetic stirrer and an internal temperature probe was charged with 4-((*tert*-butoxycarbonyl)(methyl)amino)-3-hydroxy-2-methylbutanoic acid **4** (58.7 g, 237 mmol, 1.0 equiv), CH<sub>2</sub>Cl<sub>2</sub> (concentration of **4** = 0.1 M) and 2,6-lutidine (91 ml, 783 mmol, 3.3 equiv) under a positive flow of nitrogen. The reaction mixture was cooled to -78 °C and *tert*-butyldimethylsilyl trifluoromethanesulfonate (TBSOTf) (120 ml, 522 mmol, 2.2 equiv) was added dropwise over 20 minutes. The reaction mixture was stirred at -78 °C for 1 hour and quenched with aqueous saturated sodium bicarbonate (NaHCO<sub>3</sub>; 500 ml). The layers were separated, and the aqueous layer was extracted with diethyl ether (2 x 200 ml). The combined organic extracts were washed with saturated ammonium chloride (NH<sub>4</sub>Cl; 2 x 500 ml) and brine (2 x 500 ml), dried (MgSO<sub>4</sub>), filtered, and the solvent evaporated. The residue was dissolved in MeOH:THF (1:1) and cooled to 0 °C. An aqueous solution of potassium carbonate (K<sub>2</sub>CO<sub>3</sub>; 1.5-2.2 equiv) was added, and the mixture was stirred at 0 °C for 1 hour. The reaction mixture was concentrated to remove volatiles, and the remaining aqueous layer was extracted with EtOAc. The organic layer was washed with 1 N HCl, then dried over MgSO<sub>4</sub>, filtered, and concentrated *in vacuo* to yield the crude product as a clear oil, which was co-evaporated with toluene to remove excess TBSOH and dried to provide the TBS ether **5** as a clear oil (74.1 g,



83%). (S,R)-(+)-**5**: **TLC**:  $R_f$  = 0.67 (33% EtOAc in hexanes).  $[\alpha]_D^{20}$  +3.7 ( $c$  1.0,  $\text{CHCl}_3$ ). **IR** ( $\text{cm}^{-1}$ ) 2978, 1649, 1459, 1395, 1285, 1157, 880.  **$^1\text{H}$  NMR** (500 MHz,  $\text{CDCl}_3$ , 60 °C)  $\delta$  4.15 (br s, 1H), 3.35 (dd,  $J$  = 14.5, 6.0 Hz, 1H), 3.23 (br s, 1H), 2.88 (s, 3H), 2.65 (br s, 1H), 1.44 (s, 9H), 1.21 (d,  $J$  = 7.0, 1H), 0.89 (s, 9H), 0.10 (s, 3H), 0.09 (s, 3H).  **$^{13}\text{C}$  NMR** (125 MHz,  $\text{CDCl}_3$ , 60 °C)  $\delta$  176.8, 156.4, 80.3, 72.4, 52.9, 43.9, 36.7, 28.7, 26.0, 18.2, 12.8, -4.2, -4.7. **HRMS (ESI)** calcd for  $\text{C}_{17}\text{H}_{25}\text{NO}_5\text{SiNa}$   $[\text{M} + \text{Na}]^+$ : 384.2177. Found: 384.2167.

**Preparation of *tert*-butyl ((2R,3S)-2-((*tert*-butyldimethylsilyloxy)-4-(((S)-1-(4-methoxybenzyl)oxy)propan-2-yl)amino)-3-methyl-4-oxobutyl)(methyl)carbamate (**6**):** An oven-dried, 3-liter, 3-neck, round-bottom flask was equipped with an overhead stirrer, addition funnel, and a temperature probe. Under a positive flow of nitrogen, the vessel was charged with 4-(*tert*-butoxycarbonyl(methyl)amino)-3-(*tert*-butyldimethylsilyloxy)-2-methylbutanoic acid **5** (38.1 g, 105 mmol, 1.0 equiv) dissolved in  $\text{CH}_2\text{Cl}_2$  (80% of total solvent, final concentration of **5** = 0.2 M), followed by benzotriazol-1-yl-oxytripyrrolidinophosphonium hexafluorophosphate (PyBOP; 60.4 g, 116 mmol, 1.1 equiv), and diisopropyl ethylamine (DIPEA; 55.3 ml, 316 mmol, 3.0 equiv). The resulting mixture was cooled in an ice bath before 1-(4-methoxybenzyloxy)propan-2-amine (24.7 g, 127 mmol, 1.2 equiv) was added as a solution in  $\text{CH}_2\text{Cl}_2$  (remaining 20% of total solvent) by addition funnel. The rate of addition was controlled so as to maintain an internal temperature between 3-5 °C. When the addition was complete, the mixture was warmed to ambient temperature and allowed to stir for 15 hours. The reaction was quenched with water, and extracted with  $\text{CH}_2\text{Cl}_2$ . The combined organic extracts were dried over  $\text{MgSO}_4$ , filtered, and concentrated. The yellow oil was taken up in  $\text{Et}_2\text{O}$  (500 ml), and the phosphoramidate byproducts were removed *via* filtration. The solvent was removed *in vacuo*, and the crude product was isolated. Flash chromatography on silica gel (4:1 Hexanes/EtOAc to 7:3 Hexanes/EtOAc) gave the product **6** as a colorless oil (51.9 g, 91%). (S,S,R)-**6**:  $[\alpha]_D^{20}$  -16.5 ( $c$  1.0,  $\text{CHCl}_3$ ). **IR** ( $\text{cm}^{-1}$ ) 3365, 2930, 1696, 1670, 1513, 1460, 1390, 1365, 1248, 1156.  **$^1\text{H}$  NMR** (500 MHz,  $\text{CDCl}_3$ , 55 °C)  $\delta$  7.22 (d,  $J$  = 8.5, 2H), 6.86 (d,  $J$  = 8.5, 2H), 6.75 (br s, 1H, NH), 4.46 (d,  $J$  = 11.7, 1H), 4.41 (d,  $J$  = 11.7, 1H), 4.22-4.15 (m, 1H), 4.05-3.98 (m, 1H), 3.80 (s, 3H), 3.39 (d,  $J$  = 4.6, 2H), 3.34 (dd,  $J$  = 6.4, 14.0, 1H), 3.18 (dd,  $J$  = 6.3, 14.0, 1H), 2.88 (s, 3H), 2.41 (dq,  $J$  = 2.9, 7.3, 1H), 1.46 (s, 9H), 1.22 (d,  $J$  = 7.2, 3H), 1.18 (d,  $J$  = 6.7, 3H), 0.91 (s, 9H), 0.12 (s, 3H), 0.11 (s, 3H).  **$^{13}\text{C}$  NMR** (125 MHz,  $\text{CDCl}_3$ , 55 °C)  $\delta$  173.4, 159.4, 156.0 (br), 130.6, 129.1 (2C), 113.9 (2C), 79.7 (br), 72.9, 72.8, 72.6 (br), 55.3, 53.5, 44.8, 44.5, 36.6 (br), 28.5 (3C), 25.9 (3C), 18.0, 17.9, 15.6, -4.5, -4.9. **HRMS (ESI)** calcd for  $\text{C}_{28}\text{H}_{50}\text{N}_2\text{NaO}_6\text{Si}$   $[\text{M} + \text{Na}]^+$ : 561.3330. Found: 561.3498.

**Preparation of *tert*-butyl ((2R,3R)-2-((*tert*-butyldimethylsilyloxy)-4-(((S)-1-(4-methoxybenzyl)oxy)propan-2-yl)amino)-3-methylbutyl)(methyl)carbamate (**7**):** An oven-dried, 2-liter, one-necked, round-bottom flask was equipped with a magnetic stirrer. Under a positive flow of nitrogen, the flask was charged with *tert*-butyl 2-(*tert*-butyldimethylsilyloxy)-4-(1-(4-methoxybenzyloxy)propan-2-ylamino)-3-methyl-4-oxobutyl(methyl)carbamate **6** (36.0 g, 66.8 mmol, 1.0 equiv) and anhydrous tetrahydrofuran (THF; final concentration 0.1 M). Borane dimethylsulfide complex ( $\text{BH}_3\cdot\text{DMS}$ ) (31.7 ml, 334 mmol, 5.0 equiv) was added dropwise via syringe. Afterwards, the reaction mixture was heated at 65 °C for 5 hours. After cooling to ambient temperature, excess hydride was quenched by the careful addition of MeOH. The mixture was concentrated under reduced pressure to afford a colorless oil, which was then co-evaporated with MeOH three times to remove excess  $\text{B}(\text{OMe})_3$ . The oil was then re-dissolved in MeOH and 10% aqueous potassium sodium tartrate (2:3 ratio, final concentration 0.067 M). The resulting slurry was heated at reflux for 12 hours. The volatiles were removed under reduced pressure, and the aqueous layer was extracted with EtOAc (3 x 200 ml). The combined organic layers were washed with brine (1 x 200 ml), dried over magnesium sulfate, filtered and concentrated to provide the desired amine **7** as a colorless oil (31.5 g, 90%).

(*S,R,R*)-(+)-**7**:  $[\alpha]_D^{20}$  -10.65 (*c* 2.46,  $\text{CHCl}_3$ ). IR ( $\text{cm}^{-1}$ ) 3010, 2929, 1693 1513 1461, 1389, 1247, 1152.  $^1\text{H}$  NMR (500 MHz,  $\text{CDCl}_3$ , 60 °C)  $\delta$  7.19 (d, *J* = 8.5, 2H), 6.82 (d, *J* = 8.5, 2H), 4.40 (s, 2H), 3.89 (m, 1H), 3.74 (s, 3H), 3.29 (m, 4H), 2.98 (dd, *J* = 13.5, 7.5, 1H), 2.85 (m, 4H), 2.63 (m, 1H), 2.41 (dd, *J* = 11, 9, 1H), 1.72 (m, 1H), 1.41 (s, 9H), 0.98 (d, *J* = 6.5, 1H), 0.92 (d, *J* = 6.5, 1H), 0.86 (s, 9H), 0.02 (s, 3H), 0.00 (s, 3H).  $^{13}\text{C}$  NMR (125 MHz,  $\text{CDCl}_3$ , 60 °C)  $\delta$  159.3, 155.7, 130.8, 129.1, 113.9, 79.1, 74.6, 73.3, 72.8, 55.2, 52.5, 52.0, 49.4, 38.7, 36.4, 28.6, 26.0, 18.0, 17.6, 13.7, -4.5. HRMS (ESI) calcd for  $\text{C}_{28}\text{H}_{53}\text{N}_2\text{O}_5\text{Si}$  [*M* + *H*]<sup>+</sup>: 525.3718. Found: 525.3698.

**Preparation of *tert*-butyl ((2*R*,3*R*)-2-((*tert*-butyldimethylsilyl)oxy)-4-(*N*-((*S*)-1-((4-methoxybenzyl)oxy)propan-2-yl)-5-nitro-2-((*S*)-pent-4-en-2-yloxy)benzamido)-3-methylbutyl)(methyl)carbamate (**8**):** A solution of starting material **7** (15.0 g, 28.6 mmol, 1.0 equiv) and diisopropyl ethylamine (DIEA; 19.9 ml, 114 mmol, 4.0 equiv) in  $\text{CH}_2\text{Cl}_2$  (80% of total solvent volume, final concentration of **7** = 0.12 molar) was cooled to 0 °C in an ice/water bath. Then, the acid chloride (10.0 g, 37.2 mmol, 1.3 equiv) was added to the reaction mixture as a solution in  $\text{CH}_2\text{Cl}_2$  (remaining 20% of solvent volume). Upon completion, the reaction was stirred for 2.5 hours while warming to room temperature. Analysis of the reaction by LC-MS indicated excellent conversion, and the formation of a new product. The reaction mixture was quenched with aqueous saturated  $\text{NH}_4\text{Cl}$  solution (300 ml), and the aqueous layer was extracted with  $\text{CH}_2\text{Cl}_2$  (2 x 300 ml). The combined organic layers were dried over  $\text{MgSO}_4$ , filtered, and concentrated under reduced pressure to provide the crude product, which was typically taken on without further purification. An analytical sample was obtained through purification by chromatography on silica gel, which provided a pure product (19.57 g, 90%), as a clear oil. (*S,R,R,S*)-**8**: TLC:  $R_f$  = 0.45 (30% EtOAc in hexanes). IR ( $\text{cm}^{-1}$ ) 2930 (w), 2856 (w), 1690 (m), 1636 (m), 1610 (w), 1514 (m), 1481 (m), 1460 (m), 1338 (s), 1248 (s), 1154 (s), 1078 (m).  $^1\text{H}$  NMR (500 MHz,  $\text{DMSO}-d_6$ , 140 °C)  $\delta$  8.18 (dd, *J* = 9.3, 2.4 Hz, 1H), 7.93 (d, *J* = 2.0, 1H), 7.26 (d, *J* = 9.3, 1H), 7.20 (br s, 2H), 6.89 (d, *J* = 8.3, 2H), 5.86 (ddt, *J* = 16.6, 9.8, 3.4, 1H), 5.14 (d, *J* = 17.1, 1H), 5.10 (d, *J* = 9.8, 1H), 4.76 (q, *J* = 5.9, 1H), 4.41 (s, 2H), 4.07-3.97 (m, 1H), 3.96-3.83 (m, 1H), 3.78 (s, 3H), 3.69-3.38 (br, 2H), 3.37-3.28 (m, 2H), 3.20-2.93 (br s, 2H), 2.82 (s, 3H), 2.47 (obscured m, 1H), 2.41 (dd, *J* = 14.2, 6.8, 1H), 2.24-1.93 (br s, 1H), 1.43 (s, 9H), 1.28 (d, *J* = 5.9, 3H), 1.25 (br s, 3H), 0.91 (d, *J* = 7.8, 3H), 0.83 (br s, 9H), 0.02 (br s, 6H).  $^{13}\text{C}$  NMR (125 MHz,  $\text{DMSO}-d_6$ , 130 °C)  $\delta$  166.3, 158.4, 157.7, 154.4, 140.1, 132.7, 129.7, 128.5, 128.0 (2), 124.7, 122.9, 116.8, 113.3 (2), 113.1, 78.0, 74.2, 72.5, 71.4, 70.9, 54.5, 53.4, 51.0, 39.0, 34.8 (2), 27.4 (3), 24.9 (3), 18.1, 16.8, 15.1, 12.7, -5.3, -5.6. HRMS (ESI) calcd for  $\text{C}_{40}\text{H}_{64}\text{N}_3\text{O}_9\text{Si}$  [*M* + *H*]<sup>+</sup>: 758.4406. Found: 758.4372.

**Preparation of *tert*-butyl ((2*R*,3*R*)-2-(allyloxy)-4-(*N*-((*S*)-1-((4-methoxybenzyl)oxy)propan-2-yl)-5-nitro-2-((*S*)-pent-4-en-2-yloxy)benzamido)-3-methylbutyl)(methyl)carbamate (**9**):** A solution of *tert*-butyl ((2*R*,3*R*)-2-((*tert*-butyldimethylsilyl)oxy)-4-(*N*-((*S*)-1-((4-methoxybenzyl)oxy)propan-2-yl)-5-nitro-2-((*S*)-pent-4-en-2-yloxy)benzamido)-3-methylbutyl)(methyl)carbamate (19.6 g, 25.8 mmol, 1.0 equiv) in THF (0.1 molar) was cooled to 0 °C in an ice bath. Tetrabutylammonium fluoride (TBAF) solution (1.0 M in THF, 65 ml, 65 mmol, 2.5 equiv) was added dropwise over 3 minutes, and the reaction was stirred for 14 hours, slowly warming to room temperature. Analysis of the reaction by LC-MS indicated complete disappearance of the starting material. The reaction was quenched with saturated aqueous  $\text{NH}_4\text{Cl}$  (300 ml), and extracted with EtOAc (3 x 300 ml). The combined organic layers were dried ( $\text{MgSO}_4$ ), filtered, and concentrated to provide the crude product, which was purified by flash chromatography on silica gel (13.5 g, 81%). Then, a solution of the obtained alcohol (12 g, 18.6 mmol, 1.0 equiv) in DMF (0.1 molar) was cooled to 0 °C in an ice bath. Allyl bromide (16.1 ml, 186 mmol, 10.0 equiv) was then added, followed by sodium hydride as a solid in one portion (60% dispersion in mineral oil, 1.79 g, 48 mmol, 2.4 equiv), and the reaction was stirred for 14 hours, slowly warming to room temperature. Analysis of the reaction by LC-MS indicated complete disappearance of the starting

material, and the formation of a new product. The reaction mixture was quenched with aqueous saturated  $\text{NH}_4\text{Cl}$  solution (200 ml) and extracted with EtOAc (3 x 300 ml). The combined organic extracts were dried over  $\text{MgSO}_4$ , filtered, and concentrated under reduced pressure to provide the crude product, which was purified by chromatography on silica gel to provide pure product **9** as a clear oil (12.3 g, 97%). (*S,R,R,S*)-**9**: **TLC**:  $R_f$  = 0.26 (30% EtOAc in hexanes). **IR** ( $\text{cm}^{-1}$ ) 2976 (w), 2932 (w), 1688 (m), 1634 (m), 1610 (m), 1513 (m), 1481 (m), 1453 (m), 1337 (s), 1266 (s), 1247 (s), 1153 (s), 1074 (s).  **$^1\text{H}$  NMR** (500 MHz,  $\text{DMSO}-d_6$ , 140  $^\circ\text{C}$ )  $\delta$  8.18 (dd,  $J$  = 9.3, 2.9, 1H), 7.94 (d,  $J$  = 2.9, 1H), 7.27 (d,  $J$  = 9.3, 1H), 7.21 (br s, 2H), 6.89 (d,  $J$  = 8.3, 2H), 5.85 (ddt,  $J$  = 17.1, 10.2, 6.8, 2H), 5.14 (d,  $J$  = 18.1, 2H), 5.09 (d,  $J$  = 9.8, 2H), 4.77 (q,  $J$  = 5.9, 1H), 4.41 (br s, 2H), 4.07-3.88 (br s, 2H), 3.87-3.81 (br s, 1H), 3.77 (s, 3H), 3.70-3.01 (br, 7H), 2.83 (s, 3H), 2.53-2.45 (obscured m, 1H), 2.38 (dd,  $J$  = 14.6, 7.3, 1H), 2.28-1.97 (br s, 1H), 1.42 (s, 9H), 1.28 (d,  $J$  = 5.9, 3H), 1.25 (br s, 3H), 0.95 (br s, 3H).  **$^{13}\text{C}$  NMR** (125 MHz,  $\text{DMSO}-d_6$ , 130  $^\circ\text{C}$ )  $\delta$  166.4, 158.4, 157.7, 154.3, 140.1, 134.7, 132.7, 129.7, 128.5, 128.0 (2), 124.7, 123.0, 116.8, 114.8, 113.3 (2), 113.1, 79.9, 77.9, 74.2, 71.4, 70.8, 70.1, 54.5, 53.4, 49.3, 39.1, 35.0, 34.5, 27.4 (3), 18.1, 15.1, 12.8. **HRMS (ESI)** calcd for  $\text{C}_{37}\text{H}_{54}\text{N}_3\text{O}_9$   $[\text{M} + \text{H}]^+$ : 684.3854. Found: 684.3846.

**Preparation of *tert*-butyl (((2*S*,8*R*,9*R*)-14-amino-11-((*S*)-1-((4-methoxybenzyl)oxy)propan-2-yl)-2,9-dimethyl-12-oxo-2,3,4,5,6,8,9,10,11,12-decahydrobenzo[*b*][1,9,5]dioxazacyclotetradecin-8-yl)methyl)(methyl)carbamate (**10**)**: A solution of the diolefin **9** (13.5 g, 19.8 mmol, 1.0 equiv) and Hoveyda Grubbs Catalyst II (1.24 g, 1.98 mmol, 0.10 equiv) in toluene (0.01 molar) was degassed with dry nitrogen for 15 minutes. The reaction was stirred for 14 hours at room temperature (23  $^\circ\text{C}$ ) after which analysis of the reaction by LC-MS indicated complete disappearance of the starting material, and the formation of the target material as well as some dimerized product. The solvent was evaporated under reduced pressure, and the mixture was purified by flash chromatography on silica gel using a gradient of EtOAc in hexanes. The resulting products (a mixture of geometric isomers) were redissolved in EtOAc (0.02 molar) and stirred overnight with activated carbon. The mixture was then filtered over Celite and concentrated to provide the crude products as a light brown, foamy solid (10.34 g, 80%). Then, 20 mol%  $\text{Pd}(\text{OH})_2$  on activated carbon (10.7 mg, 15  $\mu\text{mol}$ , 0.10 equiv) was added to a solution of the obtained RCM mixture (100 mg, 0.152 mmol, 1.0 equiv) in methanol (0.02 molar). Hydrogen gas was bubbled into the mixture for 30 minutes, after which the reaction was placed under a static  $\text{H}_2$  environment (balloon pressure) for 12-15 hours. The reaction mixture was filtered through Celite, washing the filter cake with EtOAc (50 ml), dichloromethane (50 ml), and finally hot EtOAc (50 ml). The filtrate was concentrated, and the crude residue was purified by flash chromatography on silica gel using a gradient of MeOH in DCM to provide the pure aniline **10** (48 mg, 51%). (*S,R,R,R*)-**10**: **IR** ( $\text{cm}^{-1}$ ) 2930 (m), 1685 (s), 1612 (s), 1512 (s), 1491 (s), 1456 (s), 1247 (s), 1225 (s), 1154 (s), 1080 (m).  **$^1\text{H}$  NMR** (500 MHz,  $\text{DMSO}-d_6$ )  $\delta$  7.22 (br s, 2H), 6.90 (d,  $J$  = 8.3, 2H), 6.70 (d,  $J$  = 8.8, 1H), 6.58 (dd,  $J$  = 8.8, 2.4, 1H), 6.42 (br s, 1H), 4.64-4.18 (br m, 5H), 4.06-3.82 (br m, 2H), 3.77 (s, 3H), 3.74-3.47 (br, 3H), 3.46-3.29 (br s, 1H), 3.28-3.15 (br s, 1H), 3.14-2.99 (br s, 1H), 2.95-2.58 (br m, 5H), 2.15-1.85 (br, 1H), 1.84-1.45 (br 4H), 1.41 (s, 9H), 1.34-1.25 (m, 3H), 1.24-0.99 (br, 6H), 0.96-0.68 (br, 3H).  **$^{13}\text{C}$  NMR** (125 MHz,  $\text{DMSO}-d_6$ )  $\delta$  170.2 (169.7, 169.1\*), 158.8 (158.6\*), 155.5 (155.2, 154.9\*), 143.5, 142.1 (141.4\*), 130.2, 129.5 (129.0\*), 127.4 (127.3\*), 114.9, 113.8 (113.6\*), 112.88 (112.80\*), 111.7, 83.7, 82.8, 78.4, 77.9 (77.7\*), 75.3, 74.9, 72.4, 72.0, 71.9, 71.7, 71.6, 70.4, 69.5, 69.3, 68.4, 65.8, 55.0, 53.6, 51.4, 50.7, 47.6, 47.0, 42.3, 38.5, 35.7, 34.5, 34.3, 33.7, 33.1, 29.9, 29.7, 29.1, 28.5, 28.1 (28.0\*), 18.7, 18.4, 18.0, 17.7, 17.3, 15.7, 14.8, 14.6, 13.0, 12.0, 11.8. **HRMS (ESI)** calcd for  $\text{C}_{35}\text{H}_{53}\text{N}_3\text{O}_7$   $[\text{M} + \text{H}]^+$ : 628.3956. Found: 628.3987.



**Preparation of Allyl-(((2*S*,8*R*,9*R*)-14-((((9*H*-fluoren-9-yl)methoxy)carbonyl)amino)-11-((*S*)-1-hydroxypropan-2-yl)-2,9-dimethyl-12-oxo-2,3,4,5,6,8,9,10,11,12-decahydrobenzo[*b*][1,9,5]dioxazacyclotetradecin-8-yl)methyl)(methyl)carbamate (**13**):** To a solution of the crude product **10** (9.04 g, 14.4 mmol) dissolved in dioxane (386 ml) at 0 °C, was added 10% NaHCO<sub>3</sub> solution (40 ml) and fluorenylmethyloxycarbonyl chloride (Fmoc-Cl; 5.40 g, 20.9 mmol, 1.5 equiv). The reaction was stirred, slowly warming to room temperature for 15 hours, after which LC/MS analysis showed that the reaction was complete. The reaction was quenched with NH<sub>4</sub>Cl solution (200 ml), and extracted EtOAc (3 x 100 ml). The combined organic extracts were dried over MgSO<sub>4</sub> or Na<sub>2</sub>SO<sub>4</sub>, filtered, and concentrated under reduced pressure. Purification of the crude residue by flash chromatography provided 11.16 g (91% over two steps) of pure Fmoc-protected product **11** as a foamy white solid.

To a solution of Fmoc-protected macrocycle **11** (34.0 g, 40.0 mmol, 1.0 equiv) in CH<sub>2</sub>Cl<sub>2</sub> (800 ml) at 0 °C was added 2,6-lutidine (18.63 ml, 160 mmol, 4.0 equiv) followed by tert-butyldimethylsilyl triflate (23.0 ml, 100 mmol, 2.5 equiv). The reaction was stirred for 2 hours while warming to room temperature. The reaction was then re-cooled to 0 °C, and more 2,6-lutidine (18.63 ml, 160 mmol, 4.0 equiv) was added (to quench the triflic acid byproduct), followed by the addition of saturated aqueous NH<sub>4</sub>Cl solution slowly. The reaction was extracted with CH<sub>2</sub>Cl<sub>2</sub> (3 x 300 ml), and the combined organic layers were dried over MgSO<sub>4</sub>, filtered, and concentrated under reduced pressure. The crude residue was then dissolved in THF (800 ml) at room temperature in a plastic bottle, and pyridine hydrofluoride (70%, 4.97 ml, 40.0 mmol, 1.0 equiv) was added. The reaction was stirred at room temperature until LC analysis showed complete conversion to the desired product. The reaction was quenched with saturated aqueous NH<sub>4</sub>Cl solution, the layers were separated, and the aqueous layer was extracted EtOAc (3 x 200 ml). The combined organic layers were dried over MgSO<sub>4</sub>, filtered, and concentrated under reduced pressure to provide the crude amine, which was used in the next step without further purification. The crude intermediate was dissolved in THF (200 ml), and cooled to 0 °C. Pyridine (12.9 ml, 160 mmol, 4.0 equiv) and allyl chloroformate (12.8 ml, 120 mmol, 3.00 equiv) were added sequentially, and the mixture was stirred for 10 minutes before warming to room temperature. The reaction was stirred for 16 hours during which it turned bright orange in color, and the starting material was no longer visible by LC/MS. The reaction was quenched with NH<sub>4</sub>Cl solution, the layers were separated, and the aqueous layer was extracted with EtOAc (3 x 100 ml). The combined organics were dried, filtered, and concentrated under reduced pressure, and the crude material was purified by flash chromatography to provide 28.0 g (84% over 2 steps) of the pure Alloc-protected macrocycle **12** as a white solid.

To a solution of the Alloc-protected compound **12** (28.0 g, 33.6 mmol, 1.0 equiv) in CH<sub>2</sub>Cl<sub>2</sub> (336 ml) and pH 7 buffer (35 ml) at 0 °C was added dichlorodicyanobenzoquinone (DDQ) (9.15 g, 40.3 mmol, 1.2 equiv) slowly. The reaction was stirred for 15 hours, slowly warming to room temperature until analysis of the reaction showed complete conversion to product. The reaction was quenched with saturated aqueous NaHCO<sub>3</sub> solution, and the layers were quickly separated to avoid a difficult emulsion. The aqueous layer was extracted with CH<sub>2</sub>Cl<sub>2</sub> (3 x 100 ml), and the combined organic layers were washed with NaHCO<sub>3</sub> solution, dried over MgSO<sub>4</sub>, filtered, and concentrated. The crude residue was purified by flash chromatography, which 22.0 g (92%) of the pure product **13** as a white solid. (*S,R,R,S*)-**13**: IR (cm<sup>-1</sup>) 3400 (br w), 3290 (br w), 2938 (w), 1684 (m), 1608 (m), 1541 (m), 1493 (m), 1450 (m), 1219 (s), 1058 (m). <sup>1</sup>H NMR (500 MHz, DMSO-*d*<sub>6</sub>, 130 °C) δ 9.03 (s, 1H), 7.95-7.82 (m, 3H), 7.82-7.65 (m, 2H), 7.65-7.55 (m, 1H), 7.48-7.24 (m, 3H), 6.92 (d, *J* = 9.0, 1H), 6.72 (d, *J* = 10.0, 1H), 6.60 (d, *J* = 10.0, 1H), 6.21 (s, 1H), 6.03-5.84 (m, 1H), 5.38-5.09 (m, 2H), 4.65-4.45 (m, 4H), 4.30 (t, *J* = 6.7, 1H), 4.28-4.18 (m, 2H), 4.13-4.02 (m, 1H), 3.90-3.55 (m, 4H), 3.52-3.22 (m, 2H), 3.20-2.70 (m, 4H), 2.52-2.48 (m,

1H), 2.27-2.19 (m, 1H), 1.99 (s, 1H), 1.86-1.48 (m, 4H), 1.42-1.16 (m, 5H), 0.86-0.68 (m, 4H). <sup>13</sup>C NMR (125 MHz, DMSO-*d*<sub>6</sub>, 130 °C) δ 169.3, 155.0, 153.0, 144.7, 143.3, 142.3, 140.2, 138.9, 137.0, 134.2, 133.0, 132.7, 128.5, 128.0, 126.8, 126.4, 126.2, 126.2, 125.9, 124.3, 124.3, 123.3, 122.9, 120.4, 120.1, 119.2, 119.0, 118.8, 115.7, 115.3, 114.8, 113.0, 111.2, 107.8, 81.7, 74.9, 73.3, 68.2, 65.4, 65.2, 64.3, 63.4, 63.2, 55.2, 54.8, 49.8, 46.4, 42.3, 38.1, 34.7, 33.7, 33.1, 28.7, 28.0, 19.7, 18.3, 17.8, 14.3, 13.6, 13.2, 11.3. **HRMS (ESI)** calcd for C<sub>41</sub>H<sub>52</sub>N<sub>3</sub>O<sub>8</sub> [M + H]<sup>+</sup>: 714.3749. Found: 714.3742.

**Preparation of [(S)-2-((2S,8R,9R)-14-(((9H-fluoren-9-yl)methoxy)carbonyl)amino)-8-(((allyloxy)carbonyl)(methyl)amino)methyl)-2,9-dimethyl-12-oxo-3,4,5,6,9,10-hexahydrobenzo[b][1,9,5]dioxazacyclotetradecin-11(2H,8H,12H)-yl)propyl benzoate (14):** To a solution of alcohol **13** (2.00 g, 2.80 mmol) in dry CH<sub>2</sub>Cl<sub>2</sub> (23 ml) was added pyridine (2.3 ml, 28 mmol) followed by benzoyl chloride (0.98 ml, 8.4 mmol) under N<sub>2</sub> atmosphere at room temperature. The resulting mixture was stirred at room temperature for 1 h. The reaction was quenched with sat. aq. NaHCO<sub>3</sub> (30 ml) and diluted with CH<sub>2</sub>Cl<sub>2</sub> (30 ml). The phases were separated and the aq. layer was washed with CH<sub>2</sub>Cl<sub>2</sub> (3 x 20 ml). The combined organic phases were washed with water (2 x 20 ml), dried (Na<sub>2</sub>SO<sub>4</sub>), and the solvent evaporated. The crude residue was purified by flash chromatography on silica gel using EtOAc in hexanes to provide 1.92 g (84%) of the desired product **14** as a clear resin. <sup>1</sup>H NMR (300 MHz, CDCl<sub>3</sub>) δ 8.05 (d, 1H), 8.00 (d, 1H), 7.77 (d, 2H), 7.66-7.50 (m, 3H), 7.48 – 7.37 (m, 4H), 7.36-7.28 (m, 2H), 7.22-7.11 (m, 1H), 6.89-6.66 (m, 2H), 6.03-5.78 (m, 1H), 5.26 – 5.06 (m, 1H), 4.72-4.40 (m, 4H), 4.32-4.22 (m, 1H), 4.18 – 4.02 (m, 1H), 4.00-3.84 (m, 1H), 3.80-3.50 (m, 1H), 3.47 (d, 2H), 3.41 – 3.15 (m, 1H), 3.12-2.73 (m, 3H), 2.19 (m, 1H), 2.04 (m, 1H), 1.91-1.69 (m, 2H), 1.67-1.45 (m, 3H), 1.37-1.08 (m, 9H), 0.99-0.80 (m, 6H), 0.77 (m, 2H). **LRMS** calculated for C<sub>48</sub>H<sub>55</sub>N<sub>3</sub>O<sub>9</sub>: 818 [M+H]<sup>+</sup>. Found 818

**Preparation of (S)-2-((2S,8R,9R)-8-(((allyloxy)carbonyl)(methyl)amino)methyl)-2,9-dimethyl-12-oxo-14-(3-phenylureido)-3,4,5,6,9,10-hexahydrobenzo[b][1,9,5]dioxazacyclotetradecin-11(2H,8H,12H)-yl)propyl benzoate (15):** A mixture of Fmoc-protected aniline **14** (1.61 g, 1.968 mmol) and piperidine (0.390 ml, 3.94 mmol) in dry DMF (19.68 ml) was stirred under N<sub>2</sub> atmosphere at room temperature for 40 minutes. Then, phenyl isocyanate (0.209 ml, 1.914 mmol) was introduced to the reaction mixture, which was stirred at room temperature for 3 hours. The reaction was diluted with water/EtOAc (10 ml) and extracted with EtOAc (3 x 20 ml). The organic phase was separated, washed with water, brine, dried (Na<sub>2</sub>SO<sub>4</sub>), and evaporated to dryness. The crude residue was purified by flash chromatography on silica gel using MeOH in CH<sub>2</sub>Cl<sub>2</sub> to provide the desired product **15** (0.77 g, 60% over two steps). <sup>1</sup>H NMR (300 MHz, CDCl<sub>3</sub>) δ 8.06 (m, 1H), 8.04 – 7.89 (m, 1H), 7.81 (m, 1H), 7.59 (m, 2H), 7.51 – 7.30 (m, 2H), 7.23 (m, 2H), 6.96 (m, 1H), 6.82 (m, 1H), 6.69 (m, 1H), 5.89 (m, 1H), 5.45 – 5.08 (m, 2H), 4.83 (m, 1H), 4.55 (m, 3H), 4.18 – 4.02 (m, 1H), 3.93 (m, 2H), 3.50 (m, 1H), 3.34 (m, 1H), 3.26 – 2.95 (m, 3H), 2.88 (m, 3H), 2.26 (m, 1H), 2.04 (m, 1H), 1.77 (m, 2H), 1.62 (m, 2H), 1.38 (m, 3H), 1.24 (m, 5H), 1.14 – 1.00 (m, 2H), 0.99 – 0.85 (m, 2H), 0.77 (m, 2H). **LRMS** calculated for C<sub>40</sub>H<sub>50</sub>N<sub>4</sub>O<sub>8</sub>: 715 [M+H]<sup>+</sup>. Found 715.

**Preparation of (S)-2-((2S,8R,9R)-8-((4-fluoro-N-methylphenylsulfonamido)methyl)-2,9-dimethyl-12-oxo-14-(3-phenylureido)-3,4,5,6,9,10-hexahydrobenzo[b][1,9,5]dioxazacyclotetradecin-11(2H,8H,12H)-yl)propyl benzoate (16):** A mixture of Alloc-protected amine **15** (0.770 g, 1.08 mmol), 1,3-dimethylpyrimidine-2,4,6(1H,3H,5H)-trione (1.26 g, 8.08 mmol) and Pd(PPh<sub>3</sub>)<sub>4</sub> (0.249 g, 0.215 mmol) in dry CH<sub>2</sub>Cl<sub>2</sub> (15 ml) was stirred under a N<sub>2</sub> atmosphere at room temperature for 1 hour. The reaction mixture was diluted with CH<sub>2</sub>Cl<sub>2</sub> (30 ml) and washed with saturated NaHCO<sub>3</sub> (2 x 20 ml) and water (2 x 20 ml). The organic phase was separated, dried (Na<sub>2</sub>SO<sub>4</sub>), and the solvent evaporated. The crude product was then re-dissolved in dry CH<sub>2</sub>Cl<sub>2</sub> (10.8 ml), then 2,6-lutidine (0.878 ml, 7.54 mmol) was added, followed by 4-fluorobenzene-1-sulfonyl chloride (0.419 g, 2.154 mmol) under a N<sub>2</sub> atmosphere. The resulting mixture was stirred at room temperature for 15 hours. The reaction was diluted with CH<sub>2</sub>Cl<sub>2</sub> (25 ml) and washed with water (2 x 20 ml). The organic layer was separated, dried (Na<sub>2</sub>SO<sub>4</sub>), and the solvent evaporated. This material was chromatographed on silica gel, using a gradient of EtOAc in hexanes to give 0.53 g (62%) of the title product **16** as colorless resin. <sup>1</sup>H NMR (300 MHz, CDCl<sub>3</sub>) δ 8.11 – 7.84 (m, 2H), 7.79 (m, 1H), 7.62 (m, 3H), 7.37 (m, 2H), 7.34 – 7.16 (m, 2H), 7.04 (m, 4H), 6.87 – 6.63 (m, 2H), 6.52 (m, 1H), 4.89 – 4.48 (m, 1H), 4.45 – 4.18 (m, 1H), 4.06 (m, 1H), 3.77 (m, 2H), 3.50 (m, 1H), 3.35 (m, 1H), 2.94 (m, 2H), 2.64 (m, 5H), 1.88 (m, 1H), 1.56 (m, 2H), 1.43 (m, 2H), 1.31 (m, 4H), 1.04 (m, 3H), 0.88 (m, 2H), 0.75 (m, 1H), 0.60 (m, 2H), 0.37 (m, 1H). LRMS calculated for C<sub>42</sub>H<sub>49</sub>FN<sub>4</sub>O<sub>8</sub>S : 789 [M+H]<sup>+</sup>. Found 789.

**Preparation of 3-[(2S,8R,9R)-11-[(2S)-1-hydroxypropan-2-yl]-2,9-dimethyl-8-[[N-methyl(4-fluorobenzene)sulfonamido]methyl]-12-oxo-2,3,4,5,6,8,9,10,11,12-decahydro-1,7,11-benzodioxazacyclotetradecin-14-yl]-1-phenylurea (19):** To a solution of Bz-protected alcohol **16** (0.490 g, 0.621 mmol) in MeOH (12.4 ml) was added potassium carbonate (K<sub>2</sub>CO<sub>3</sub>; 0.472 g, 3.42 mmol) under a N<sub>2</sub> atmosphere. The suspension was stirred at room temperature for 15 hours. The reaction mixture was then quenched with saturated NH<sub>4</sub>Cl (20 ml) and extracted with EtOAc (2 x 20 ml). The organic phase was separated, washed with water and brine, dried (Na<sub>2</sub>SO<sub>4</sub>), and the solvent evaporated. This material was chromatographed on silica, using MeOH in CH<sub>2</sub>Cl<sub>2</sub> to afford the desired product **17** (0.40 g, 94%) as colorless resin. <sup>1</sup>H NMR (300 MHz, CDCl<sub>3</sub>) δ 7.95 – 7.51 (m, 3H), 7.39 (m, 1H), 7.34 – 7.07 (m, 5H), 7.07 – 6.91 (m, 1H), 6.91 – 6.60 (m, 2H), 4.65 (s, 1H), 4.33 (s, 1H), 3.93 (m, 4H), 3.56 (m, 2H), 3.10 (m, 2H), 2.96 – 2.55 (m, 5H), 2.47 – 2.27 (m, 1H), 2.04 (m, 1H), 1.64 (m, 3H), 1.47 (m, 4H), 1.38 – 1.22 (m, 2H), 1.22 – 1.09 (m, 3H), 1.09 – 0.90 (m, 2H), 0.79 (m, 2H). LRMS calculated for C<sub>35</sub>H<sub>45</sub>FN<sub>4</sub>O<sub>7</sub>S : 685 [M+H]<sup>+</sup>. Found 685.

**Preparation of N-(((2S,8R,9R)-11-((S)-1-azidopropan-2-yl)-2,9-dimethyl-12-oxo-14-(3-phenylureido)-2,3,4,5,6,8,9,10,11,12-decahydrobenzo[b][1,9,5]dioxazacyclotetradecin-8-yl)methyl)-4-fluoro-N-methylbenzenesulfonamide (18):** To a solution of alcohol **17** (0.401 g, 0.586 mmol) in dry THF (2.9 ml) under N<sub>2</sub> was added 2,3,4,6,7,8,9,10-octahydropyrimido[1,2-a]azepine (0.265 ml, 1.76 mmol) followed by diphenyl phosphorazidate (DPPA; 0.189 ml, 0.878 mmol). The reaction mixture was stirred for 16 hours, then concentrated and chromatographed on silica, using MeOH/CH<sub>2</sub>Cl<sub>2</sub> to afford the desired product **18** (0.36 g, 87%) as a colorless resin. <sup>1</sup>H NMR (300 MHz, CDCl<sub>3</sub>) δ 8.24 – 7.64 (m, 2H), 7.57 – 7.33 (m, 2H), 7.31 – 7.05 (m, 4H), 7.03 – 6.77 (m, 3H), 6.77 – 6.53 (m, 1H), 4.67 – 4.27 (m, 3H), 4.23 – 4.09 (m, 1H), 4.01 – 3.84 (m, 2H), 3.83 – 3.61 (m, 4H), 3.61 – 3.29 (m, 2H), 3.25 – 3.02 (m, 2H), 3.06 – 2.55 (m, 4H), 2.27 – 1.94 (m, 1H), 1.92 – 1.32 (m, 6H), 1.30 – 1.14 (m, 3H), 1.14 – 1.01 (m, 2H), 0.98 – 0.85 (m, 1H), 0.83 – 0.62 (m, 1H). **LRMS (ESI)** calcd for C<sub>35</sub>H<sub>44</sub>FN<sub>7</sub>O<sub>6</sub>S [M + H]<sup>+</sup>: 710.3. Found: 710.0.

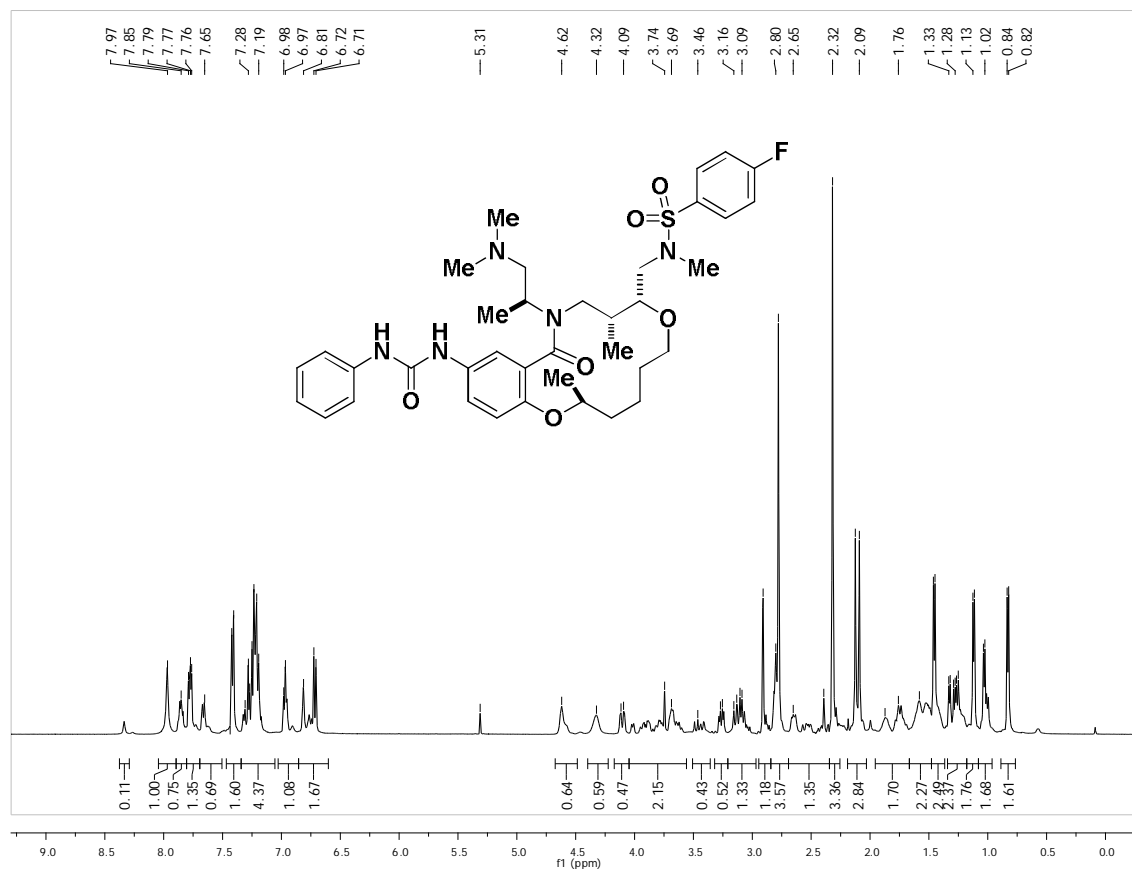
**Preparation of N-(((2S,8R,9R)-11-((S)-1-aminopropan-2-yl)-2,9-dimethyl-12-oxo-14-(3-phenylureido)-2,3,4,5,6,8,9,10,11,12-decahydrobenzo[b][1,9,5]dioxazacyclotetradecin-8-yl)methyl)-4-fluoro-N-methylbenzenesulfonamide (19):** To a solution of azide **18** (0.33 g, 0.47 mmol) in THF (15 ml) and H<sub>2</sub>O (0.9 ml) was added triphenylphosphine (PPh<sub>3</sub>) (0.305 g, 1.16 mmol). The reaction mixture was stirred 16 hours, then diluted with EtOAc (30 ml), dried (Na<sub>2</sub>SO<sub>4</sub>), and the solvent evaporated. This material was chromatographed on silica, using MeOH/CH<sub>2</sub>Cl<sub>2</sub> to afford the 0.25 g (79%) of **19** as a colorless resin. <sup>1</sup>H NMR (300 MHz, CDCl<sub>3</sub>) δ 8.96 – 8.20 (m, 2H), 7.92 – 7.65 (m, 2H), 7.58 – 7.33 (m, 2H), 7.33 – 7.05 (m, 4H), 7.08 – 6.85 (m, 1H), 6.84 – 6.62 (m, 1H), 4.73 – 4.32 (m, 1H), 4.16 – 3.53 (m, 4H), 3.48 – 3.24 (m, 1H), 3.21 – 2.92 (m, 4H), 2.91 – 2.79 (m, 2H), 2.80 – 2.51 (m, 4H), 2.31 – 1.89 (m, 2H), 1.89 – 1.37 (m, 6H), 1.37 – 1.14 (m, 6H), 1.10 – 0.89 (m, 2H), 0.67 – 0.32 (m, 2H). **LRMS (ESI)** calcd for Chemical Formula: C<sub>35</sub>H<sub>46</sub>FN<sub>5</sub>O<sub>6</sub>S [M + H]<sup>+</sup>: 684.3. Found: 684.5.

**Preparation of N-(((2S,8R,9R)-11-((S)-1-(dimethylamino)propan-2-yl)-2,9-dimethyl-12-oxo-14-(3-phenylureido)-2,3,4,5,6,8,9,10,11,12-decahydrobenzo[b][1,9,5]dioxazacyclotetradecin-8-yl)methyl)-4-fluoro-N-methylbenzenesulfonamide (20):** To a solution of amine **19** (223 mg, 0.326 mmol) in dry CH<sub>2</sub>Cl<sub>2</sub> (6.5 ml) was added formaldehyde (37% in water, 0.146 ml, 1.96 mmol) followed by MgSO<sub>4</sub> (471 mg, 3.91 mmol). The mixture was stirred for 1 hour, then sodium triacetoxyborohydride (691 mg, 3.26 mmol) was added and the mixture stirred for 16 hours. The mixture was diluted with water (25 ml) and CH<sub>2</sub>Cl<sub>2</sub> (30 ml), the phases separated, and the aqueous phase was extracted with CH<sub>2</sub>Cl<sub>2</sub> (2 x 20 ml). The combined organic phases were washed with water, dried (Na<sub>2</sub>SO<sub>4</sub>), and the solvent evaporated. This material was chromatographed on silica gel, using a gradient of MeOH in CH<sub>2</sub>Cl<sub>2</sub> to afford the probe **20** in 93% purity as a colorless resin. Additional purification by preparative HPLC yielded product >99 % purity (73.1 mg, 31% yield).

<sup>1</sup>H NMR (500 MHz, CDCl<sub>3</sub>) δ 7.97 (s, 1H), 7.89 – 7.82 (m, 1H), 7.80 – 7.73 (m, 1H), 7.70 – 7.60 (m, 1H), 7.47 – 7.35 (m, 2H), 7.34 – 7.11 (m, 4H), 7.03 – 6.87 (m, 1H), 6.85 – 6.65 (m, 2H), 4.67 – 4.47 (m, 1H), 4.46 – 4.20 (m, 1H), 4.19 – 3.97 (m, 1H), 3.96 – 3.54 (m, 2H), 3.52 – 3.34 (m, 1H), 3.33 – 3.18 (m, 1H), 3.17 – 2.99 (m, 1H), 2.91 (s, 1H), 2.84 – 2.69 (m, 4H), 2.69 – 2.35 (m, 1H), 2.32 (s, 3H), 2.19 – 2.01 (m, 3H), 1.96 – 1.65 (m, 2H), 1.64 – 1.48 (m, 2H), 1.48 – 1.34 (m, 3H), 1.35 – 1.18 (m, 2H), 1.18 – 1.07 (m, 2H), 1.7 – 0.92 (m, 2H), 0.91 – 0.75 (m, 2H). <sup>13</sup>C NMR (125 MHz, CDCl<sub>3</sub>) δ 172.7, 172.4, 166.0, 164.0, 153.3, 147.5, 139.4, 133.3, 130.0, 128.8, 128.6, 126.1, 122.1, 119.8, 119.4, 119.0, 118.8, 116.6, 116.4, 116.2, 113.4, 111.9, 83.2, 74.3, 71.6, 71.2, 69.8, 69.4, 68.4, 63.6, 63.1, 62.7, 53.6, 53.1, 51.9, 51.2, 51.0, 50.7, 50.4, 46.4, 46.0, 45.8, 45.2, 43.4, 43.1, 40.8, 38.4, 37.3, 36.7, 34.6, 34.4, 30.5, 29.3, 28.8, 18.4, 18.3, 18.2, 17.9, 17.2, 16.9, 15.8, 14.7, 13.6, 12.7. **HRMS (ESI)** calcd for Chemical Formula: C<sub>37</sub>H<sub>50</sub>FN<sub>5</sub>O<sub>6</sub>S [M + H]<sup>+</sup>: 712.3539. Found: 712.3511.

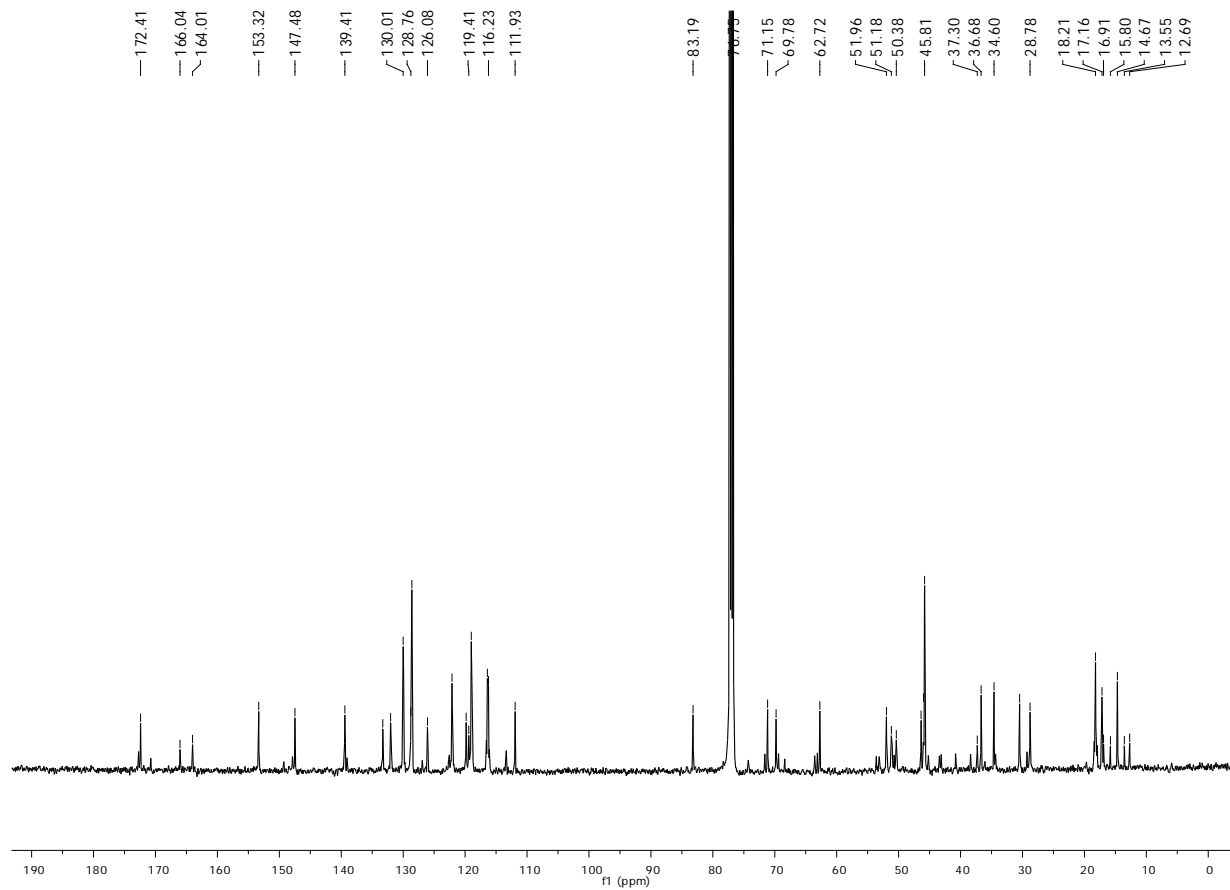
## Appendix D: NMR and LC Data of Probe and Analogs

### <sup>1</sup>H NMR Spectrum (CDCl<sub>3</sub>, 500 MHz) of the Probe (ML238)

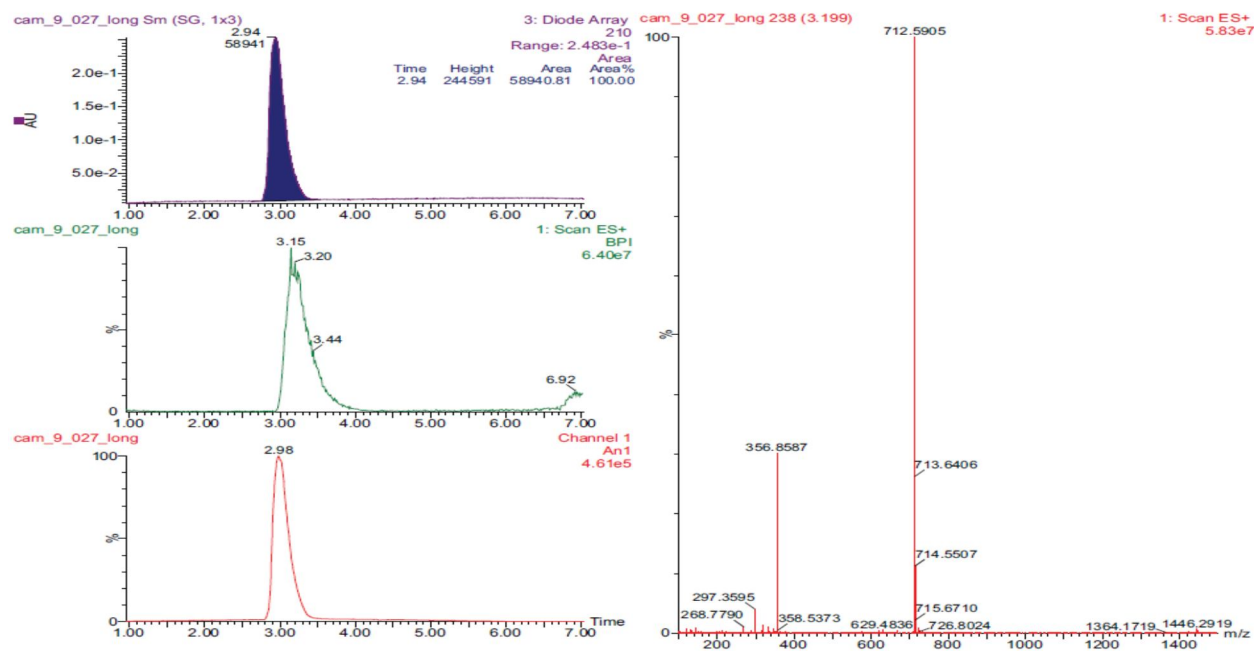




**$^{13}\text{C}$  NMR Spectrum ( $\text{CDCl}_3$ , 500 MHz) of the Probe (ML238)**



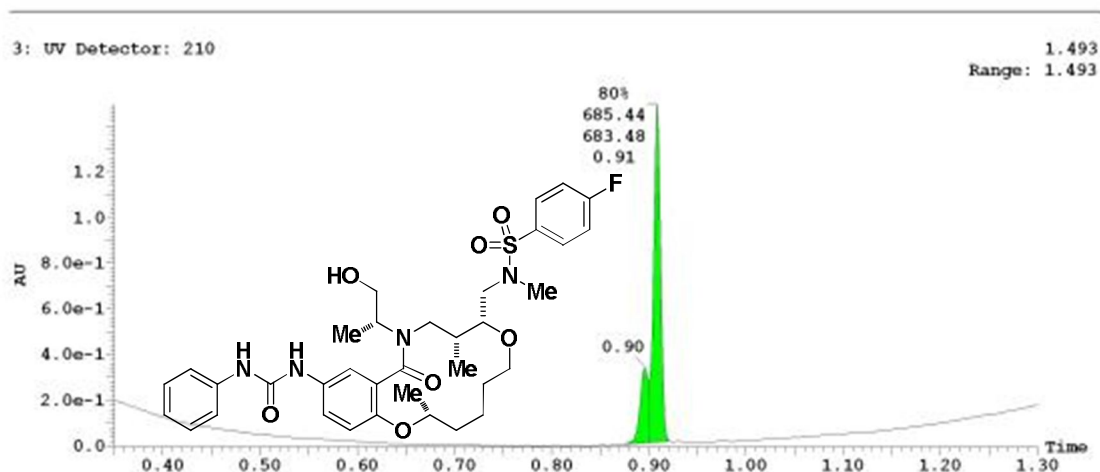
# LCMS Chromatogram of the Probe (ML238) showing 100% purity



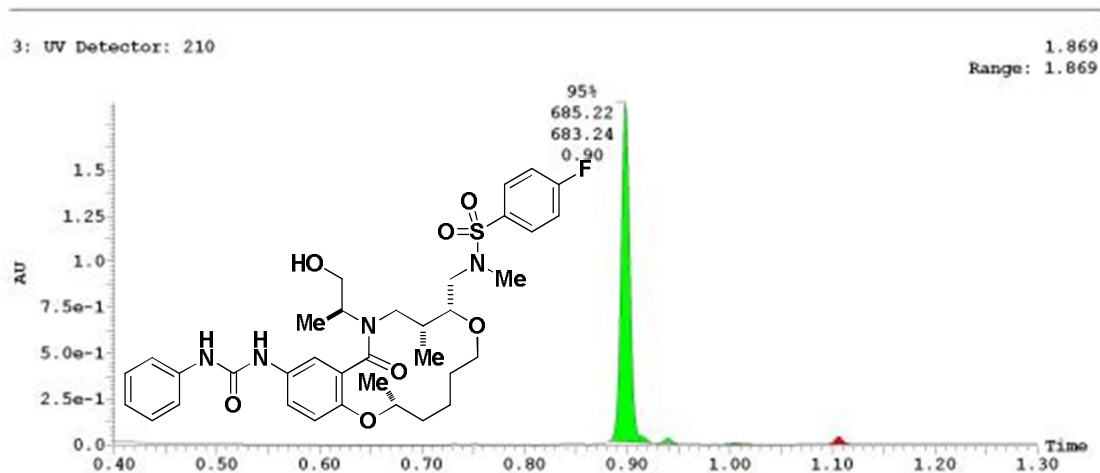


## Spectroscopic Data for Analogs

### UPLC Chromatogram of Analog CID 49849936



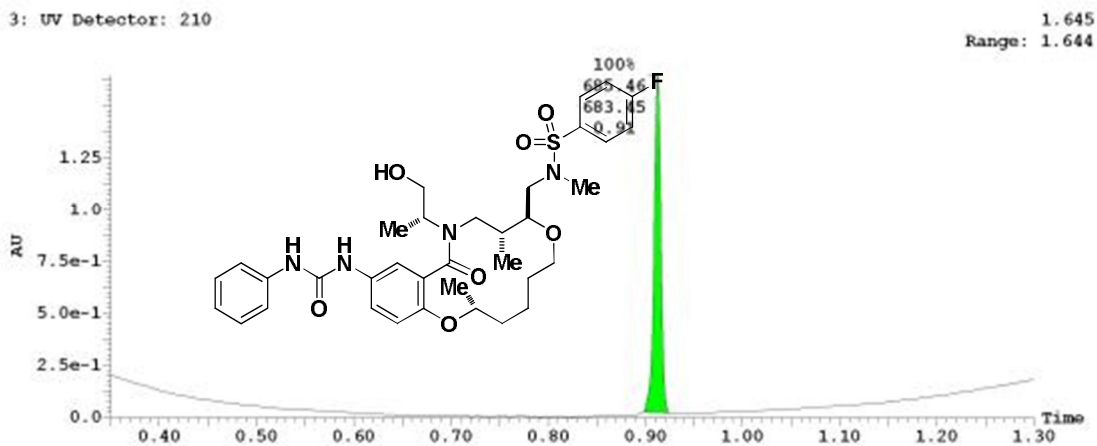
### UPLC Chromatogram of Analog CID 44487559



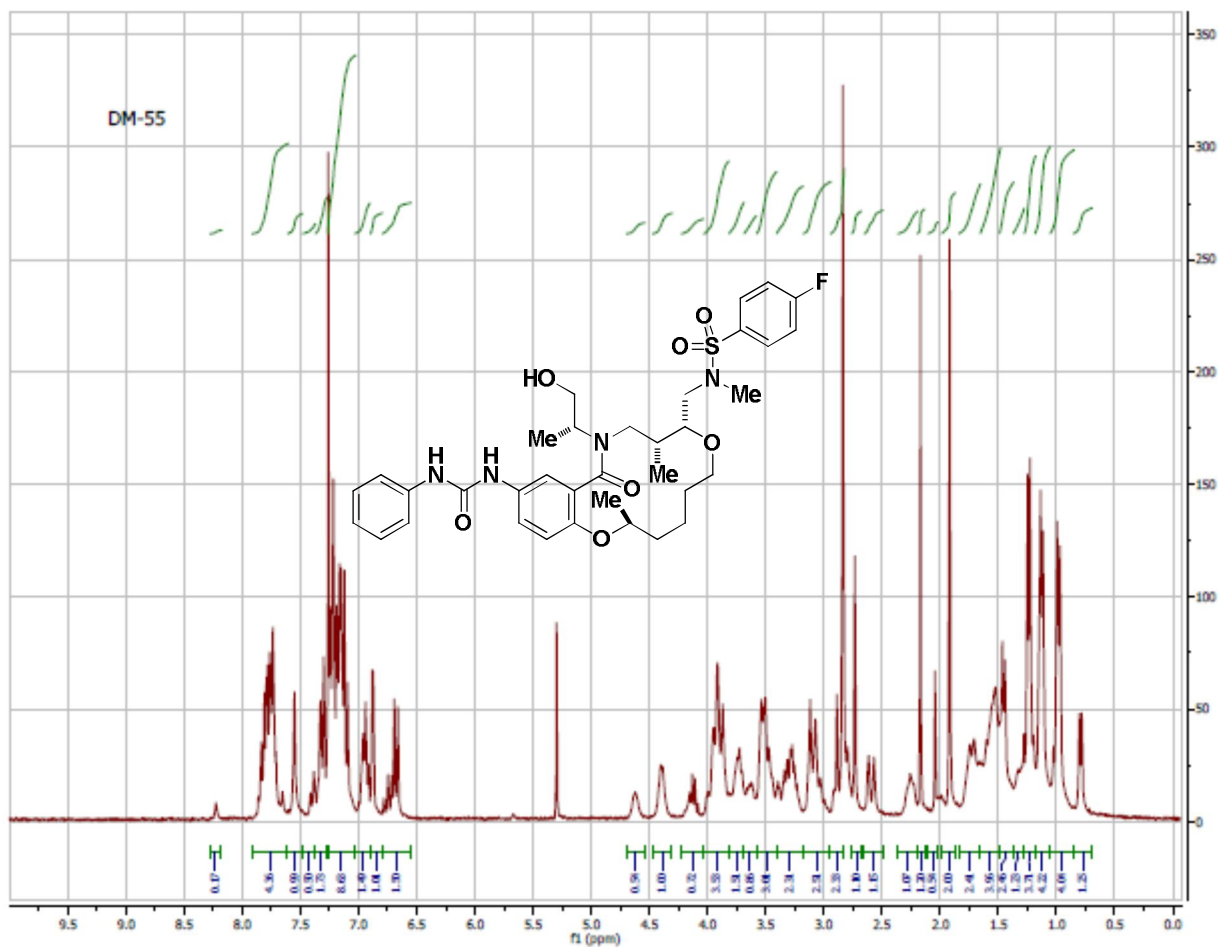
### UPLC Chromatogram of Analog CID 44489738



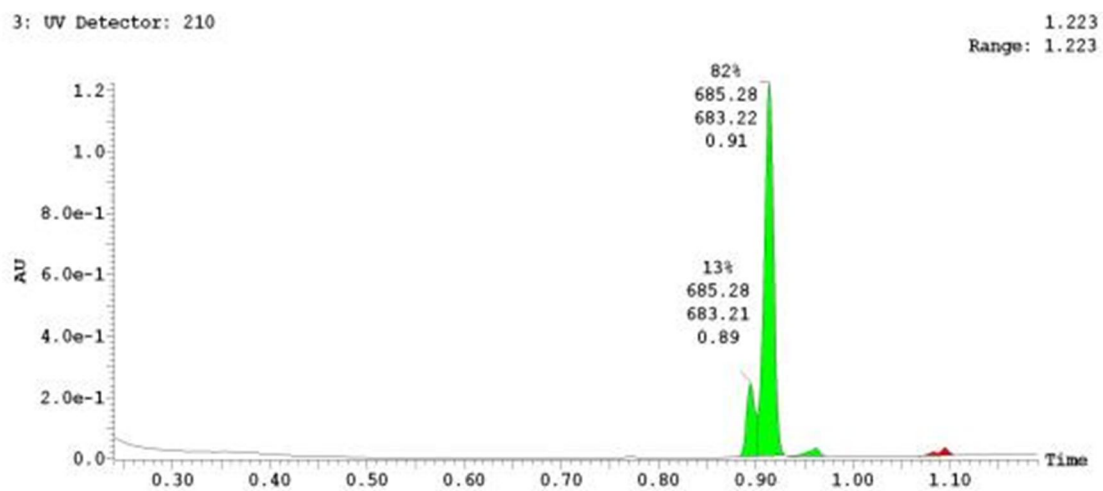
### UPLC Chromatogram of Analog CID9849919



**$^1\text{H}$  NMR Spectrum (300 MHz,  $\text{CDCl}_3$ ) of Analog CID 44483977**

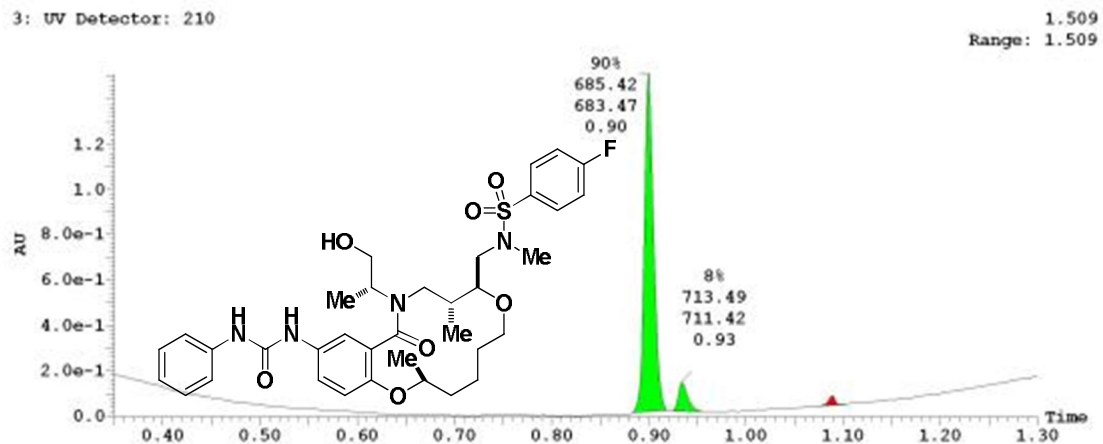


**UPLC Chromatogram of Analog CID 44483977**

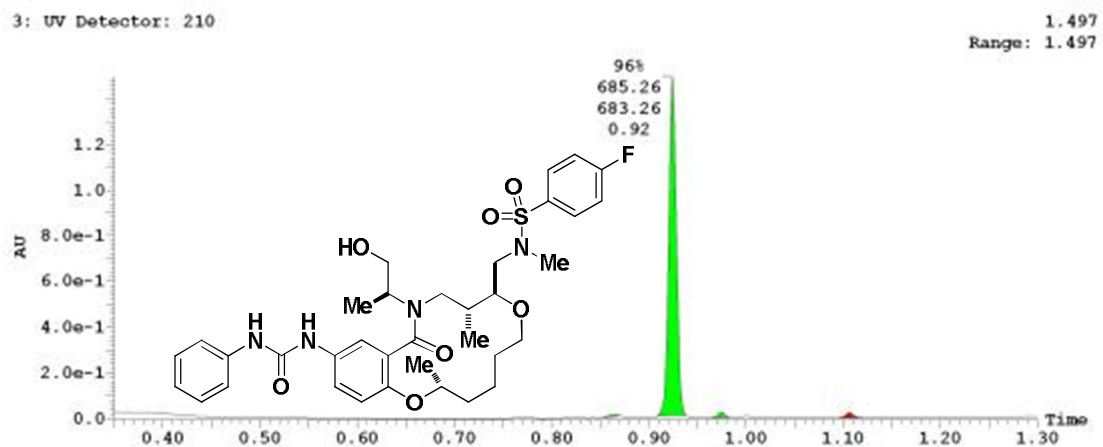




### UPLC Chromatogram of Analog CID 44485781

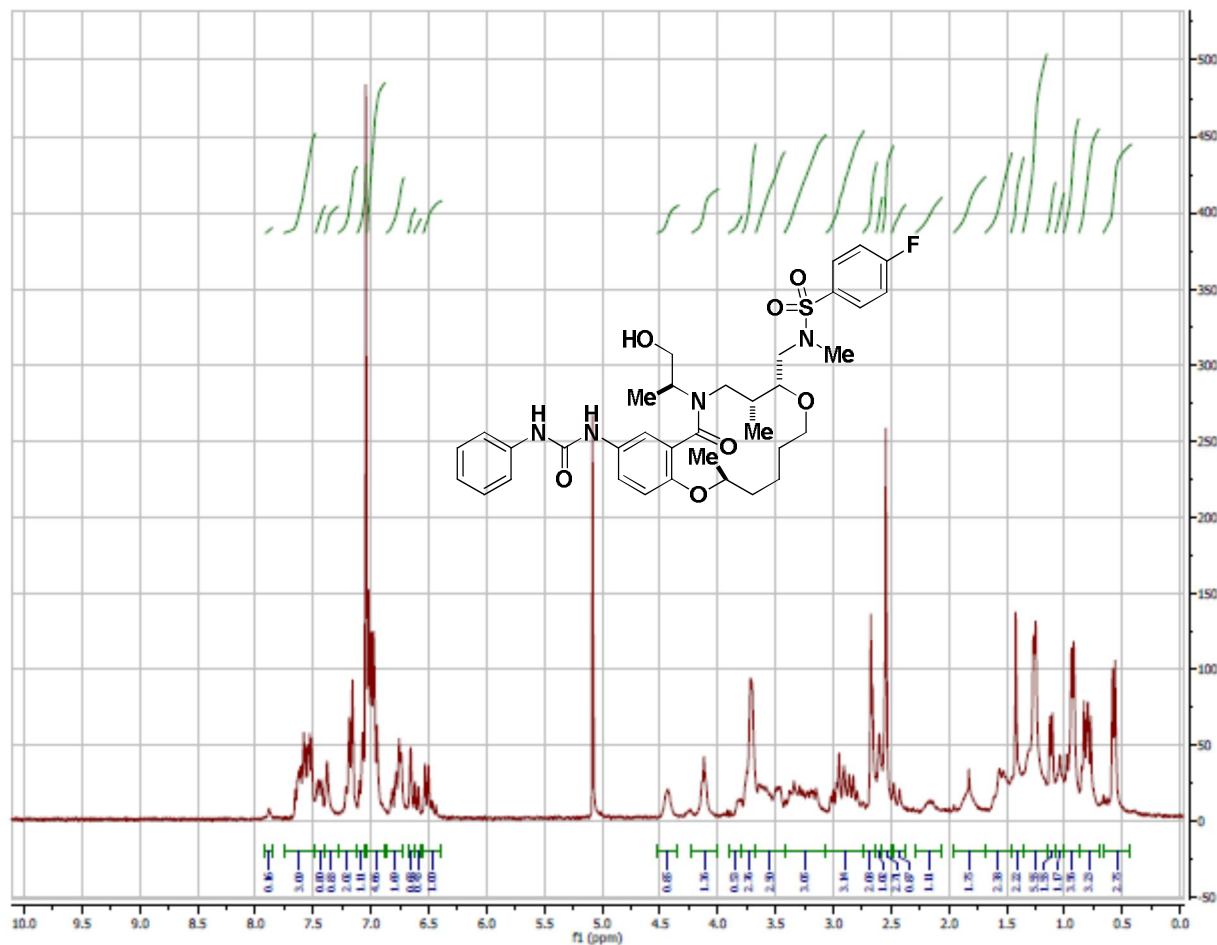


### UPLC Chromatogram of Analog CID 44486410

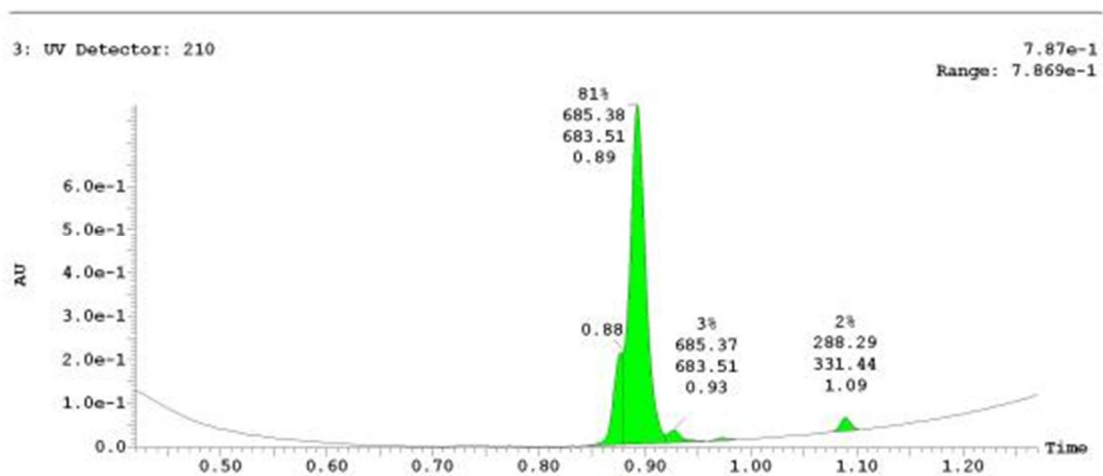




<sup>1</sup>H NMR Spectrum (300 MHz, CDCl<sub>3</sub>) of Analog CID 44487502

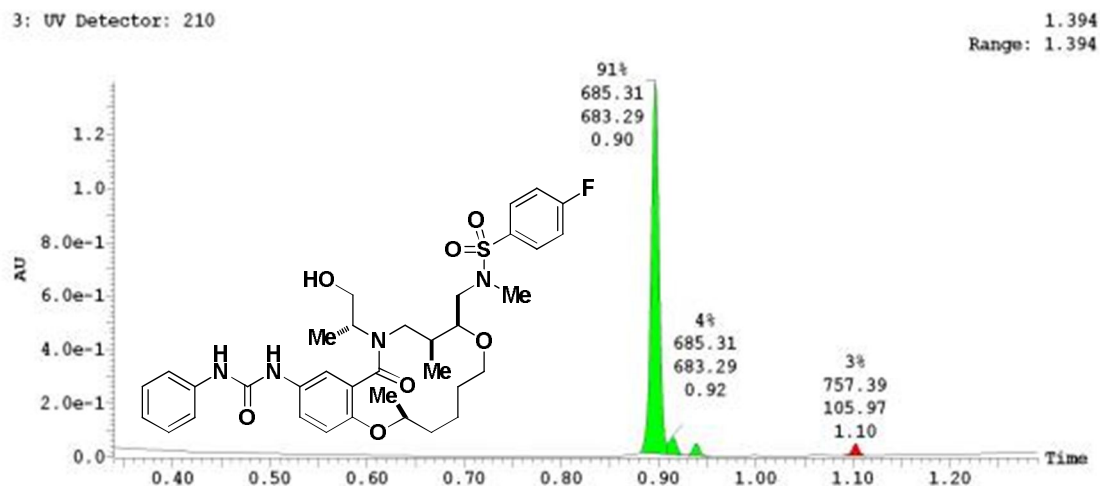


UPLC Chromatogram of Analog CID 44487502

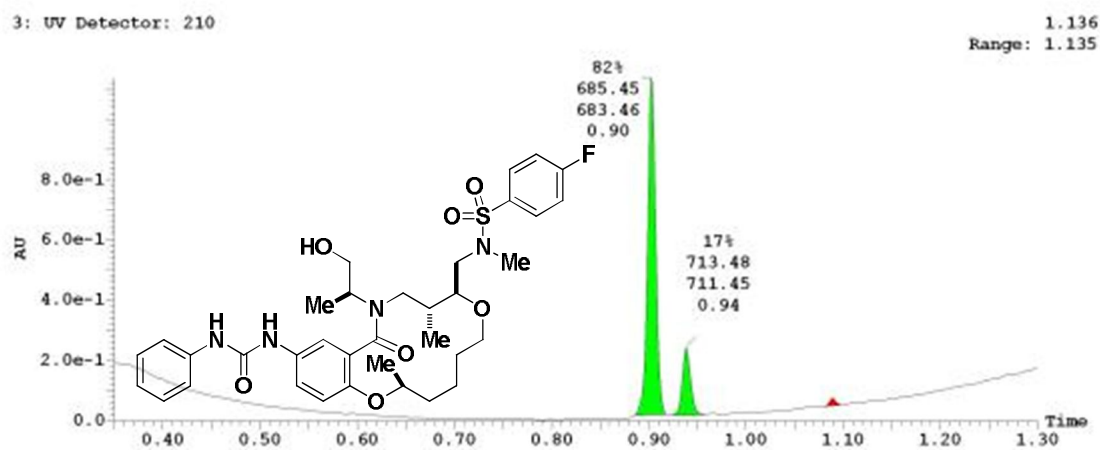




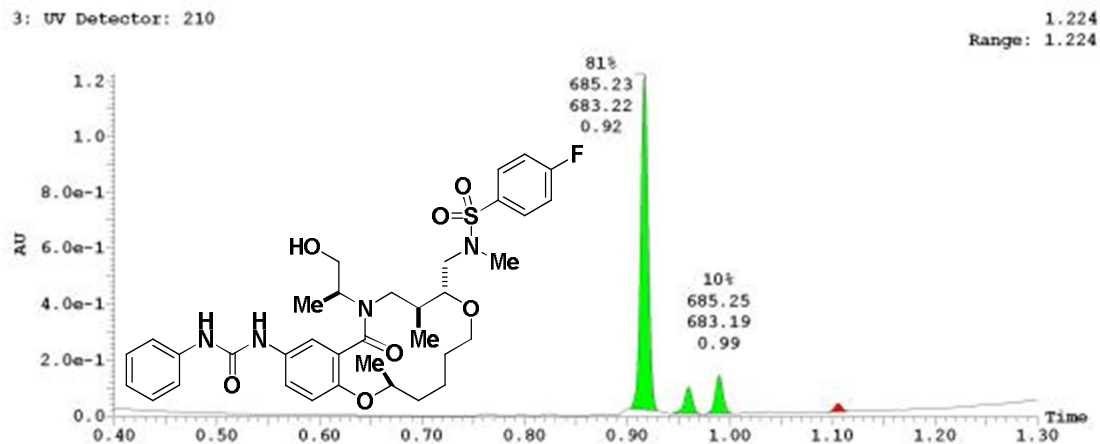
### UPLC Chromatogram of Analog CID 44487483



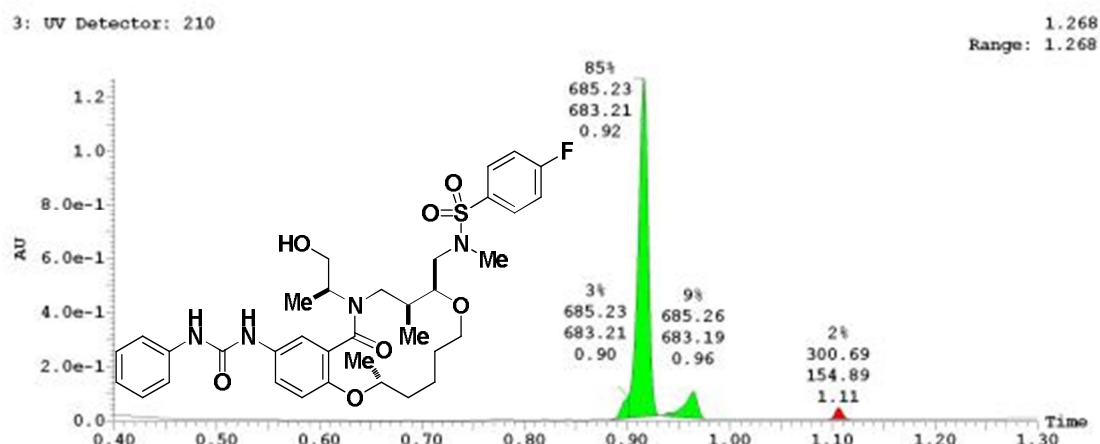
### UPLC Chromatogram of Analog CID 44486382



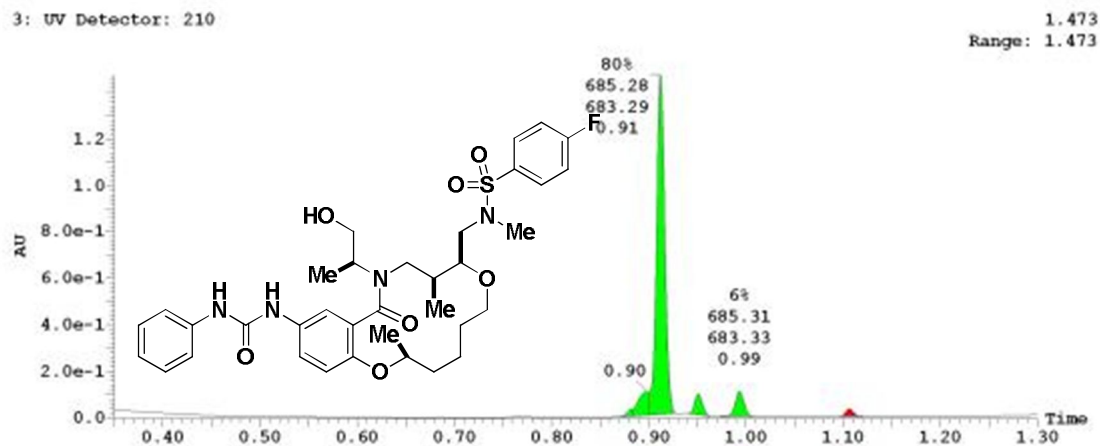
### UPLC Chromatogram of Analog CID 44488751



### UPLC Chromatogram of Analog CID 44487451



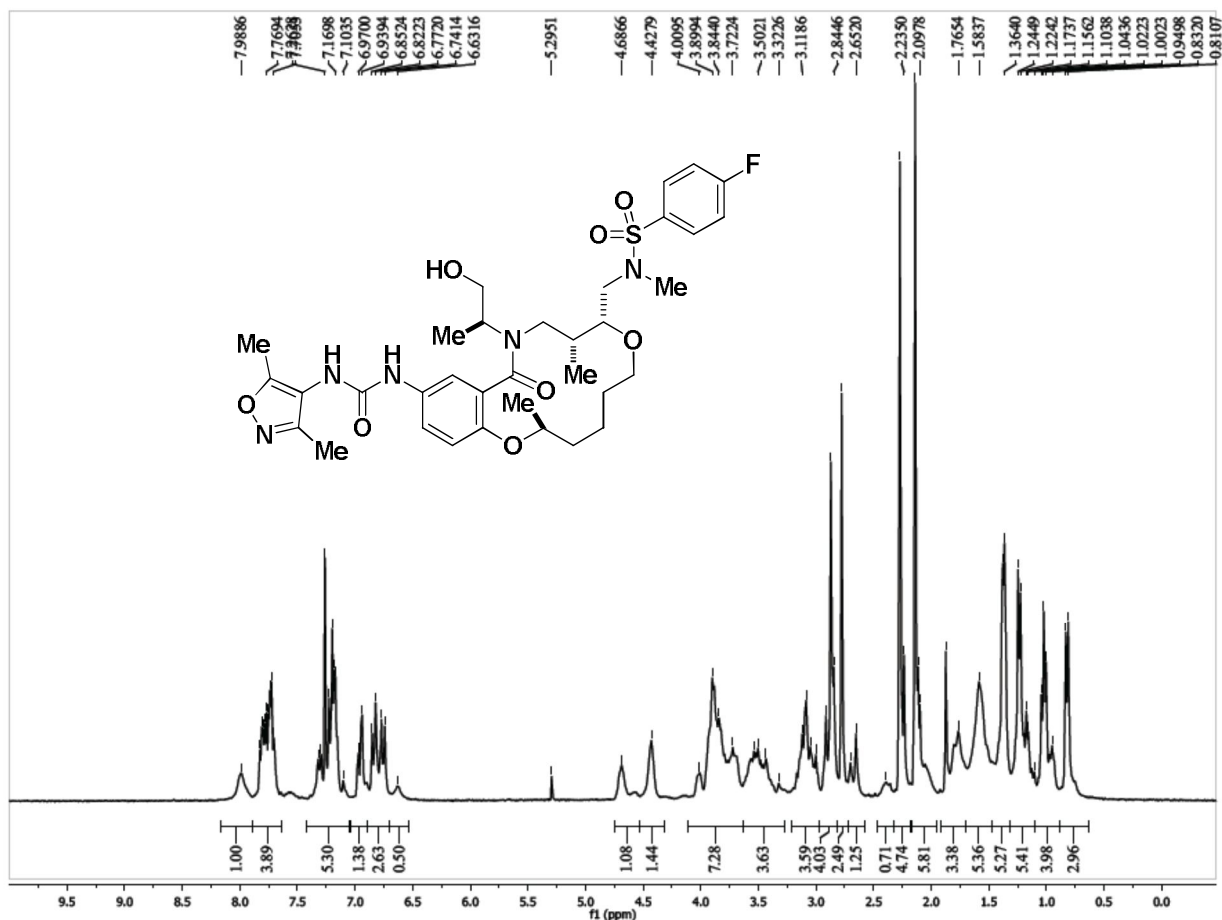
### UPLC Chromatogram of Analog CID44485115



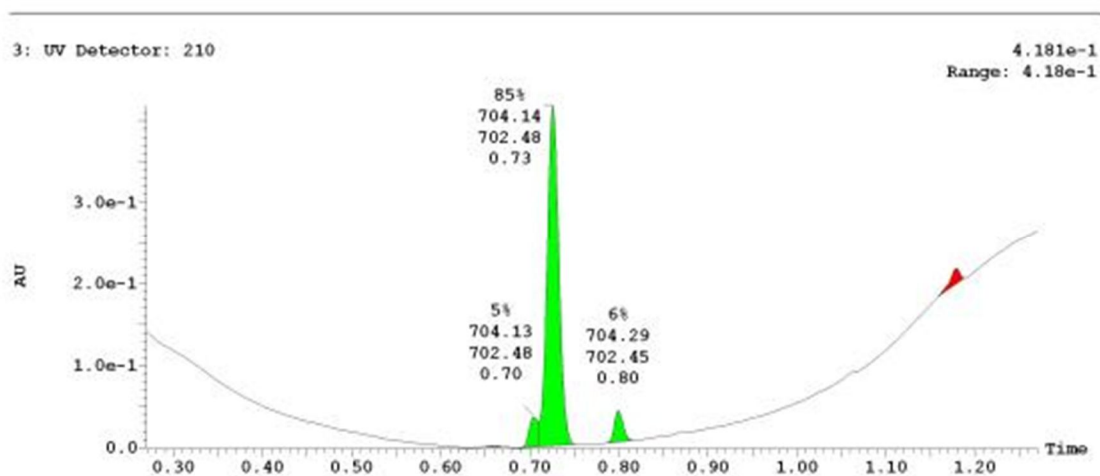




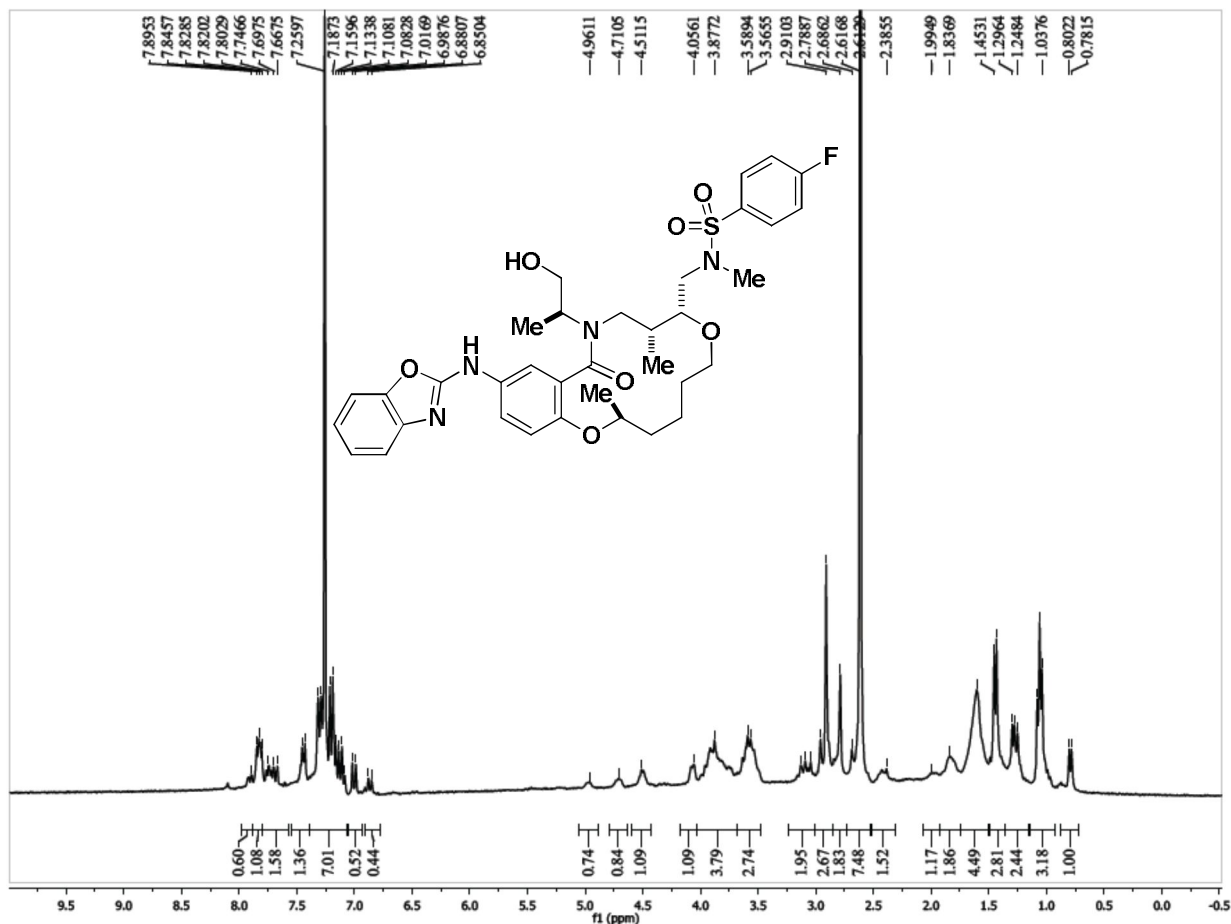
<sup>1</sup>H NMR Spectrum (300 MHz, CDCl<sub>3</sub>) of Analog CID 49843020



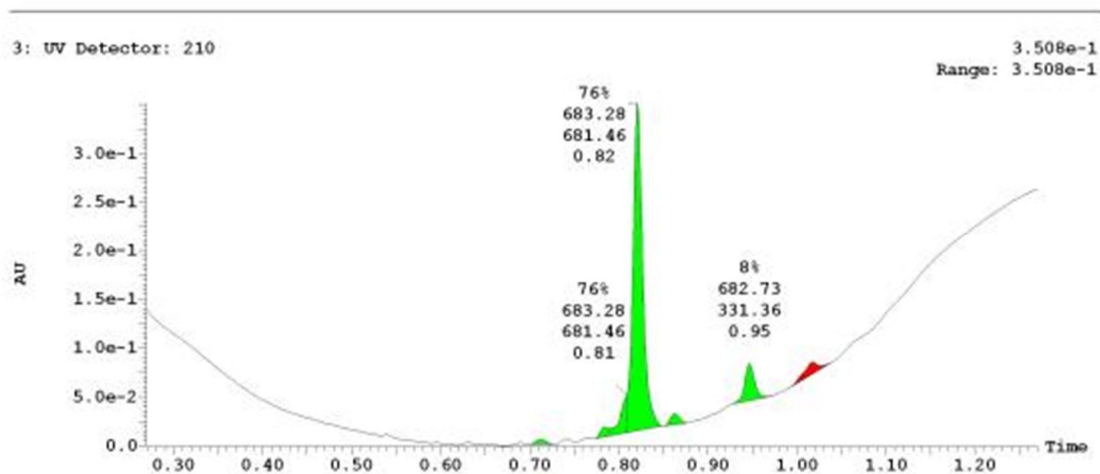
UPLC Chromatogram of Analog CID 49843020



<sup>1</sup>H NMR Spectrum (300 MHz, CDCl<sub>3</sub>) of Analog CID 49849904

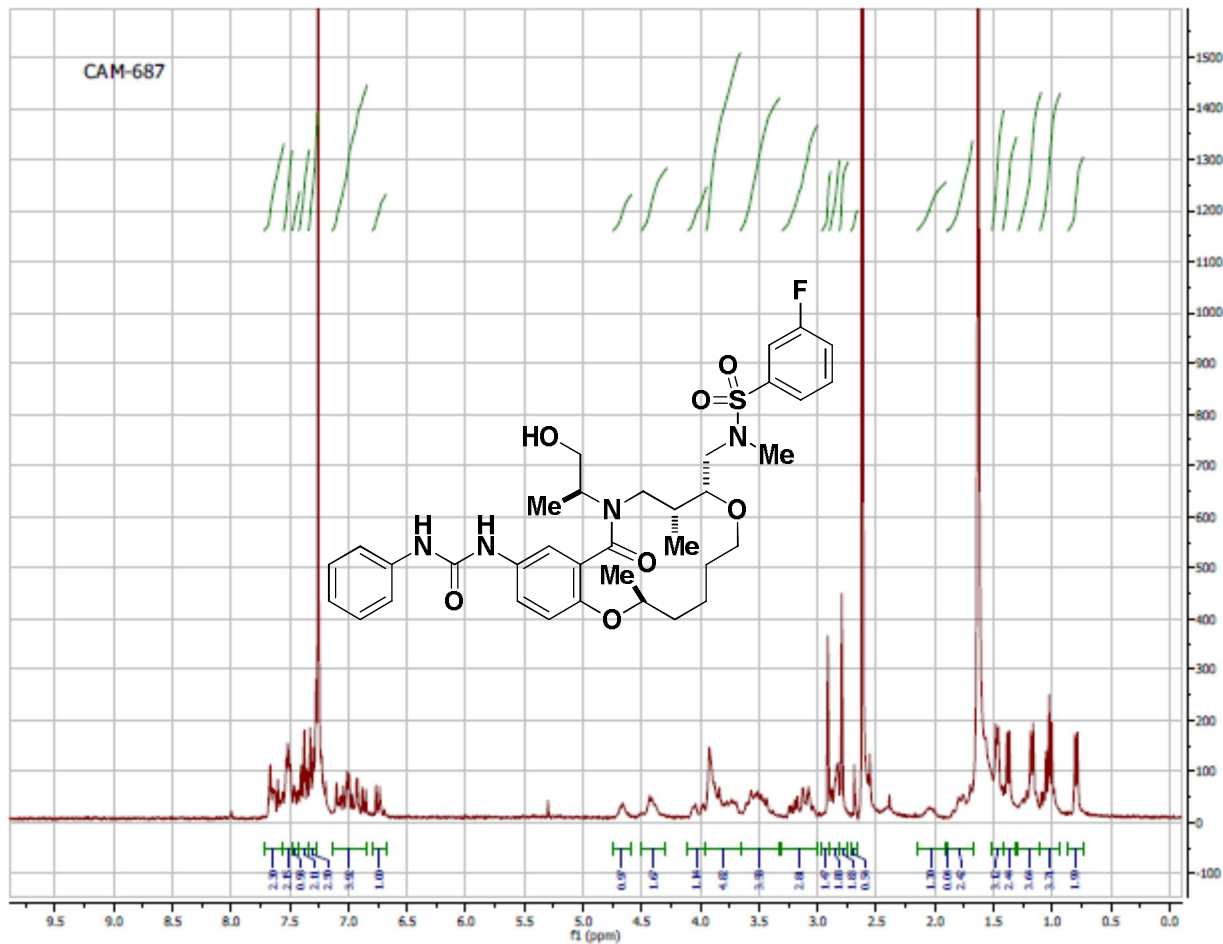


UPLC Chromatogram of Analog CID 49849904





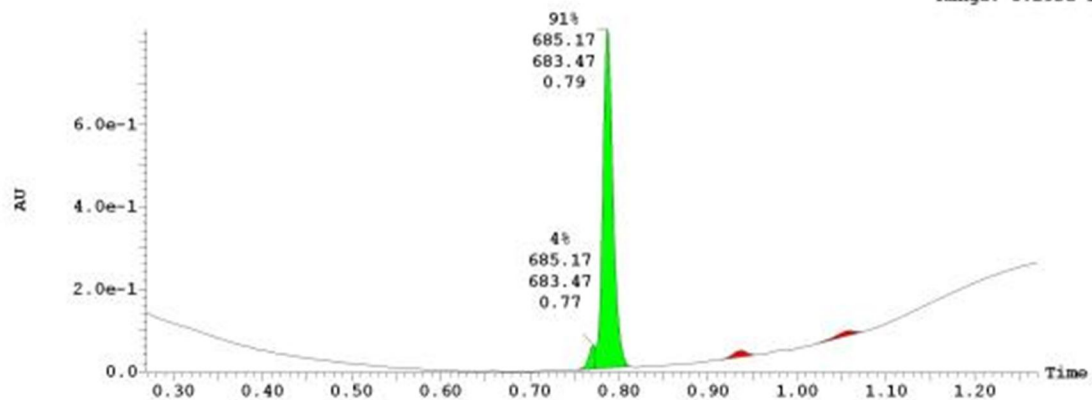
<sup>1</sup>H NMR Spectrum (300 MHz, CDCl<sub>3</sub>) of Analog CID 49849918



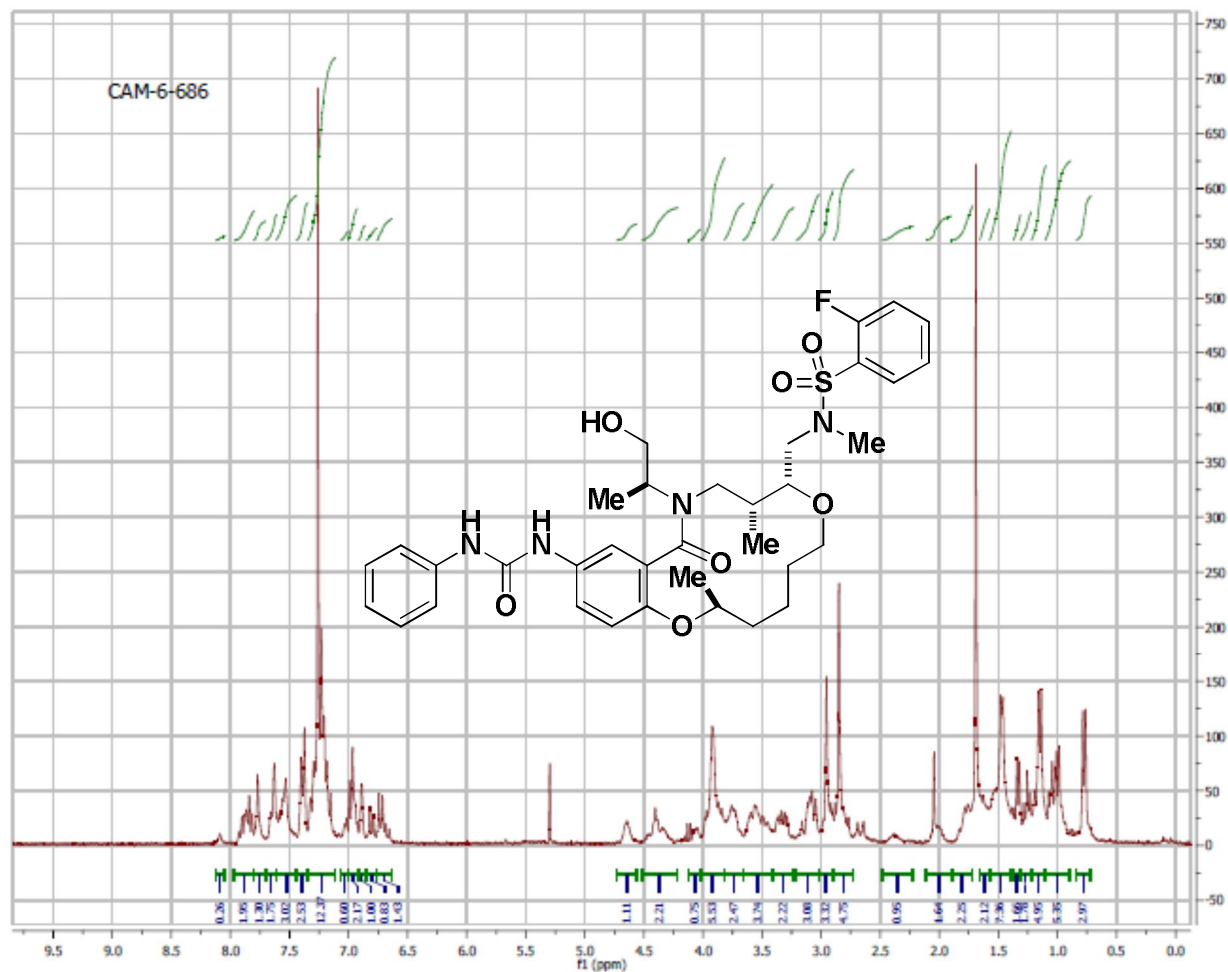
UPLC Chromatogram of Analog CID 49849918

3: UV Detector: 210

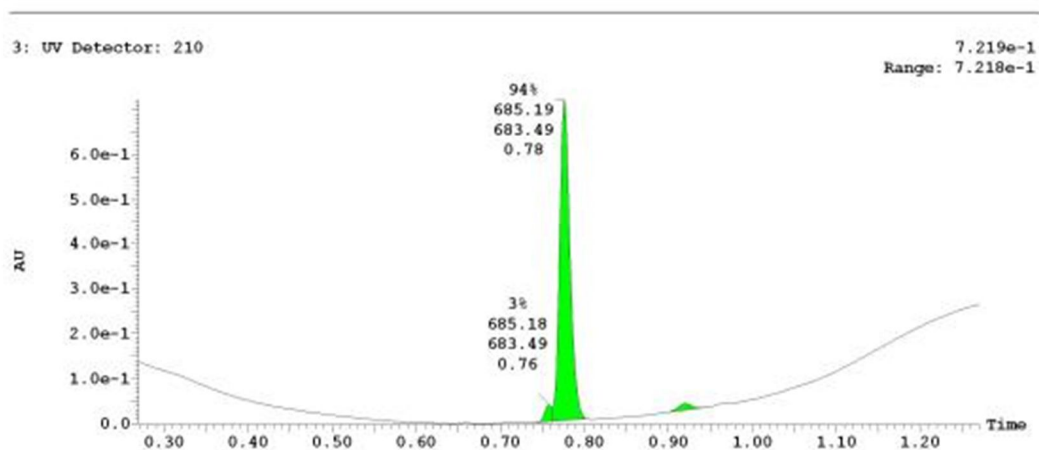
8.296e-1  
Range: 8.295e-1



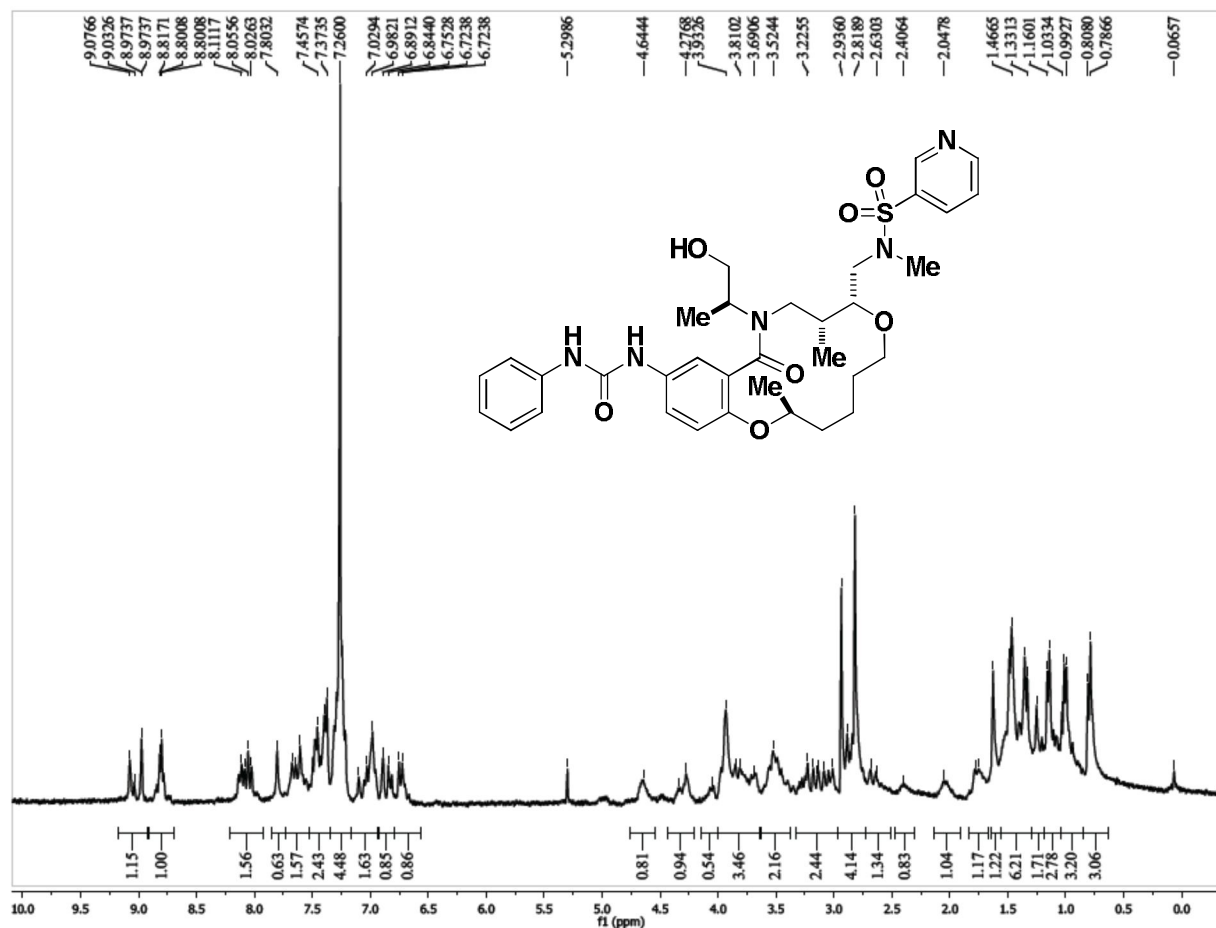
<sup>1</sup>H NMR Spectrum (300 MHz, CDCl<sub>3</sub>) of Analog CID 49849913



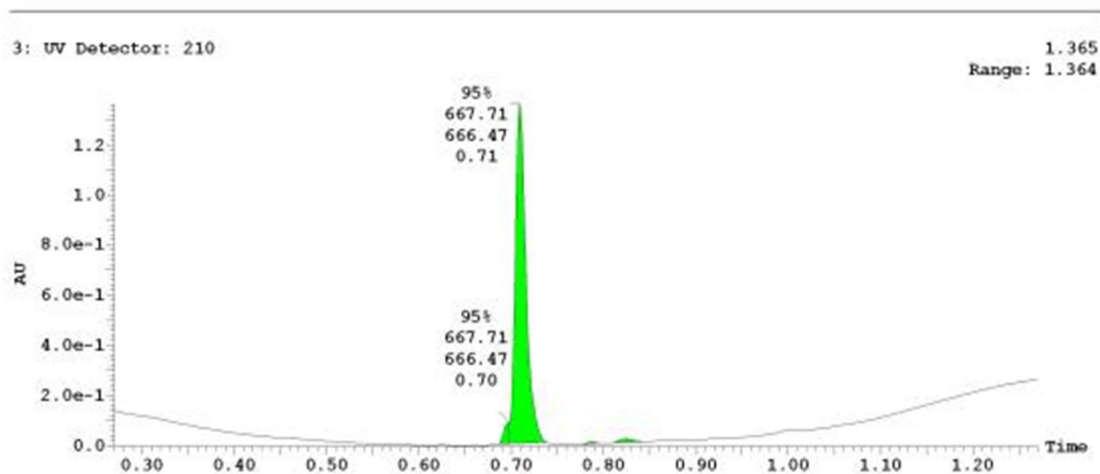
UPLC Chromatogram of Analog CID 49849913



<sup>1</sup>H NMR Spectrum (300 MHz, CDCl<sub>3</sub>) of Analog CID 49849924

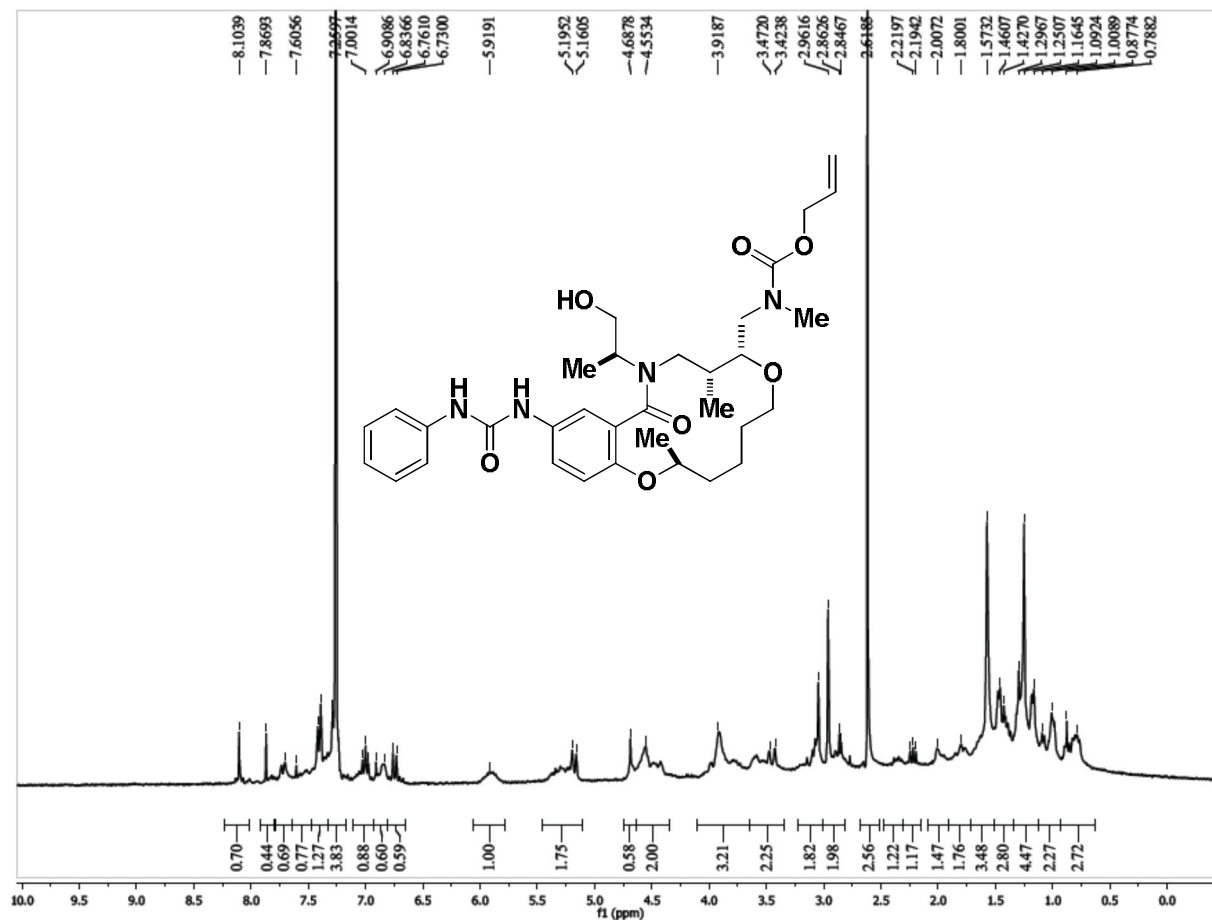


UPLC Chromatogram of Analog CID 49849924

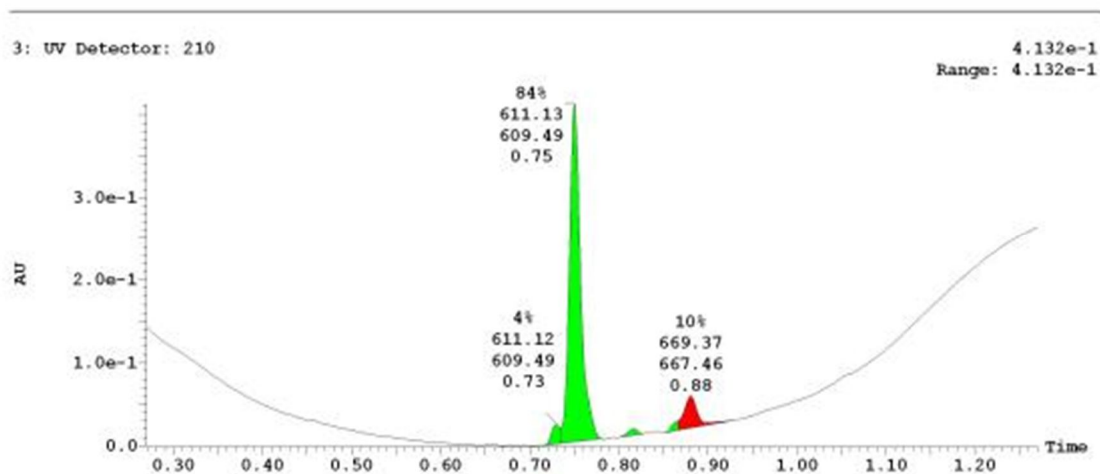




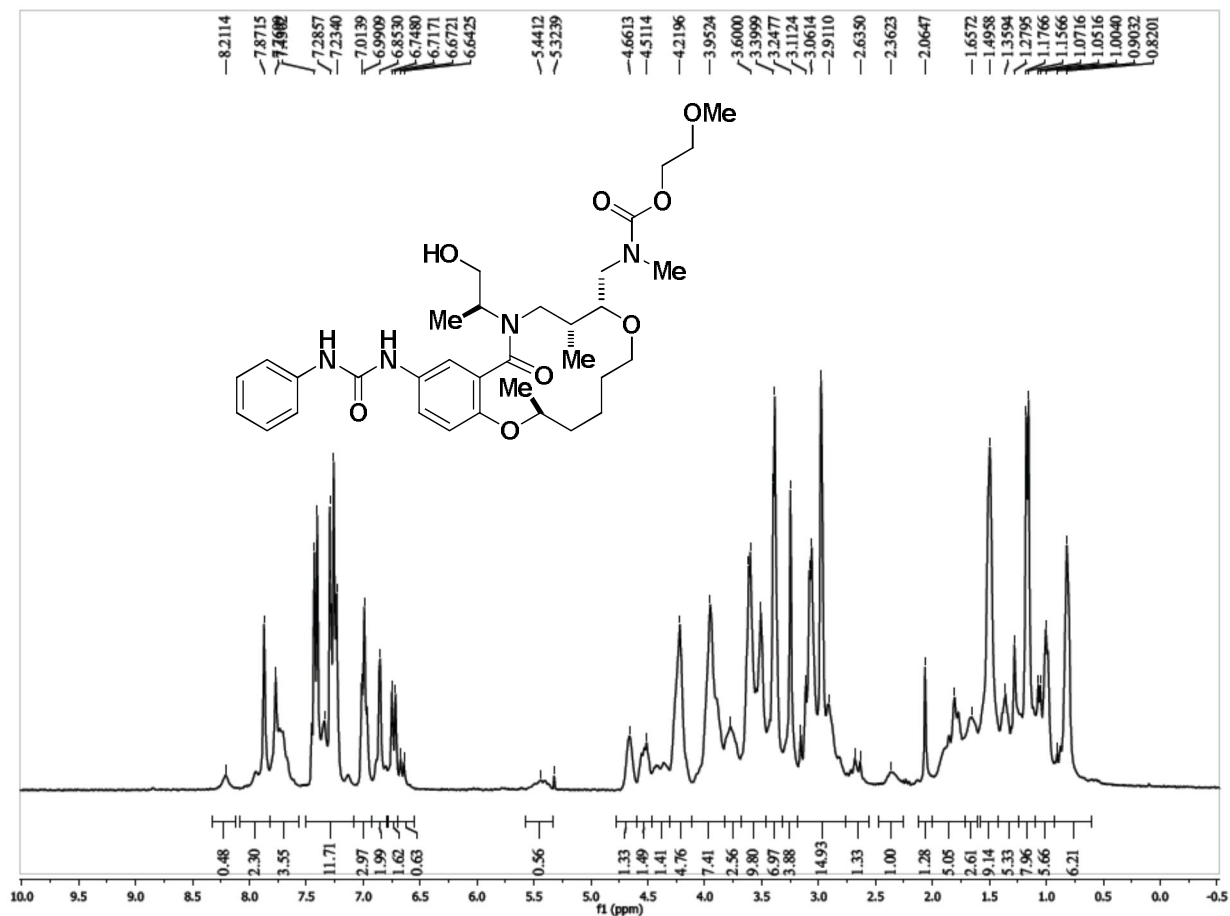
<sup>1</sup>H NMR Spectrum (300 MHz, CDCl<sub>3</sub>) of Analog CID 49849917



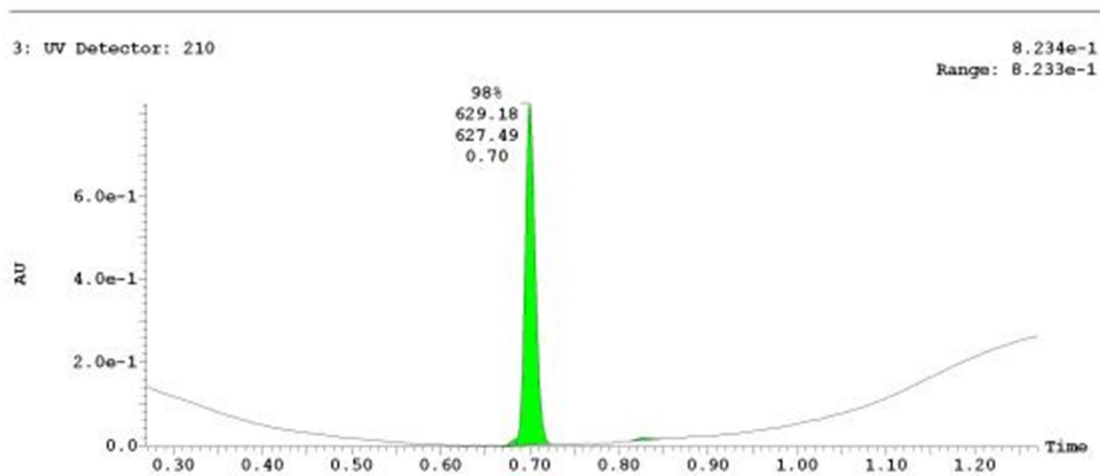
UPLC Chromatogram of Analog CID 49849917



<sup>1</sup>H NMR Spectrum (300 MHz, CDCl<sub>3</sub>) of Analog CID 49849932



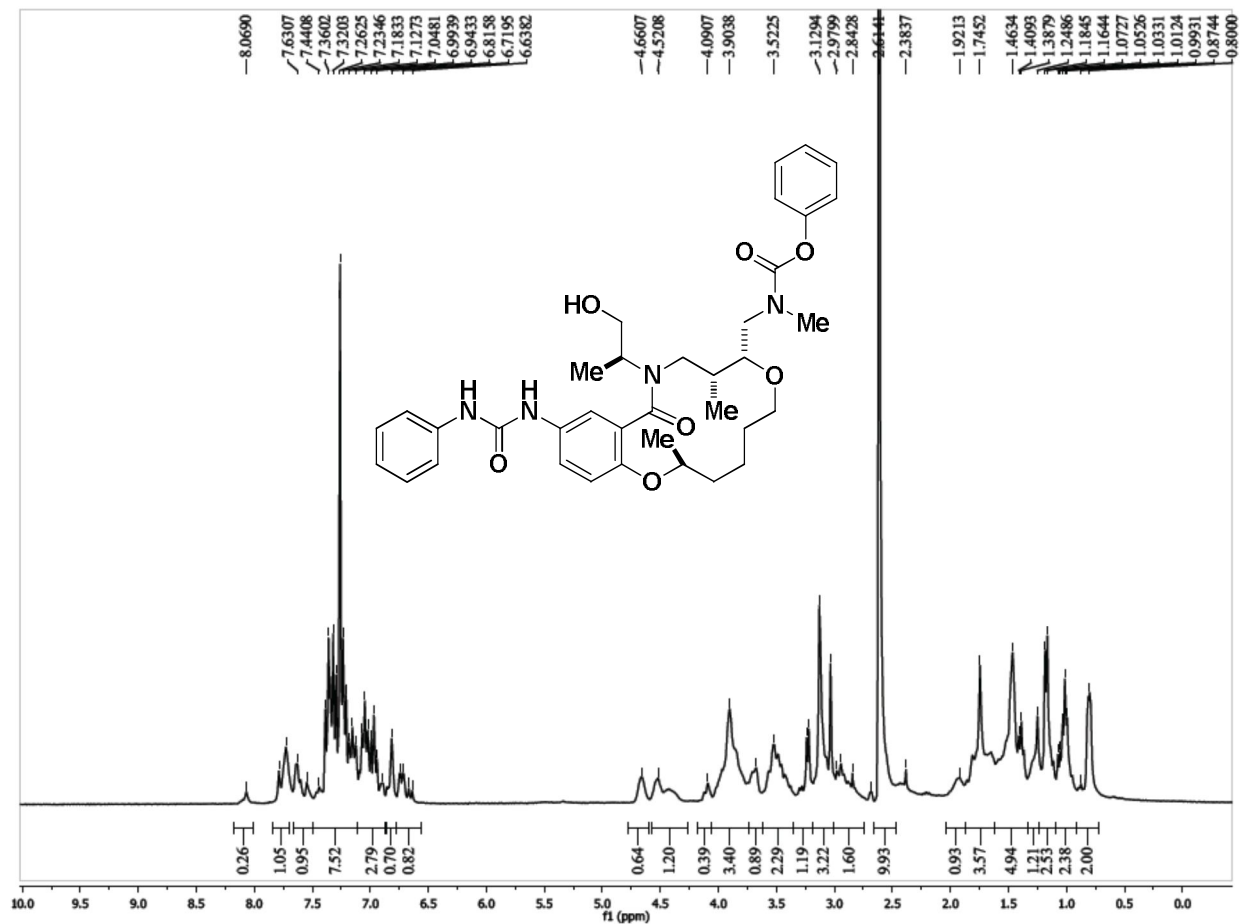
UPLC Chromatogram of Analog CID 49849932



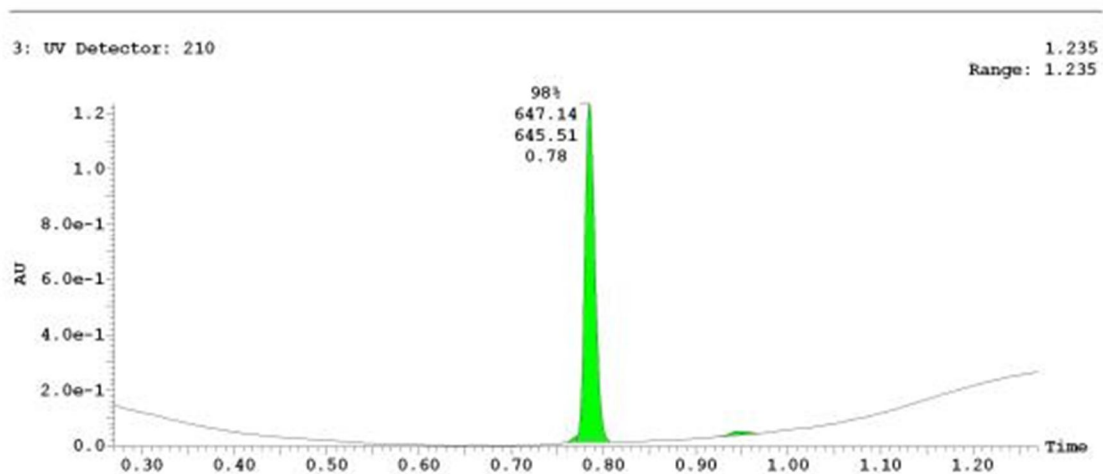




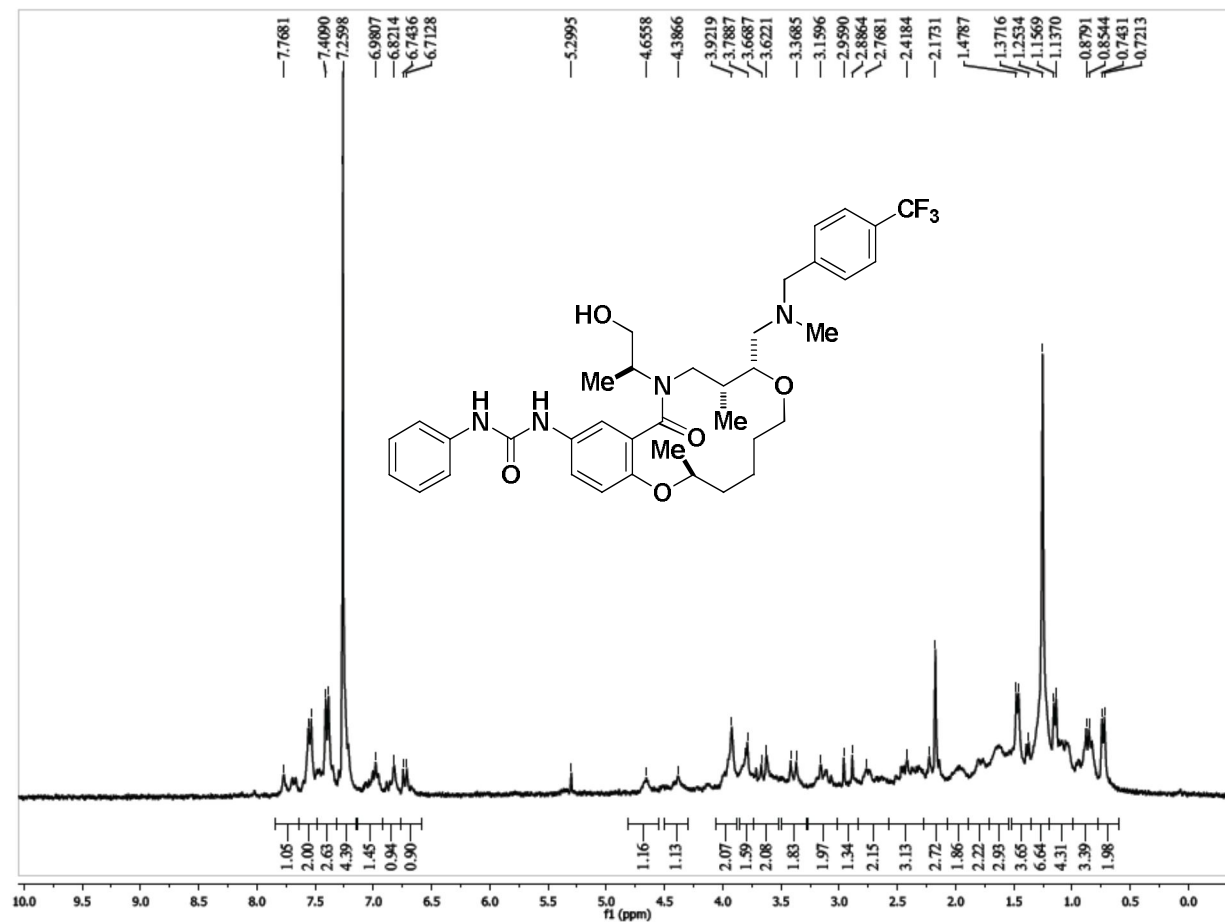
<sup>1</sup>H NMR Spectrum (300 MHz, CDCl<sub>3</sub>) of Analog CID 49849908



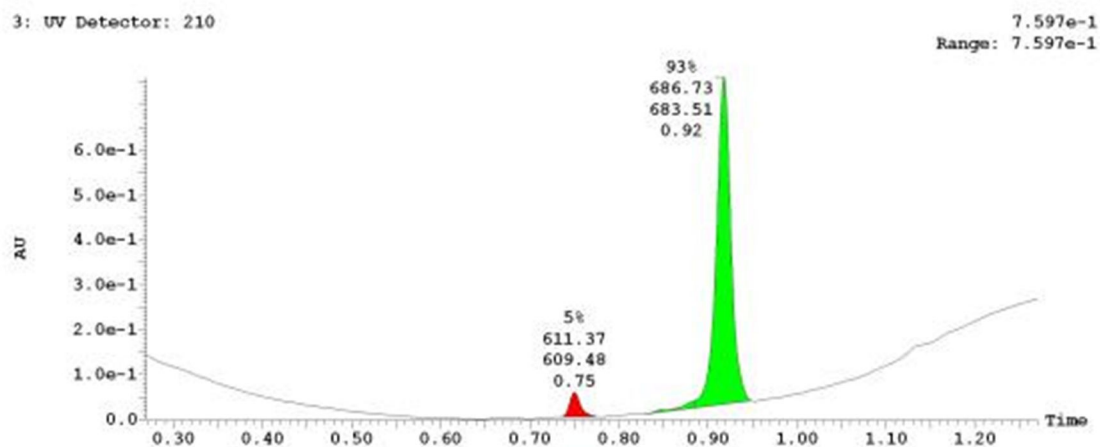
UPLC Chromatogram of Analog CID 49849908



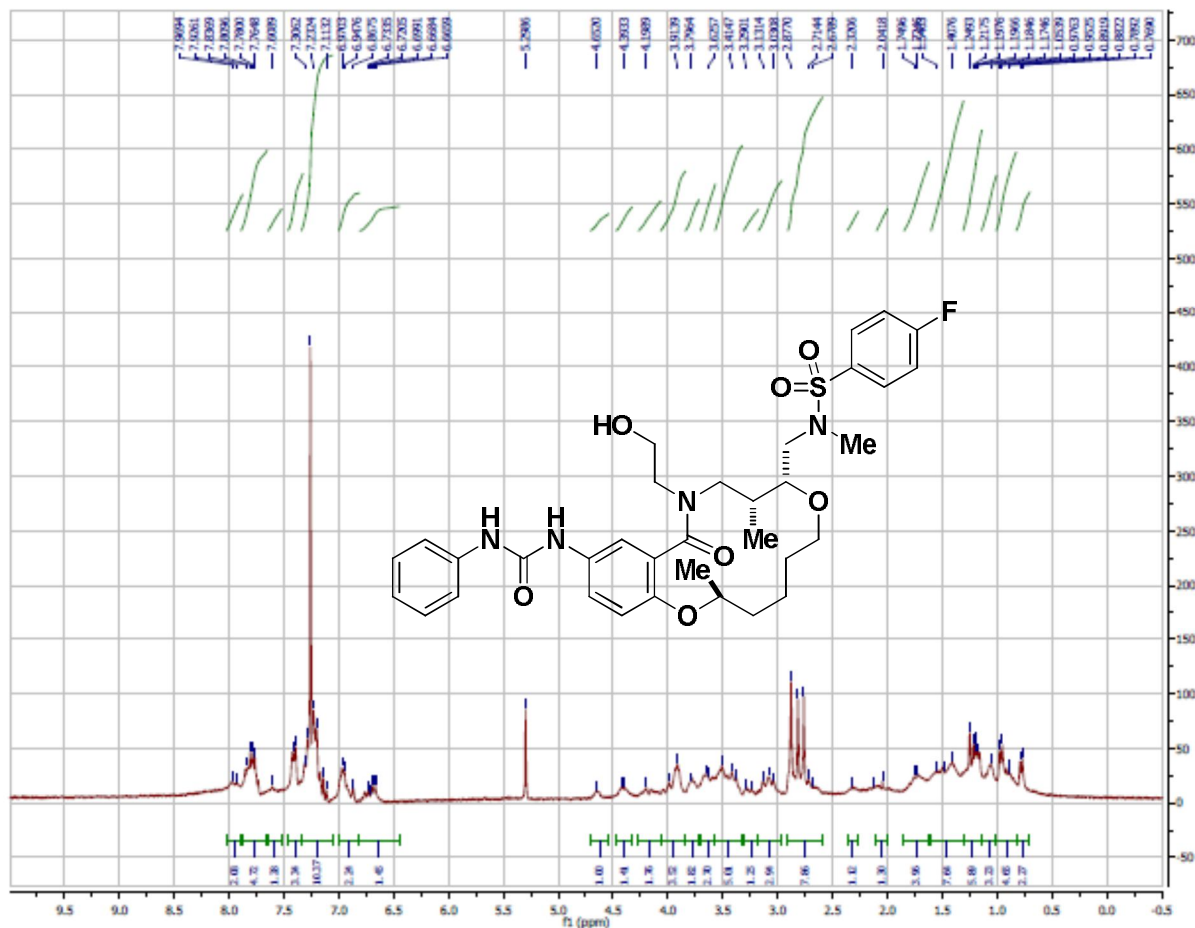
<sup>1</sup>H NMR Spectrum (300 MHz, CDCl<sub>3</sub>) of Analog CID 49843214



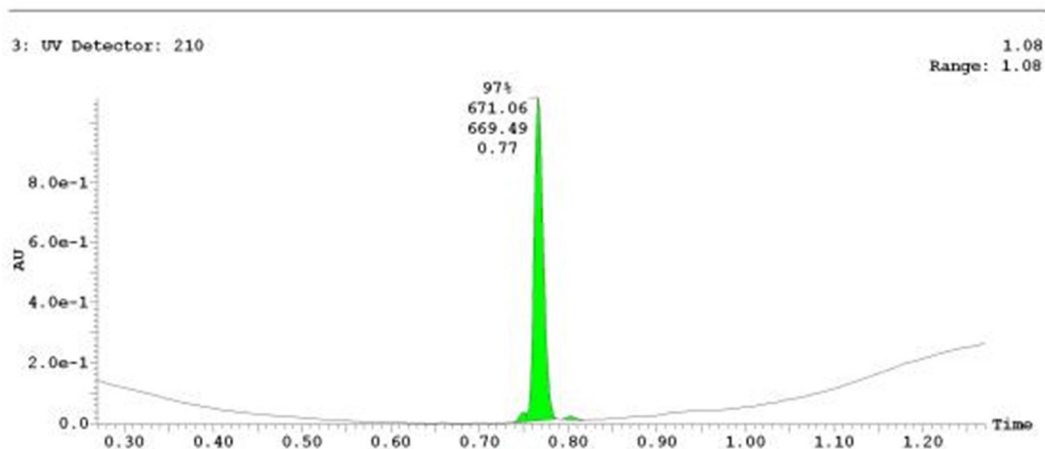
UPLC Chromatogram of Analog CID 49843214



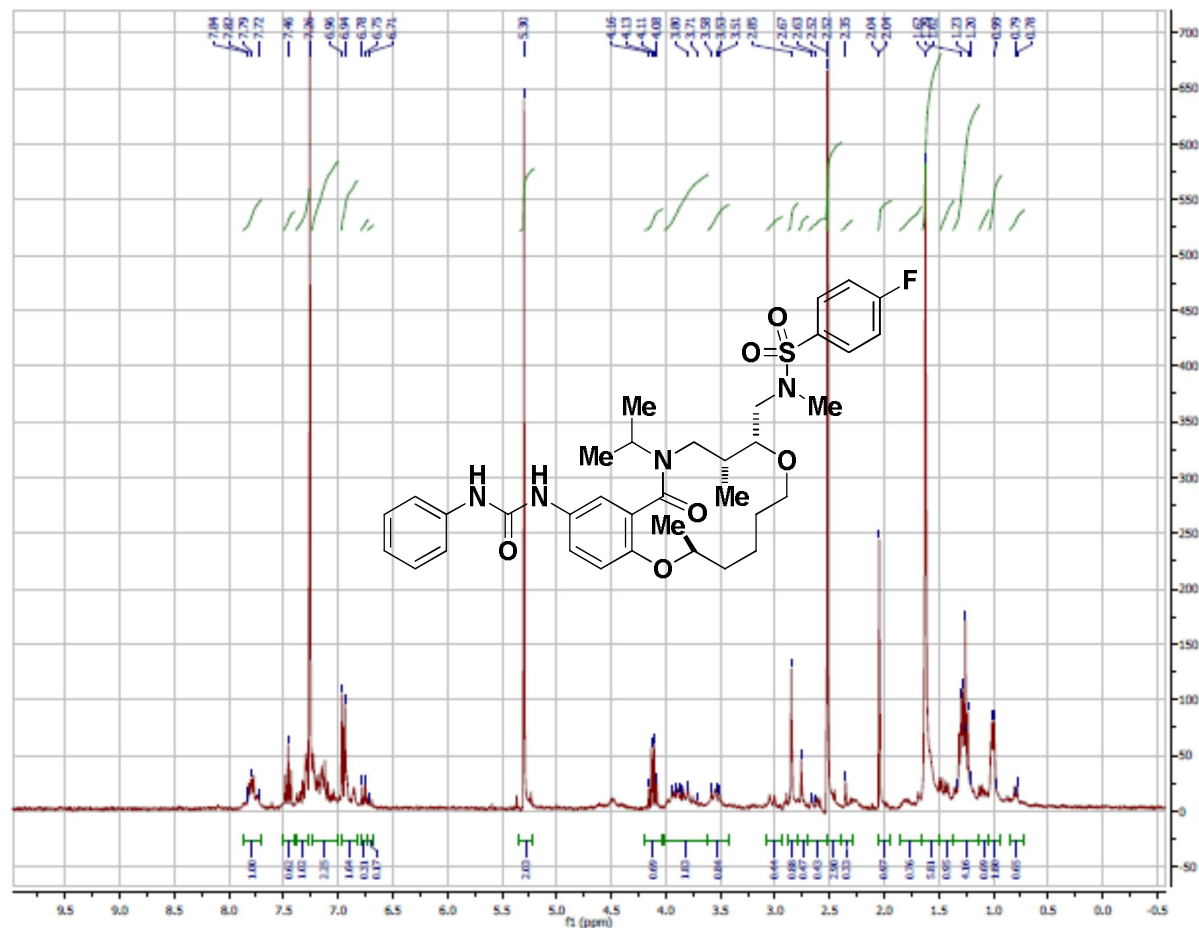
<sup>1</sup>H NMR Spectrum (300 MHz, CDCl<sub>3</sub>) of Analog CID 49849923



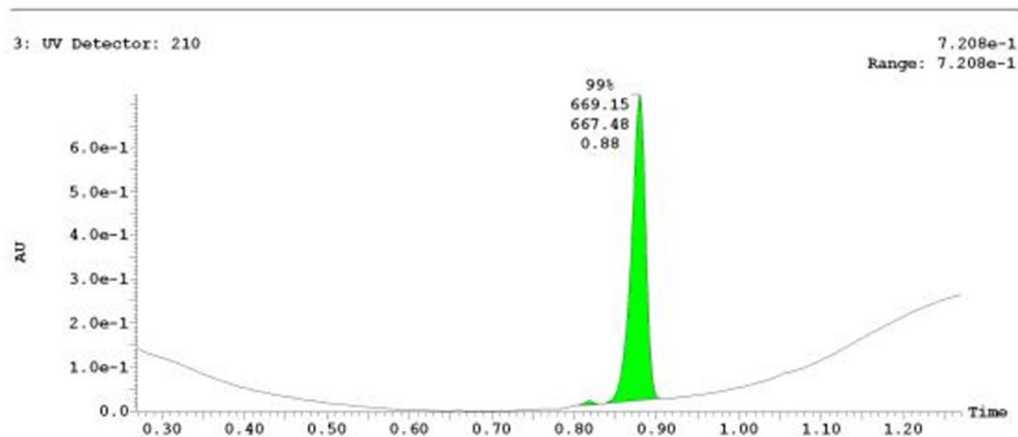
UPLC Chromatogram of Analog CID 49849923



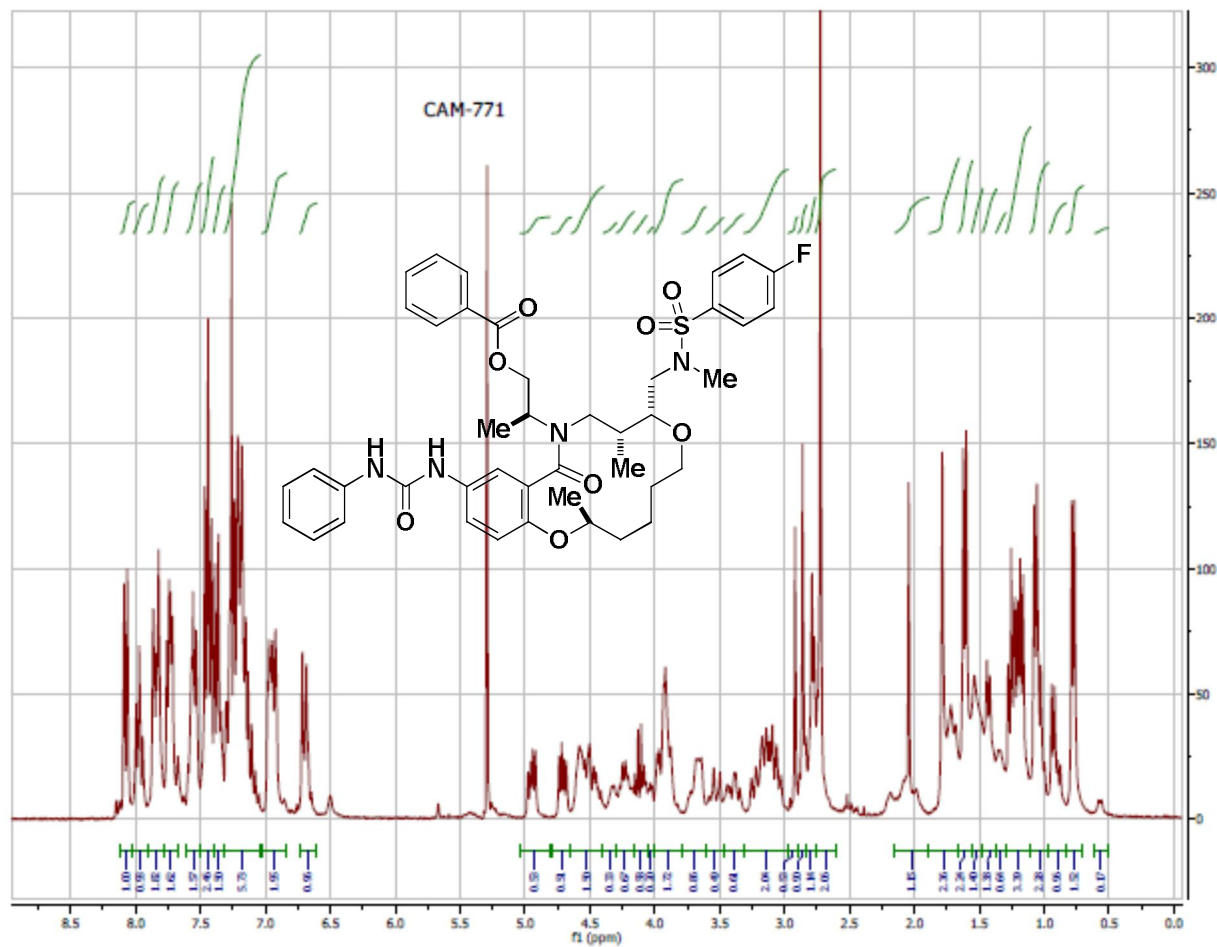
<sup>1</sup>H NMR Spectrum (300 MHz, CDCl<sub>3</sub>) of Analog CID 49849935



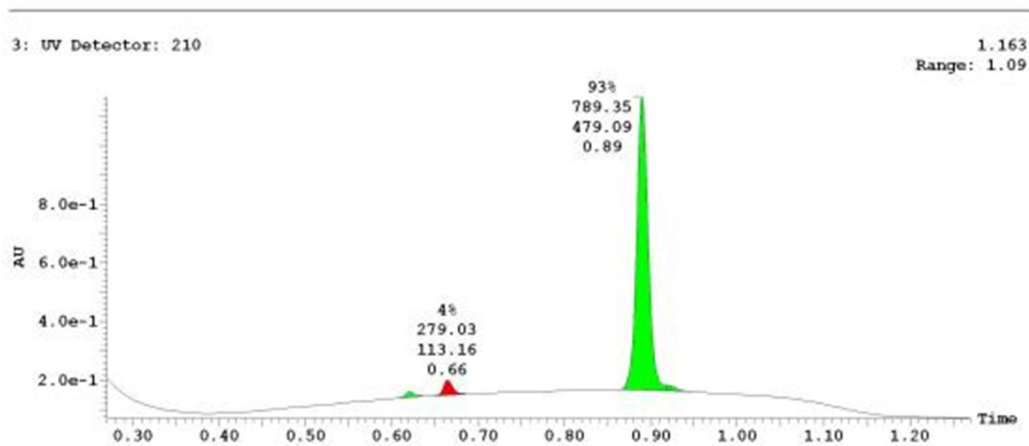
UPLC Chromatogram of Analog CID 49849935



**$^1\text{H}$  NMR Spectrum (300 MHz,  $\text{CDCl}_3$ ) of Analog CID 49849915**

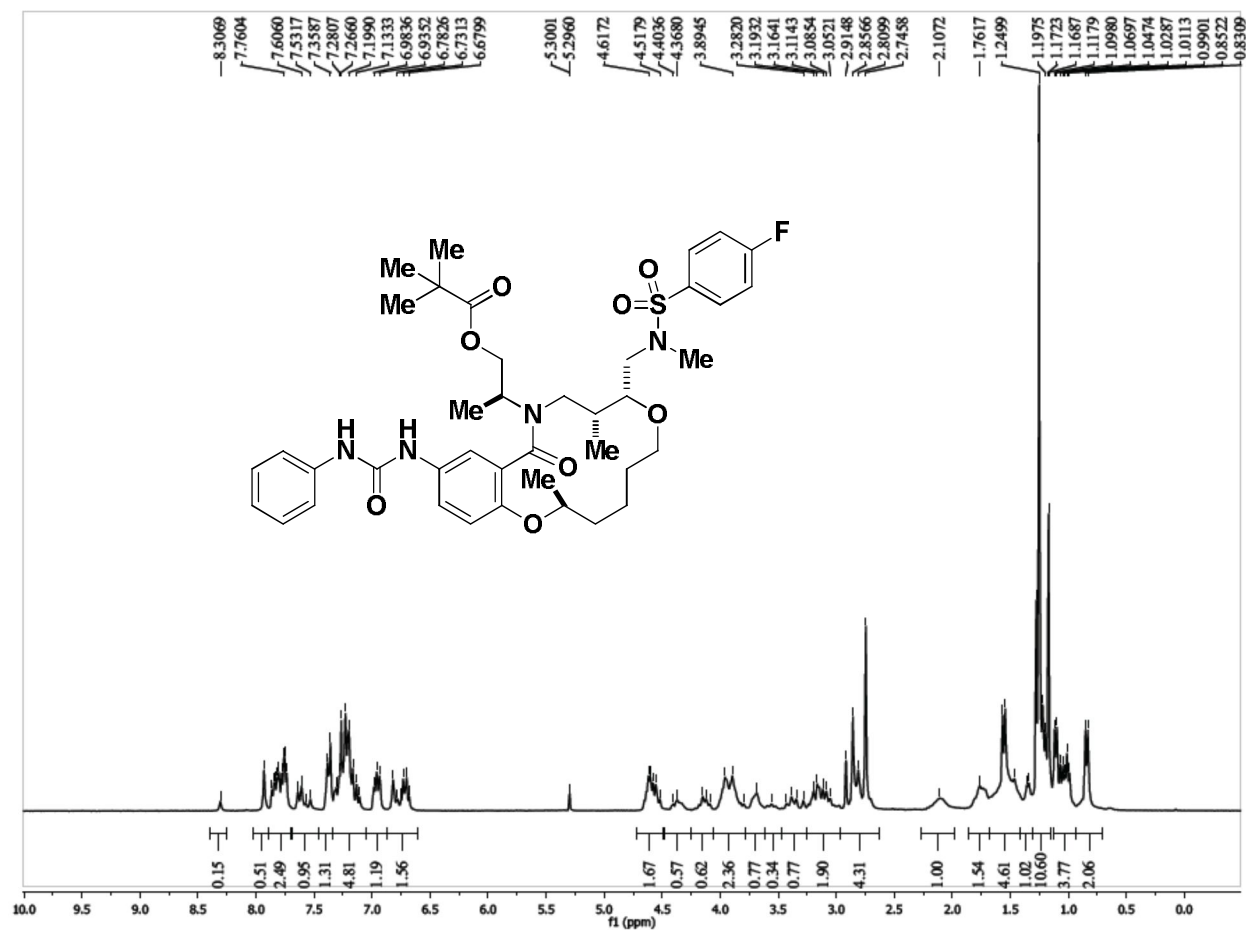


**UPLC Chromatogram of Analog CID 49849915**





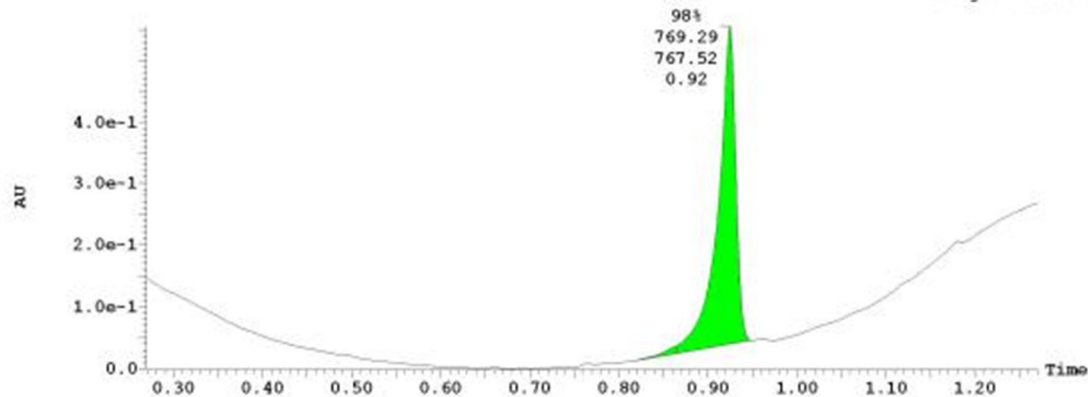
**<sup>1</sup>H NMR Spectrum (300 MHz, CDCl<sub>3</sub>) of Analog CID 49849931**



**UPLC Chromatogram of Analog CID 49849931**

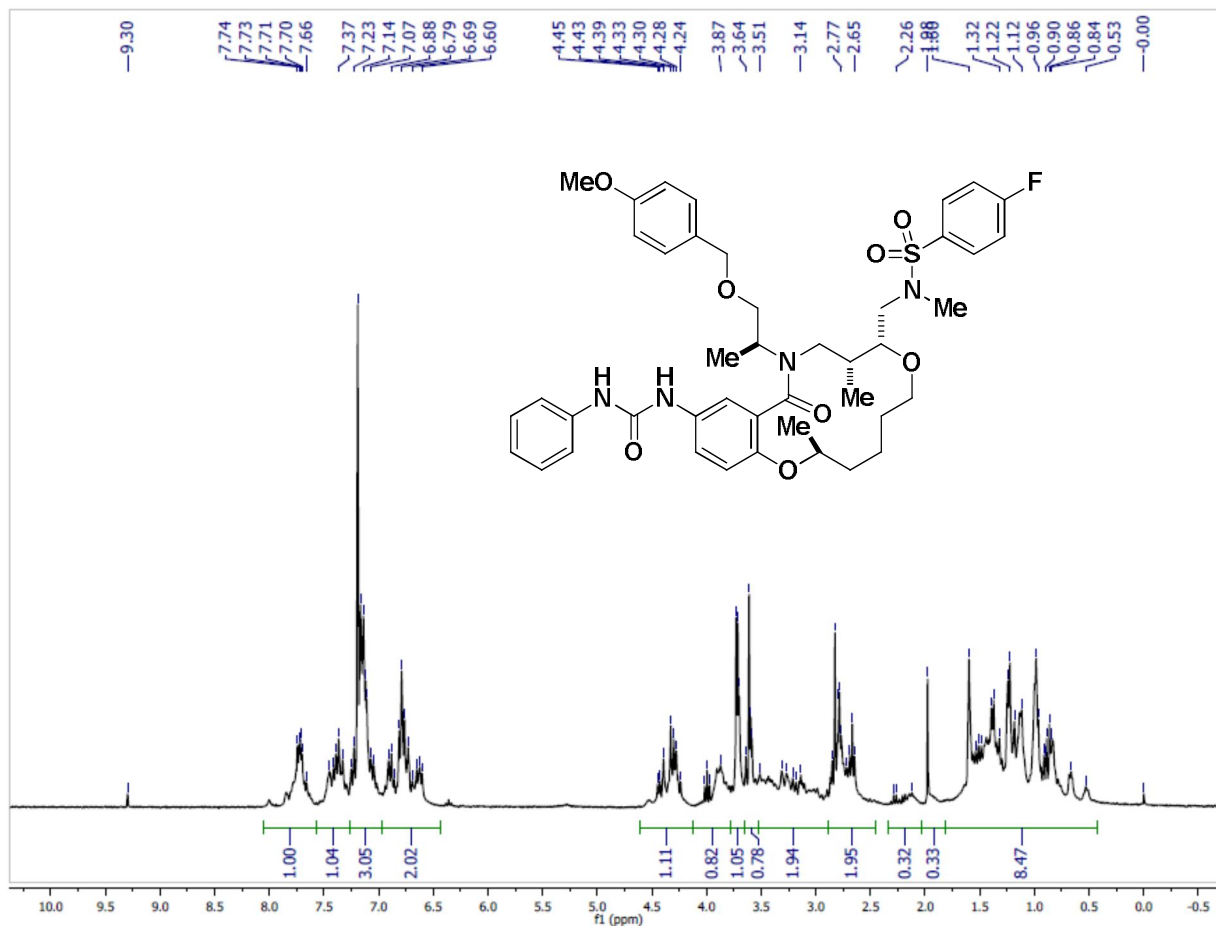
3: UV Detector: 210

5.548e-1  
Range: 5.548e-1

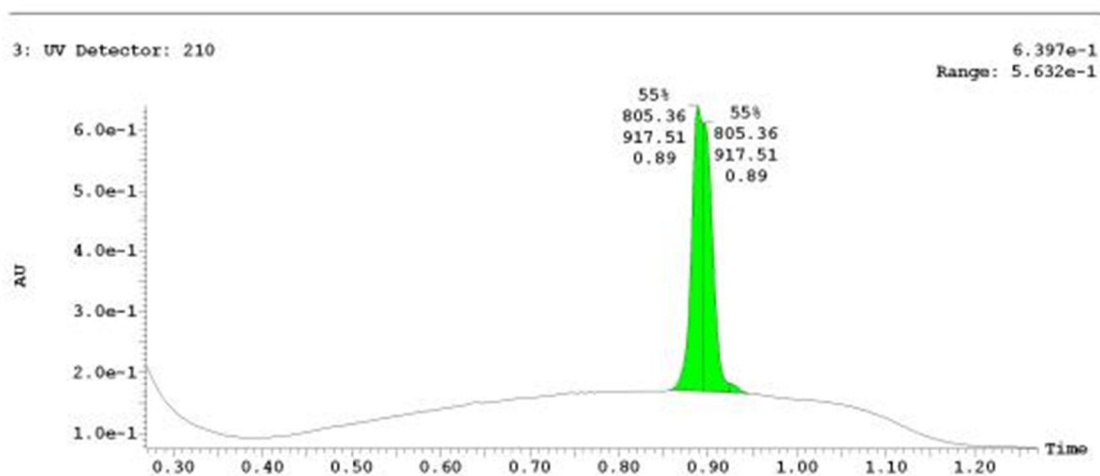




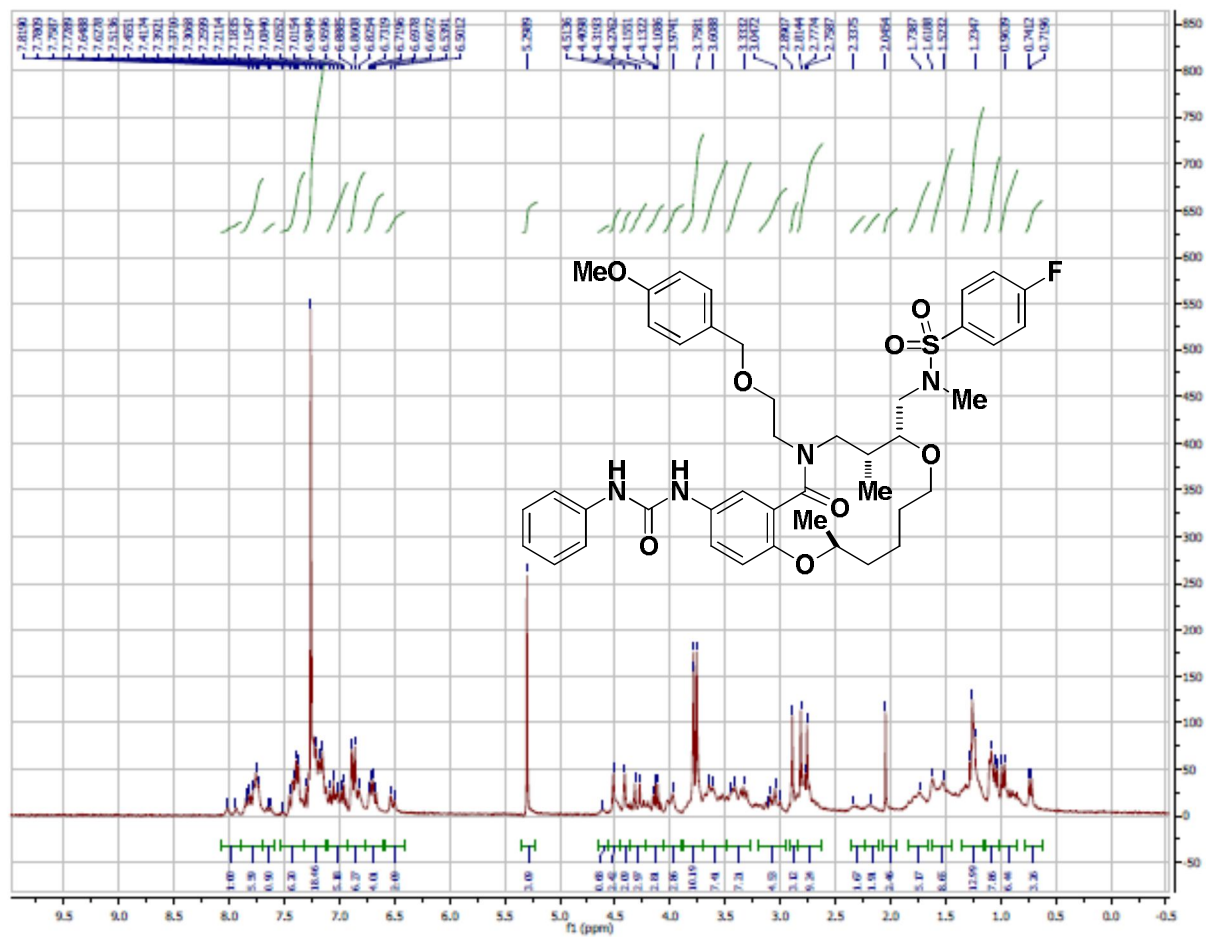
<sup>1</sup>H NMR Spectrum (300 MHz, CDCl<sub>3</sub>) of Analog CID 49849909



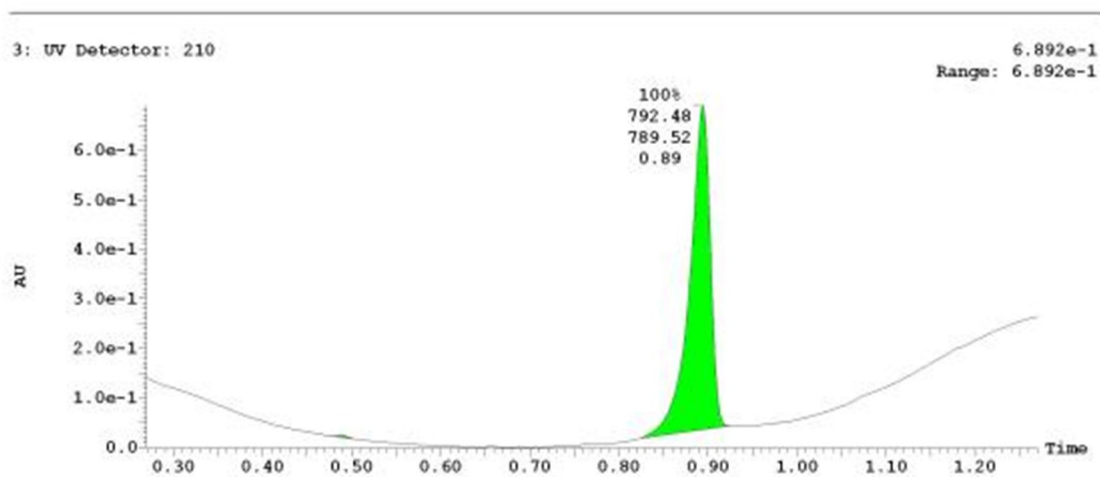
UPLC Chromatogram of Analog CID 49849909



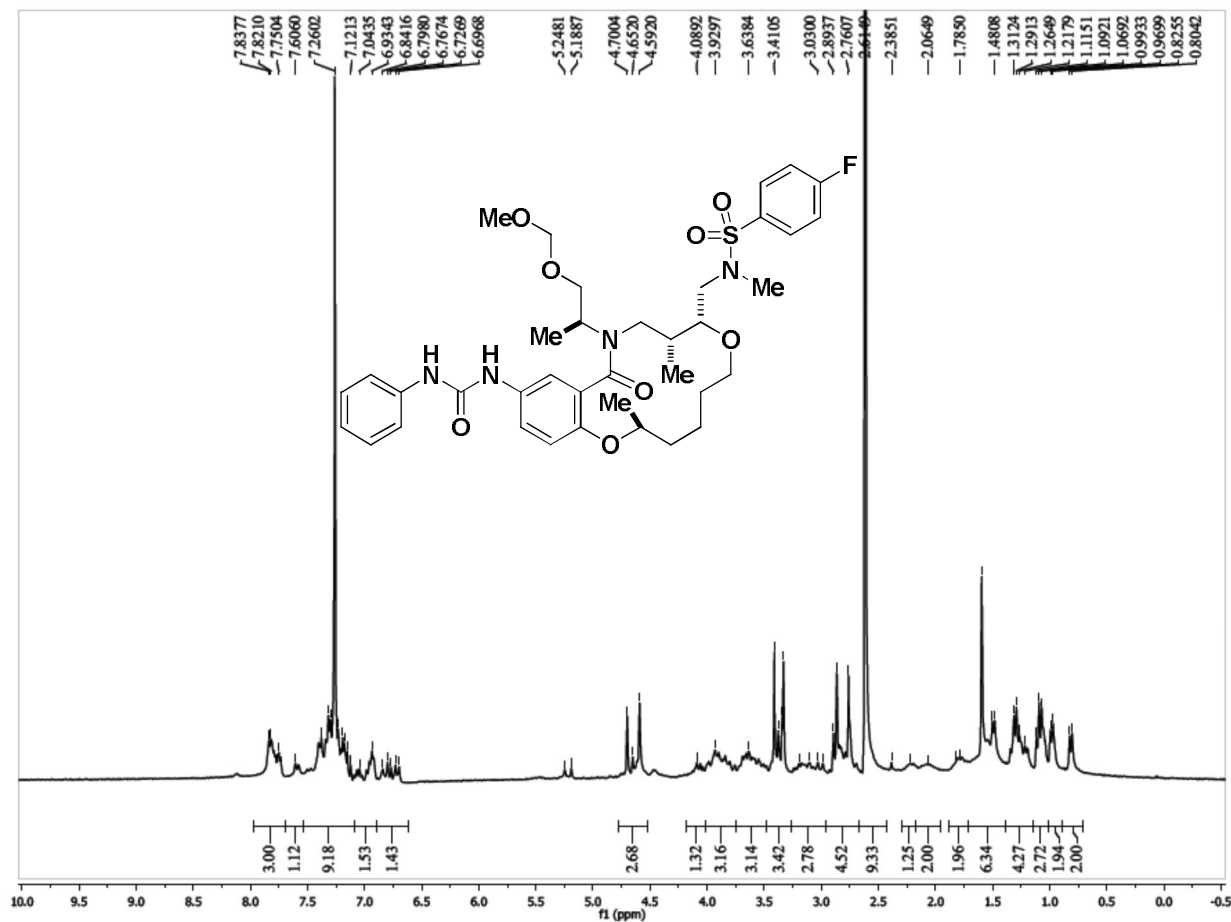
<sup>1</sup>H NMR Spectrum (300 MHz, CDCl<sub>3</sub>) of Analog CID 49849903



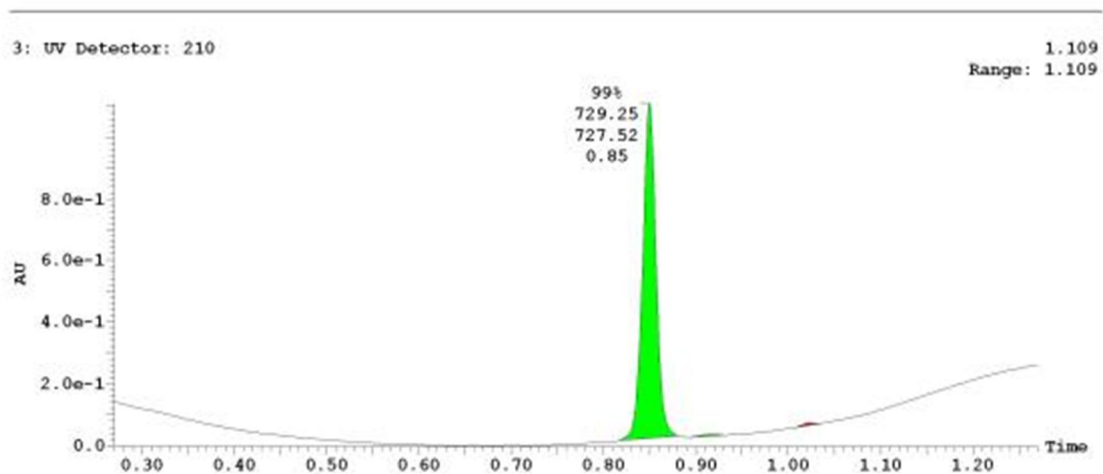
UPLC Chromatogram of Analog CID 49849903



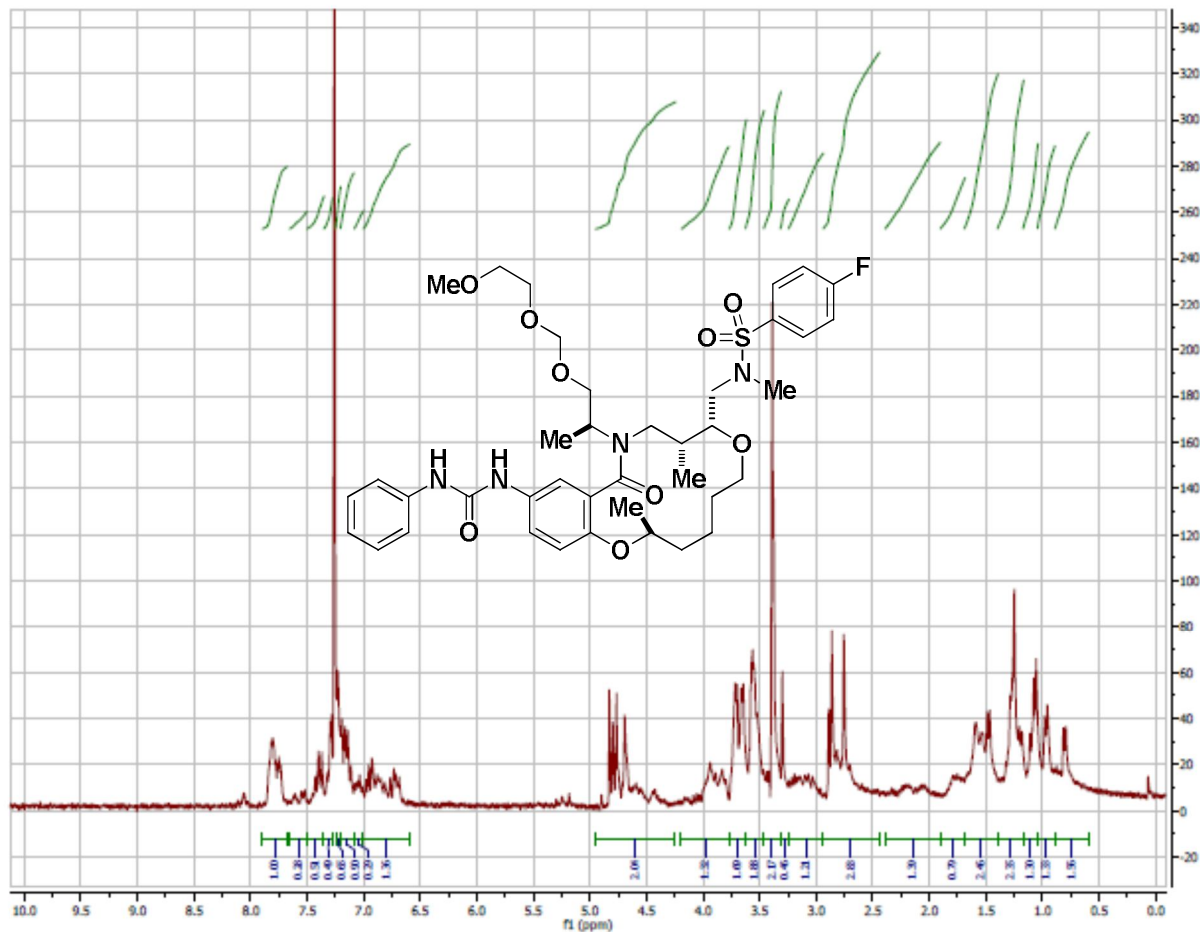
<sup>1</sup>H NMR Spectrum (300 MHz, CDCl<sub>3</sub>) of Analog CID 49849928



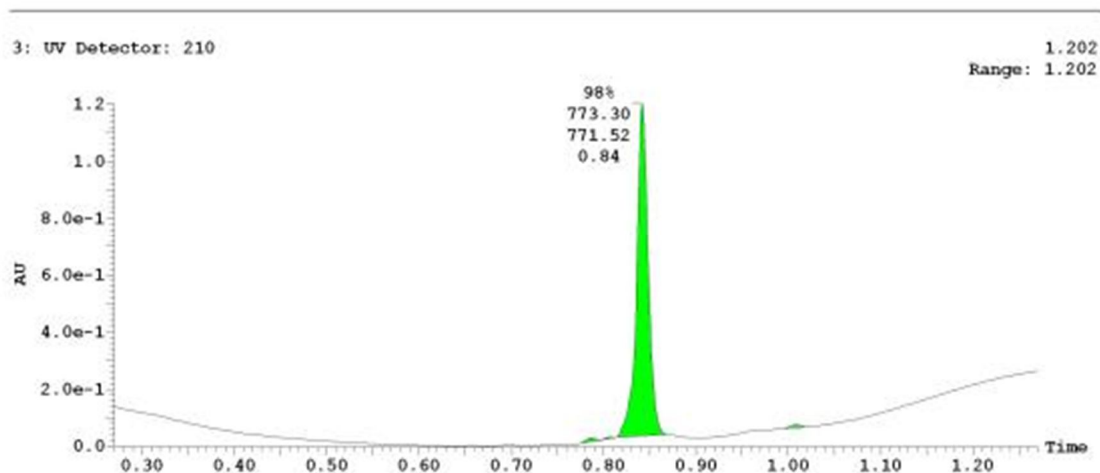
UPLC Chromatogram of Analog CID 49849928



**<sup>1</sup>H NMR Spectrum (300 MHz, CDCl<sub>3</sub>) of Analog CID 49849921**

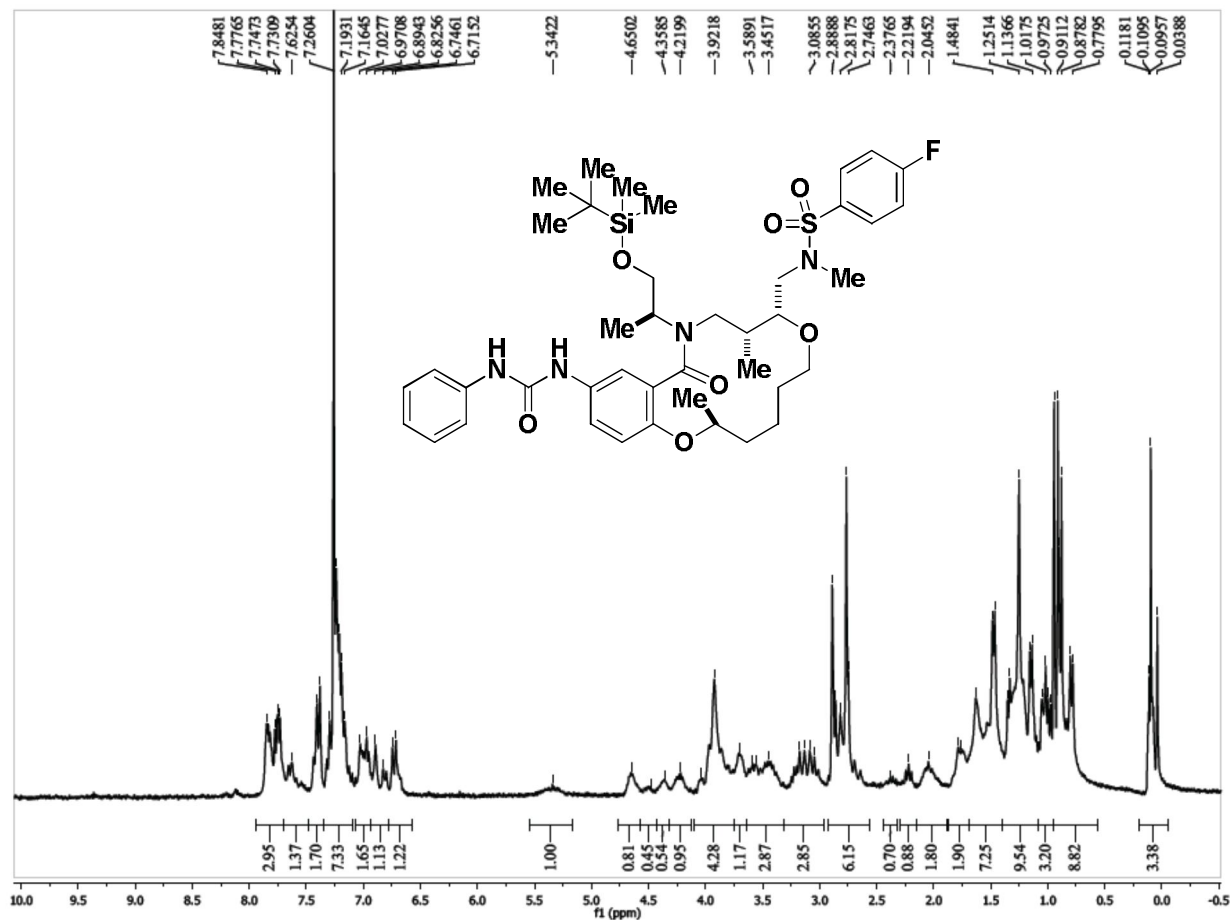


**UPLC Chromatogram of Analog CID 49849921**

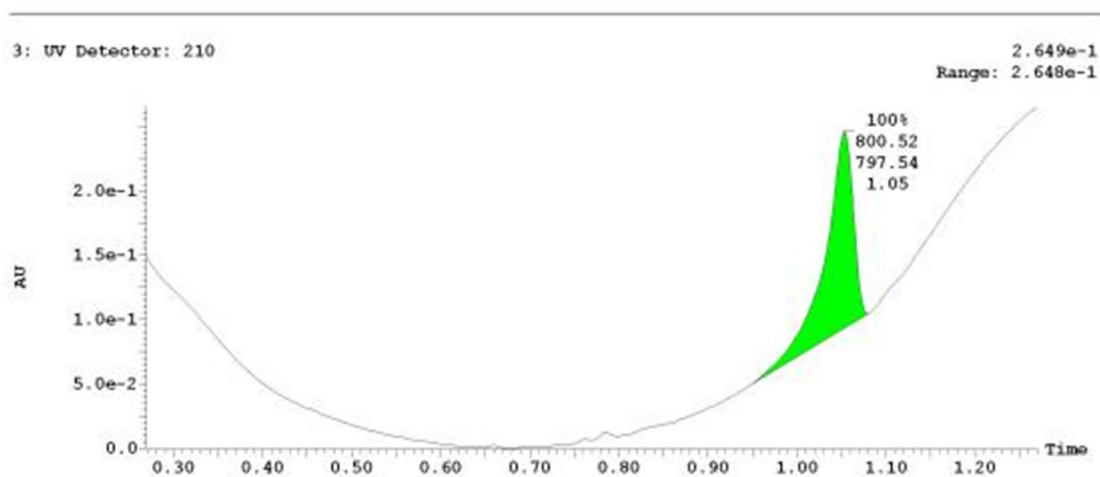




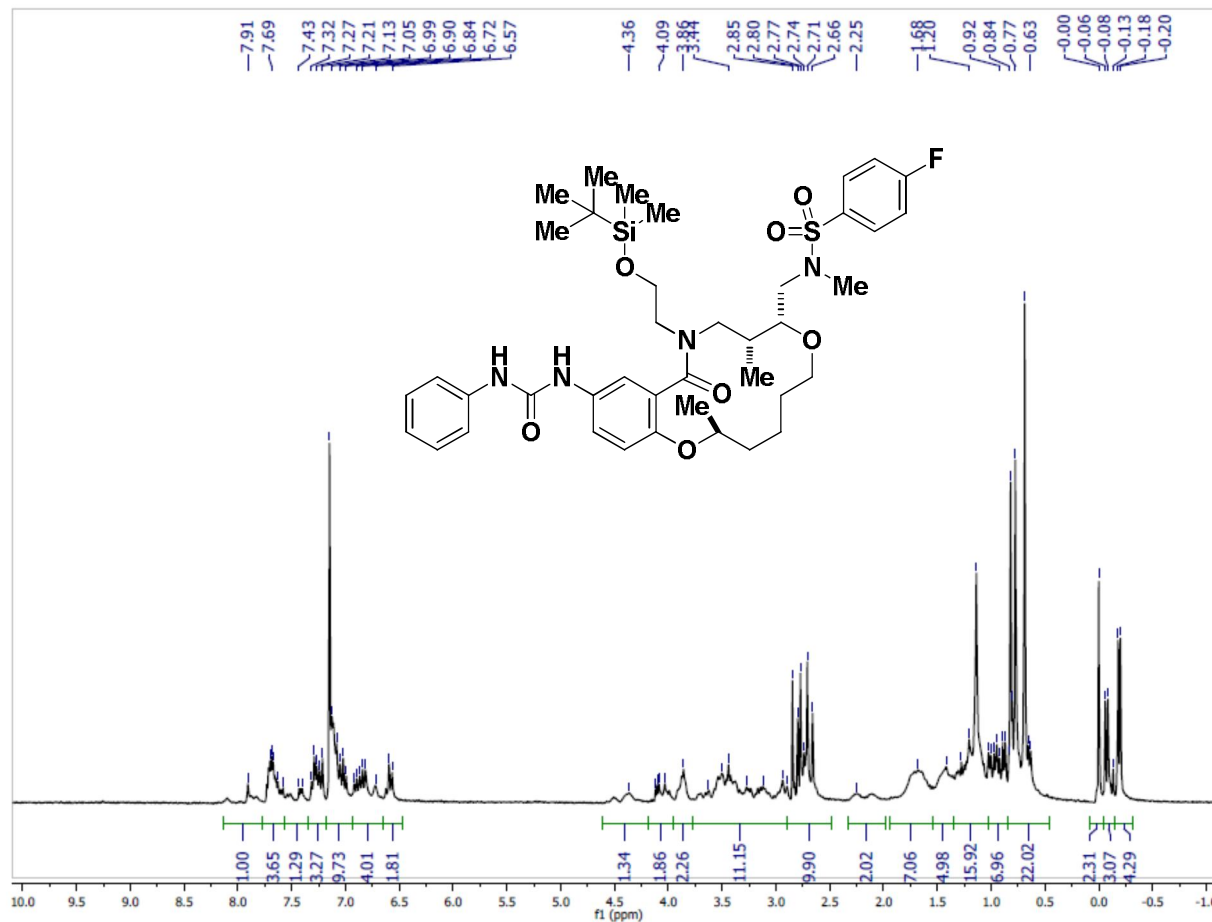
<sup>1</sup>H NMR Spectrum (300 MHz, CDCl<sub>3</sub>) of Analog CID 49849916



UPLC Chromatogram of Analog CID 49849916



<sup>1</sup>H NMR Spectrum (300 MHz, CDCl<sub>3</sub>) of Analog CID 49849934

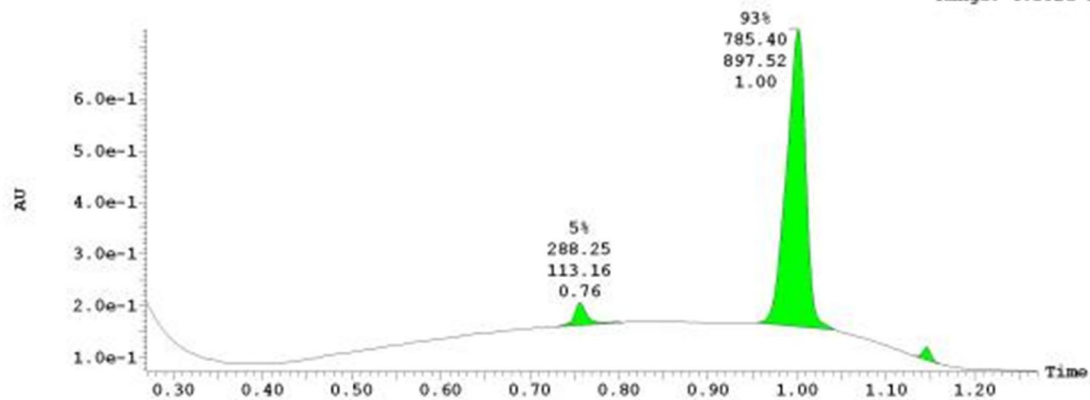


UPLC Chromatogram of Analog CID 49849934

3: UV Detector: 210

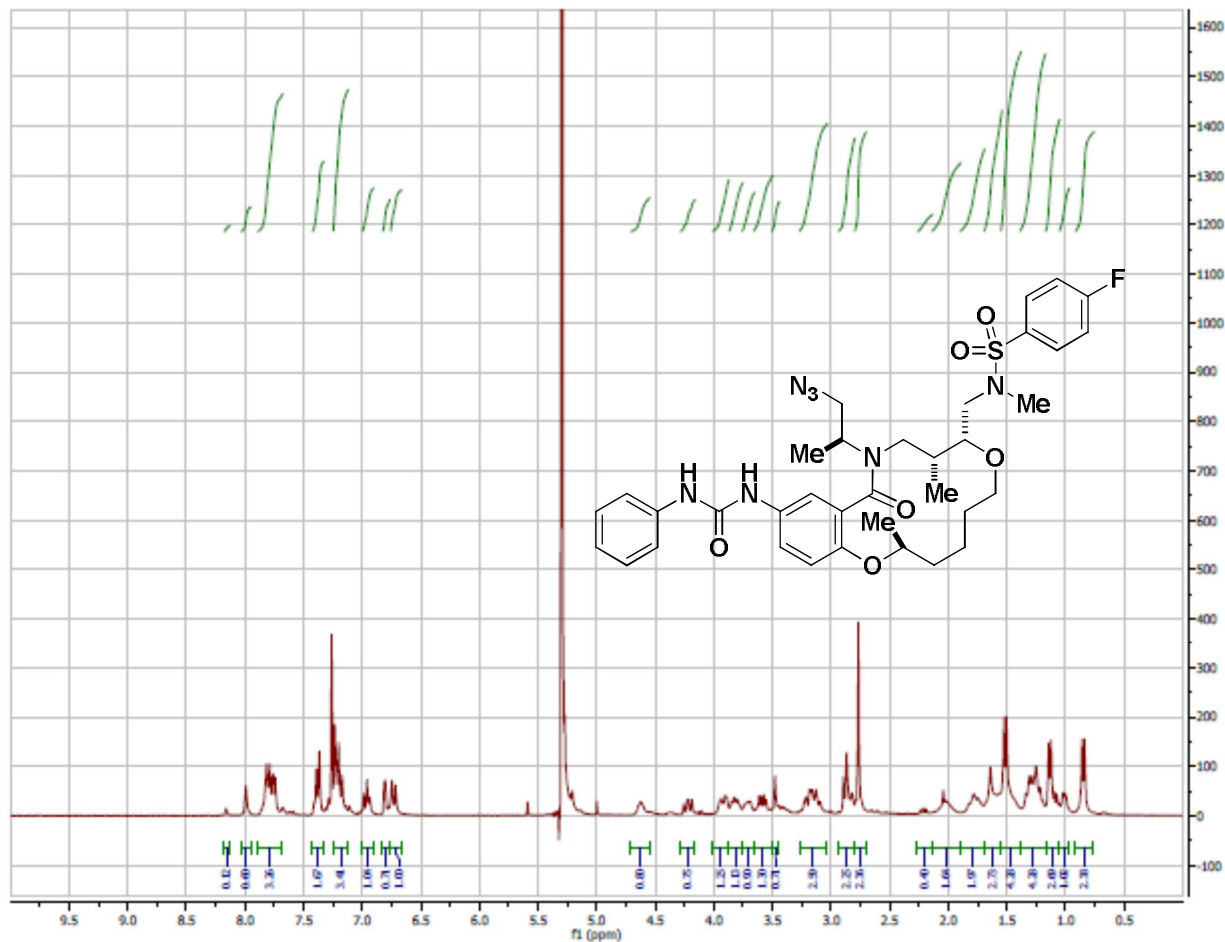
7.338e-1

Range: 6.592e-1





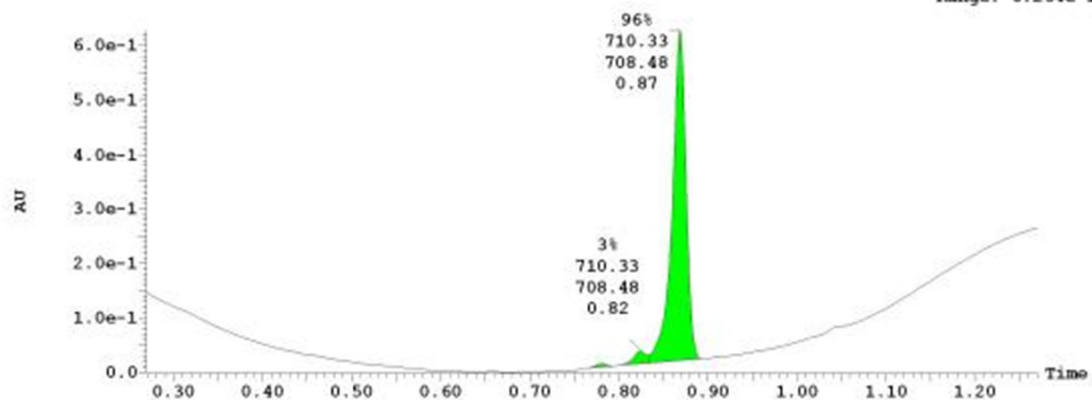
<sup>1</sup>H NMR Spectrum (300 MHz, CDCl<sub>3</sub>) of Analog CID 49849906



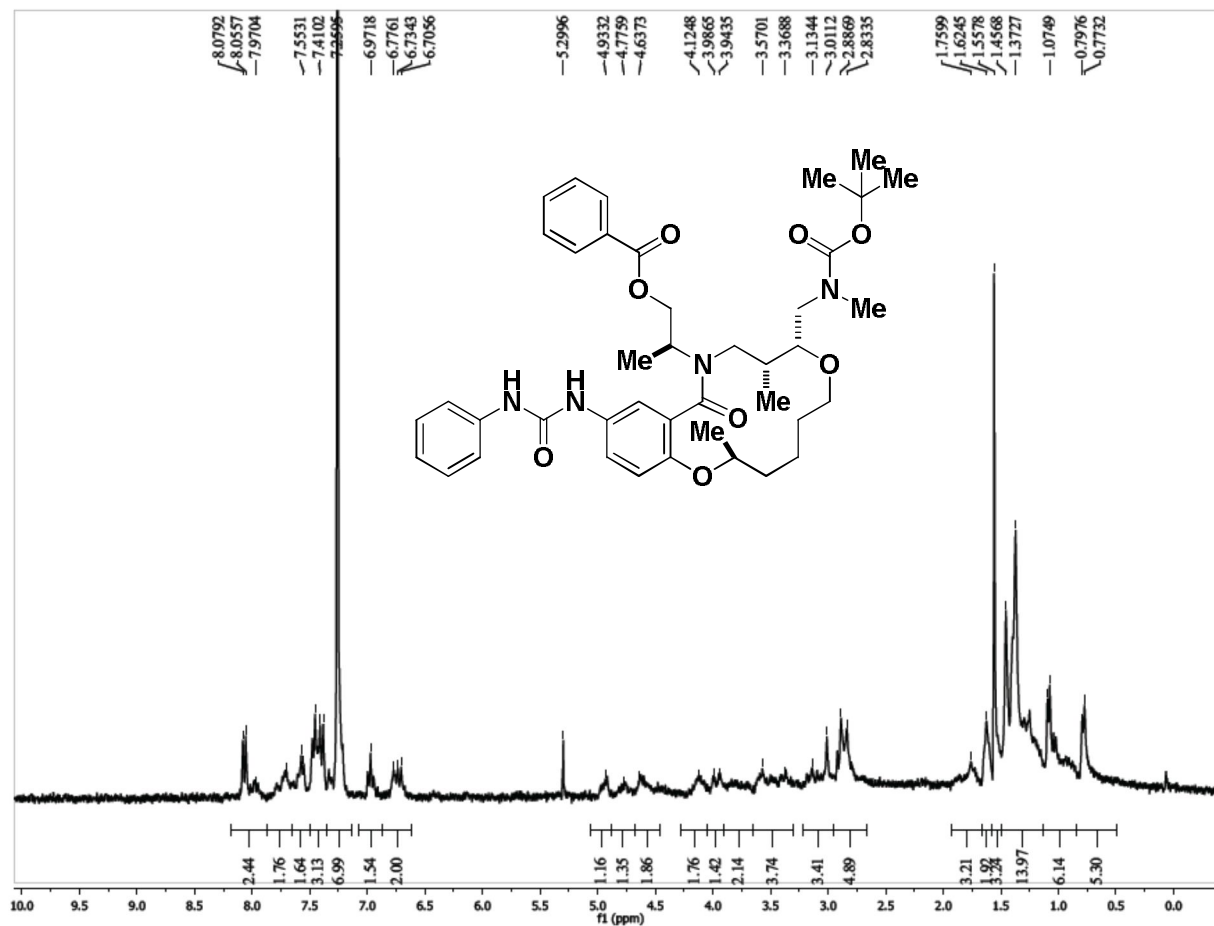
UPLC Chromatogram of Analog CID 49849906

3: UV Detector: 210

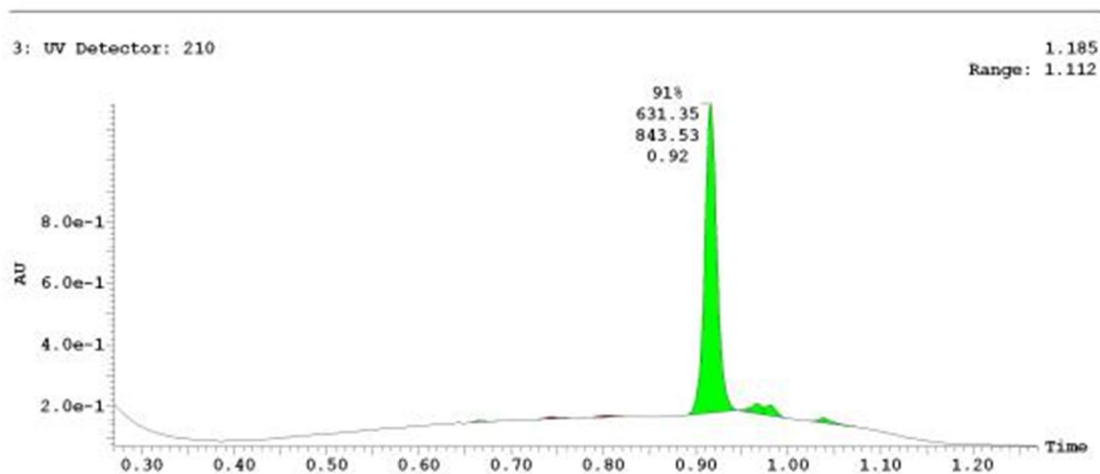
6.264e-1  
Range: 6.264e-1



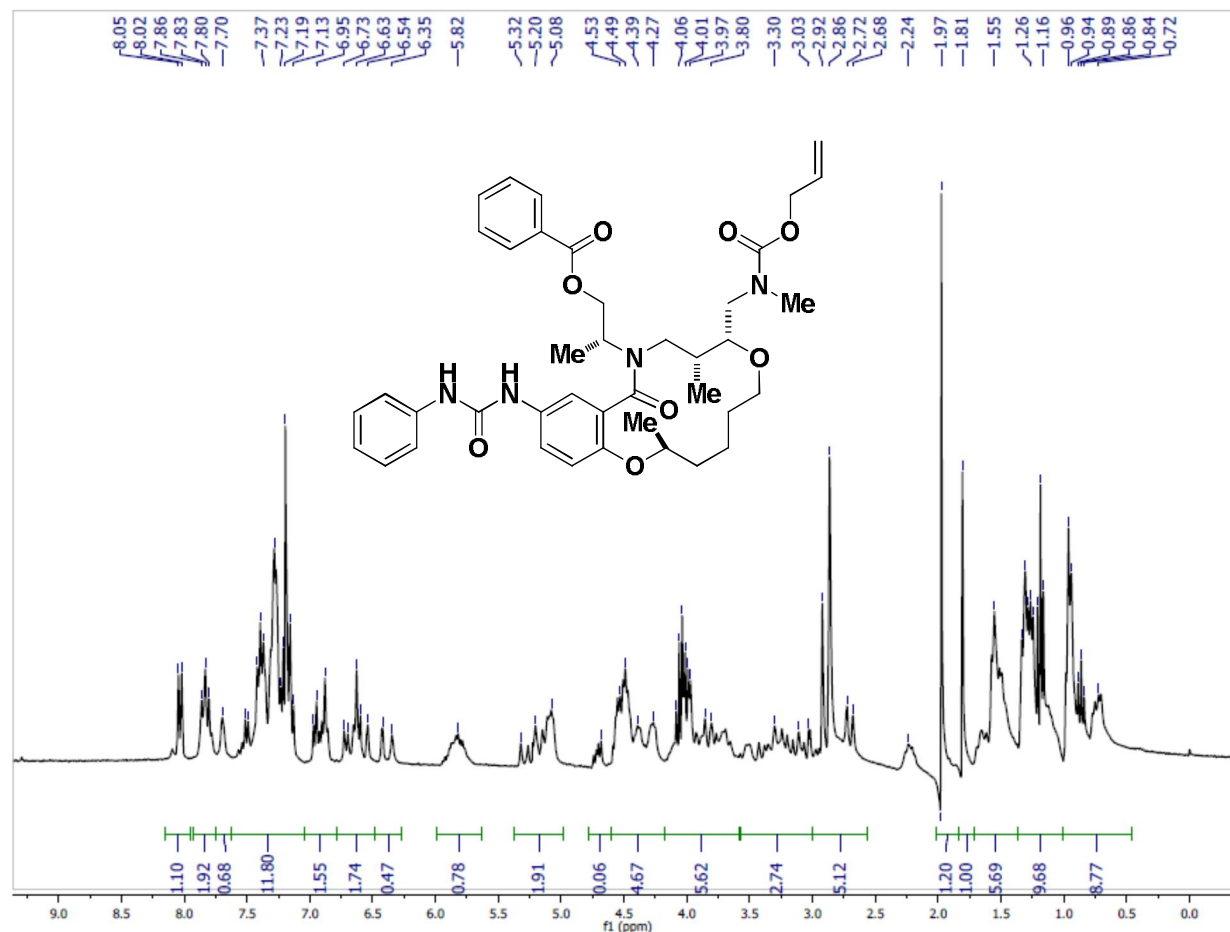
<sup>1</sup>H NMR Spectrum (300 MHz, CDCl<sub>3</sub>) of Analog CID 49849907



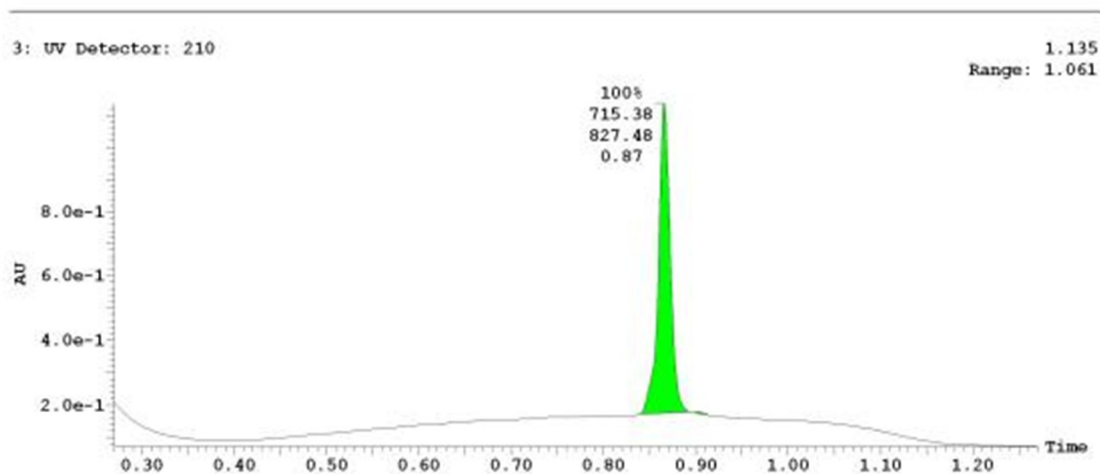
UPLC Chromatogram of Analog CID 49849907



**<sup>1</sup>H NMR Spectrum (300 MHz, CDCl<sub>3</sub>) of Analog CID 49849911**

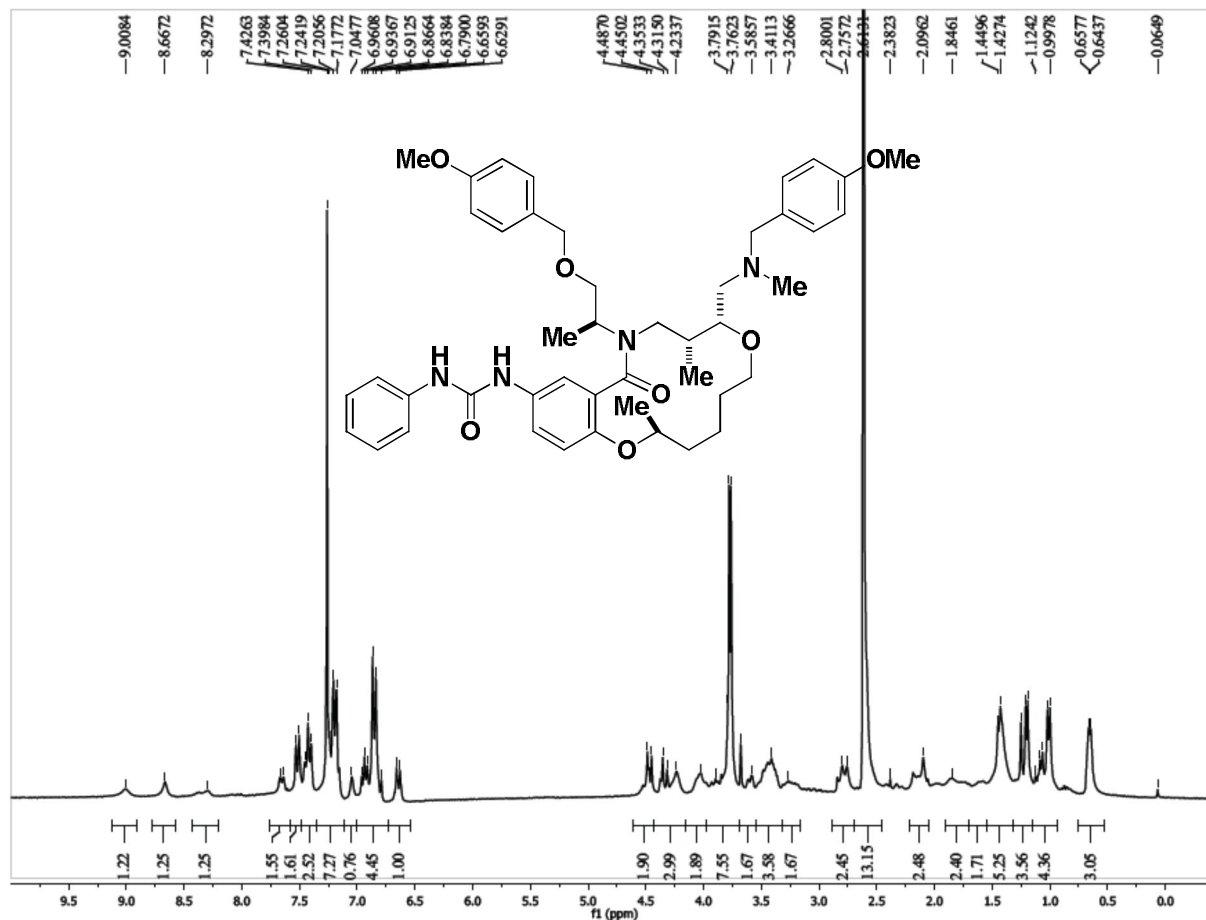


**UPLC Chromatogram of Analog CID 49849911**

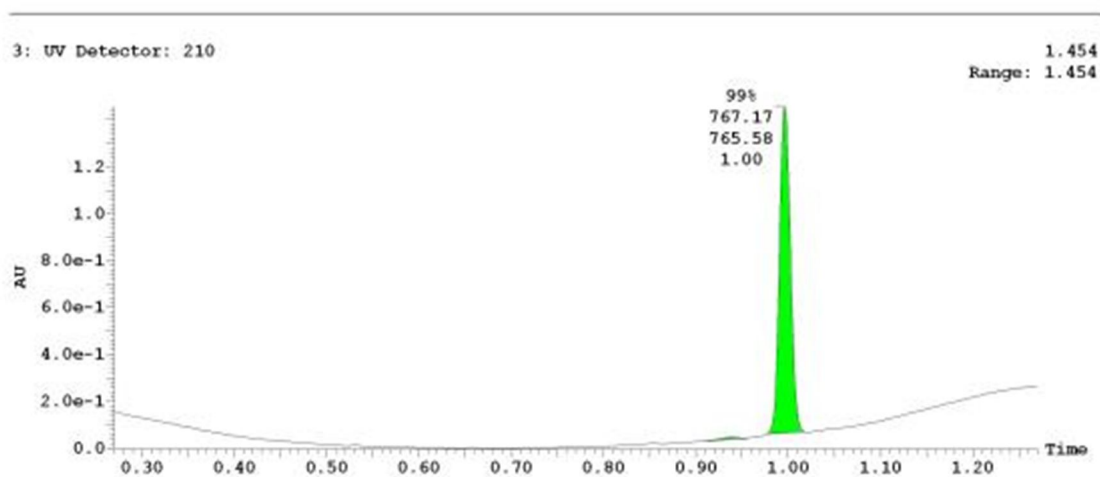




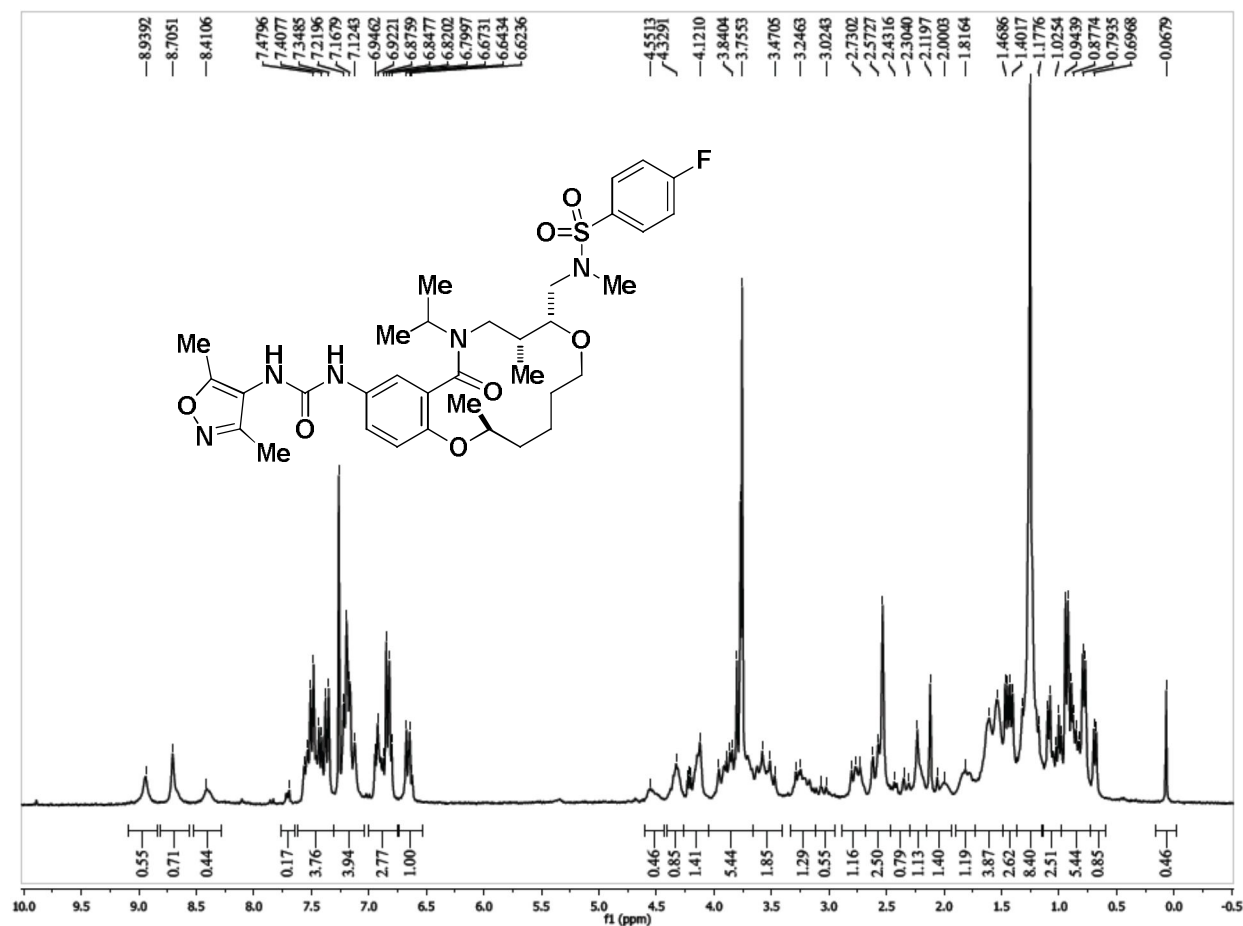
<sup>1</sup>H NMR Spectrum (300 MHz, CDCl<sub>3</sub>) of Analog CID 49849925



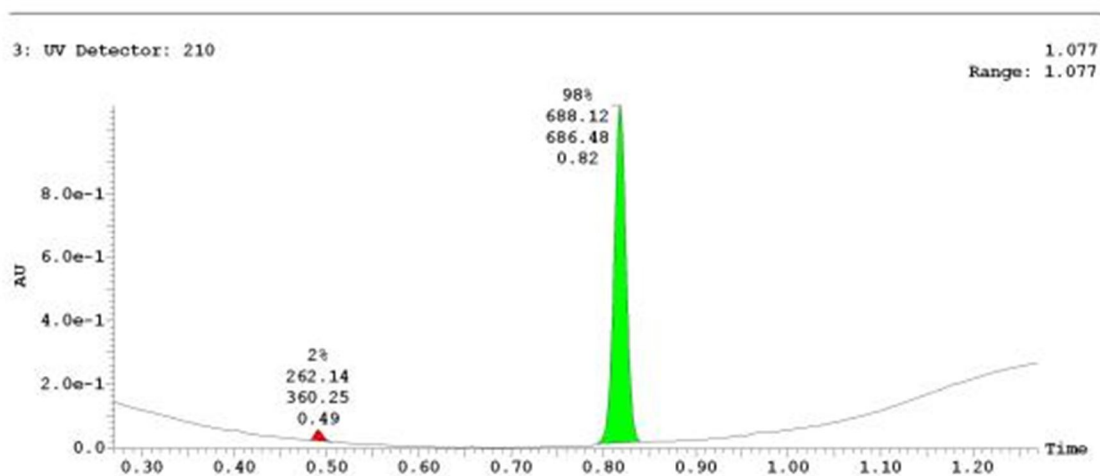
UPLC Chromatogram of Analog CID 49849925



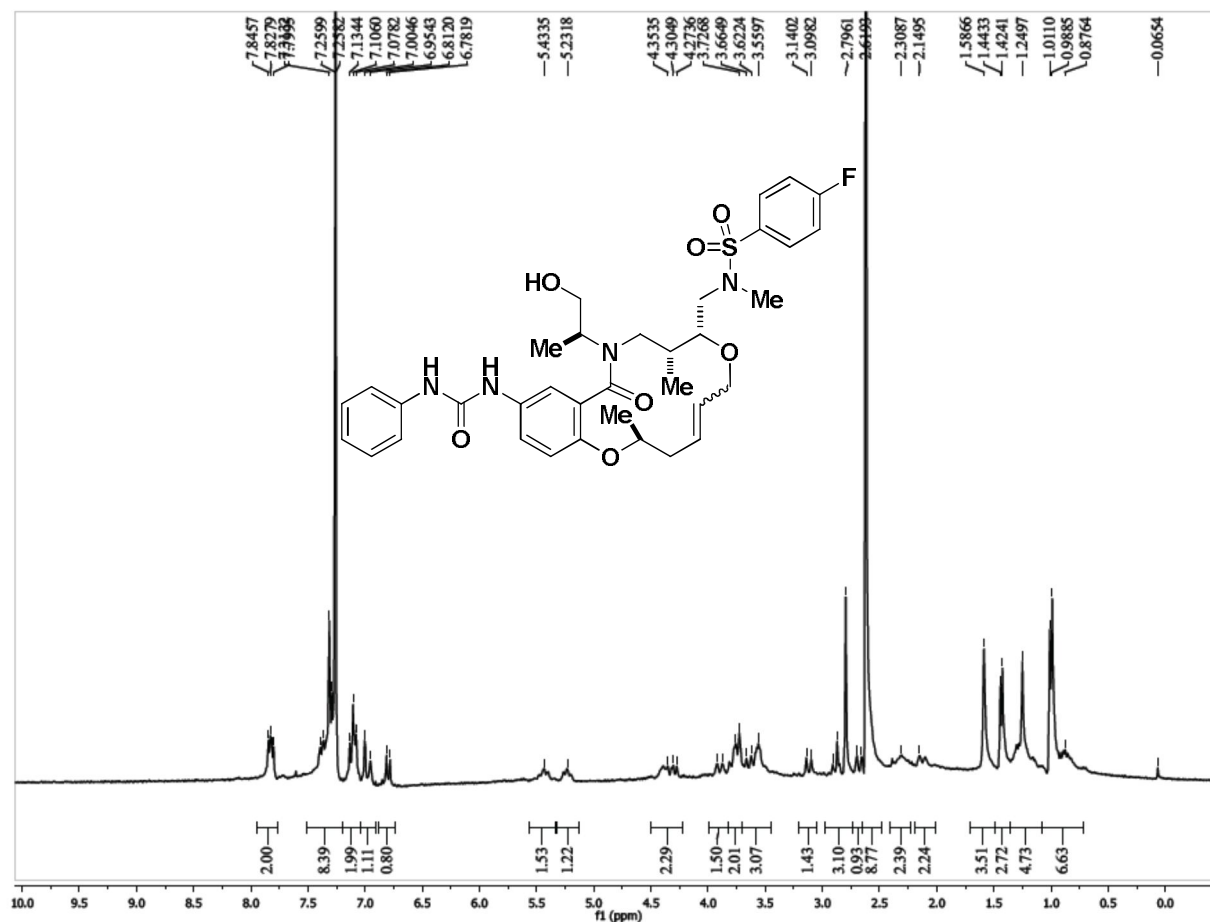
<sup>1</sup>H NMR Spectrum (300 MHz, CDCl<sub>3</sub>) of Analog CID 49849905



UPLC Chromatogram of Analog CID 49849905



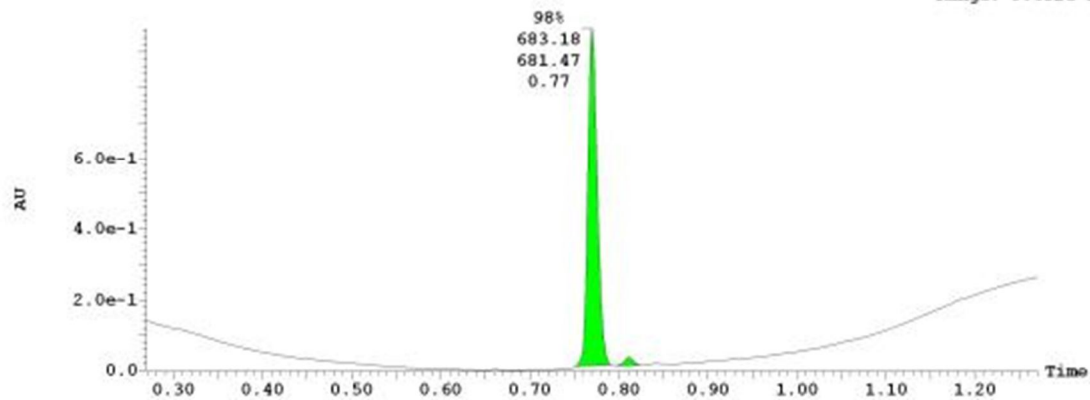
<sup>1</sup>H NMR Spectrum (300 MHz, CDCl<sub>3</sub>) of Analog CID 49849910



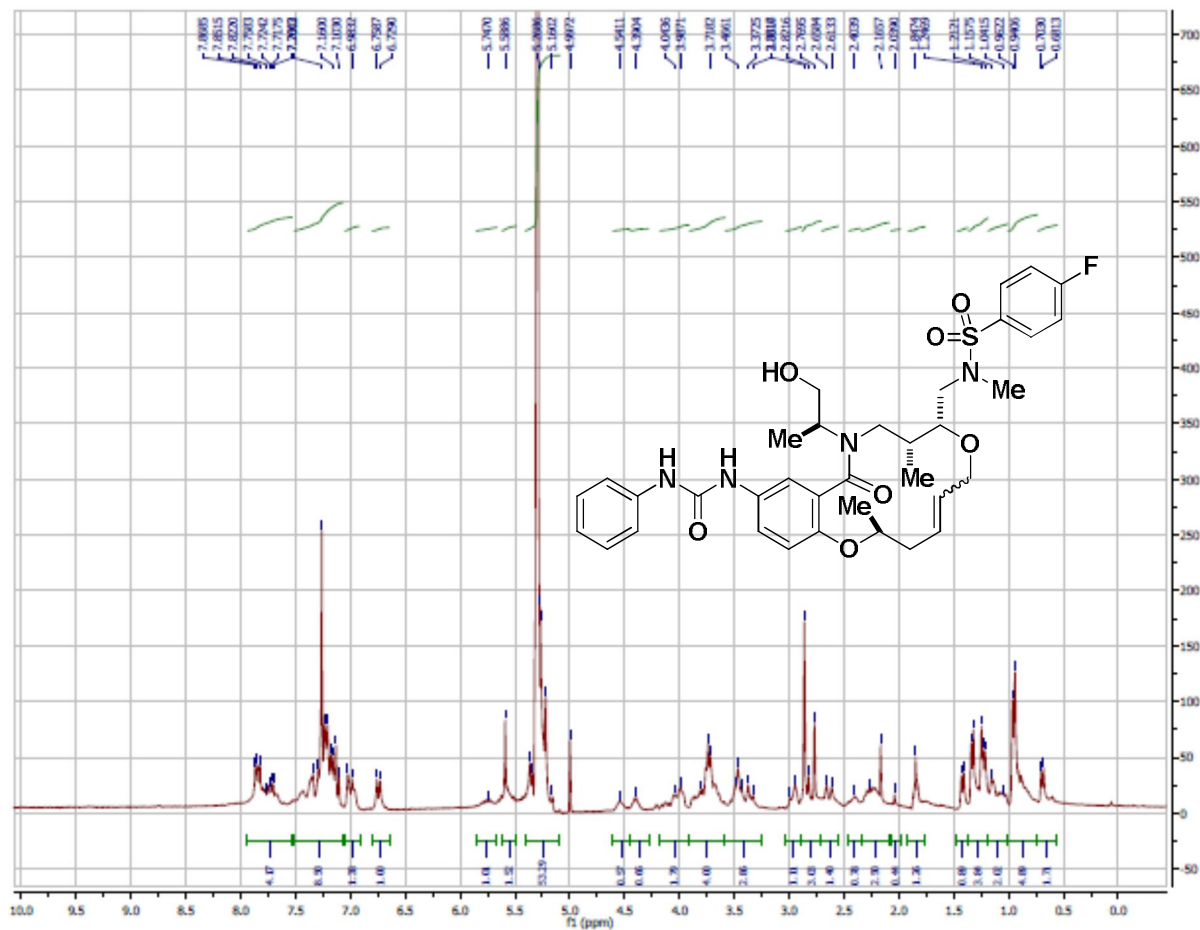
UPLC Chromatogram of Analog CID 49849910

3: UV Detector: 210

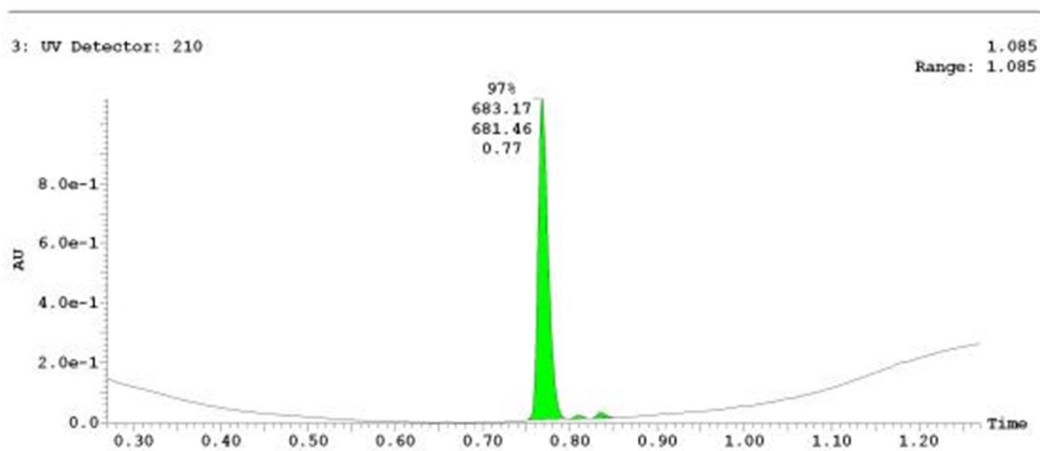
9.652e-1  
Range: 9.652e-1



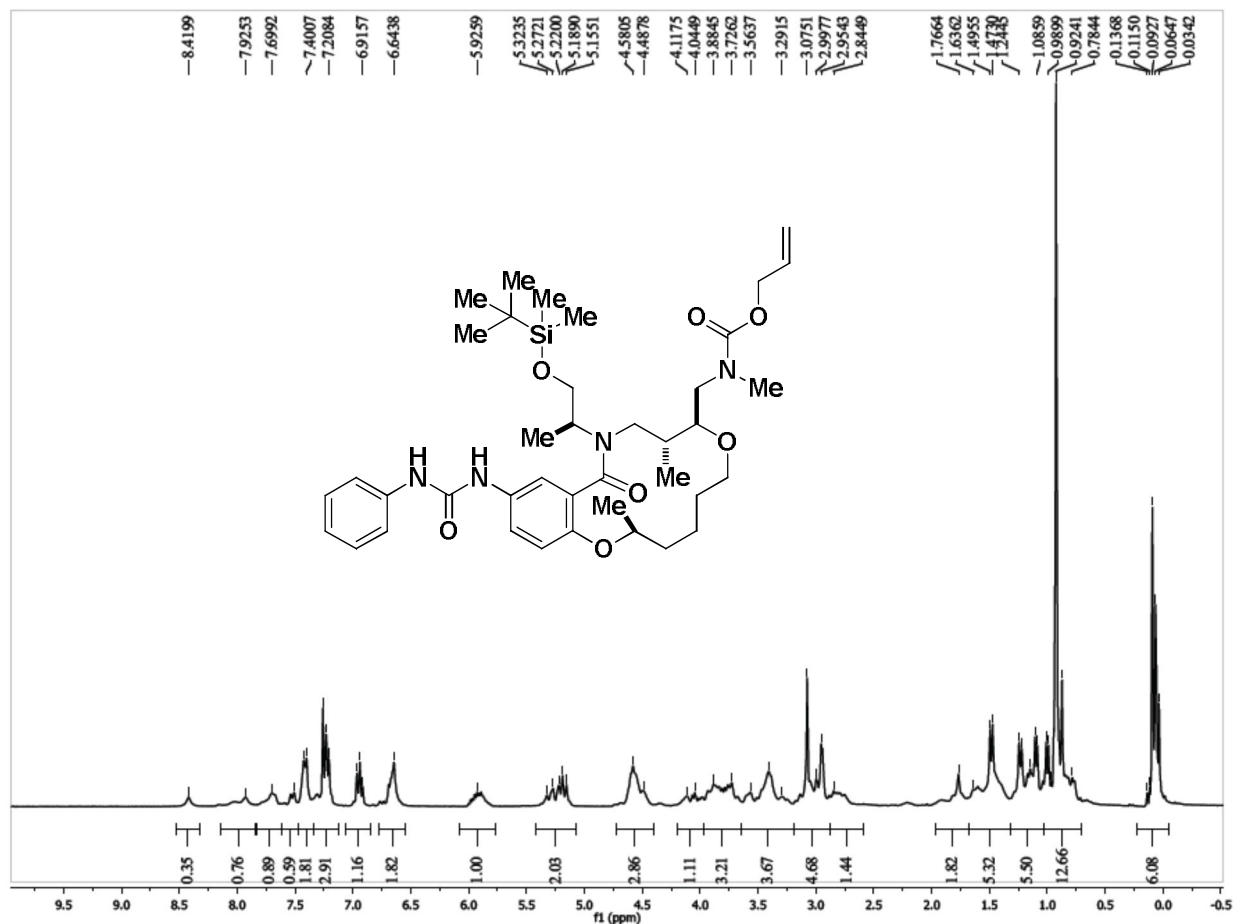
**$^1\text{H}$  NMR Spectrum (300 MHz,  $\text{CDCl}_3$ ) of Analog CID 49849926**



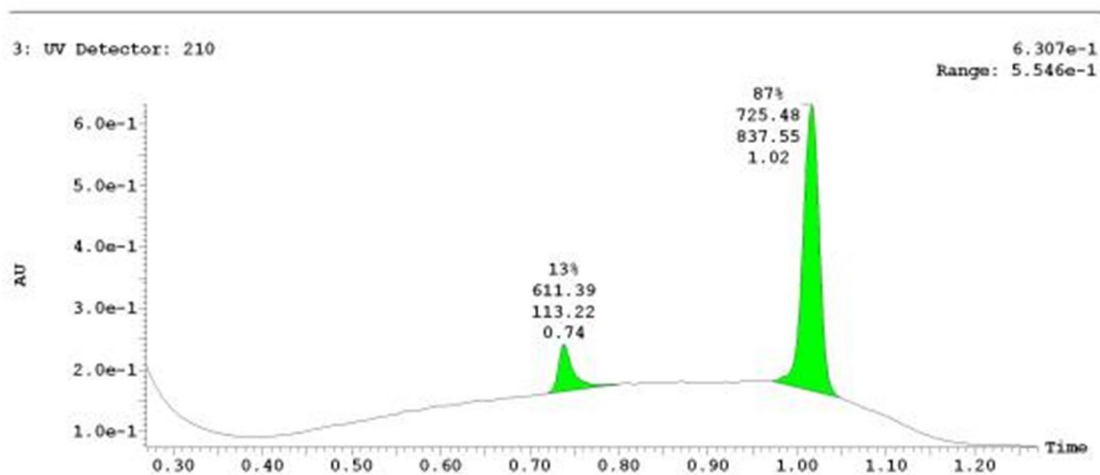
**UPLC Chromatogram of Analog CID 49849926**



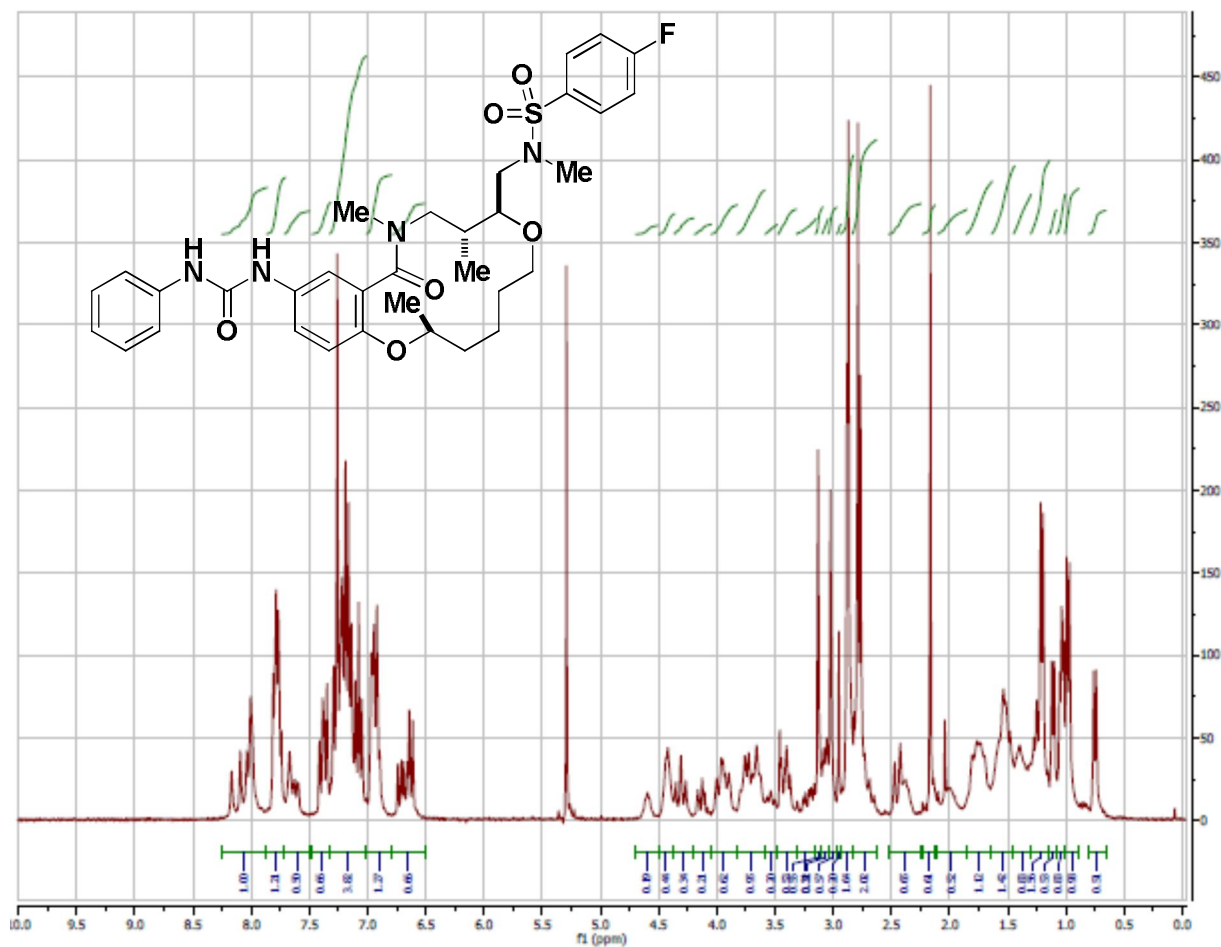
<sup>1</sup>H NMR Spectrum (300 MHz, CDCl<sub>3</sub>) of Analog CID 49849937



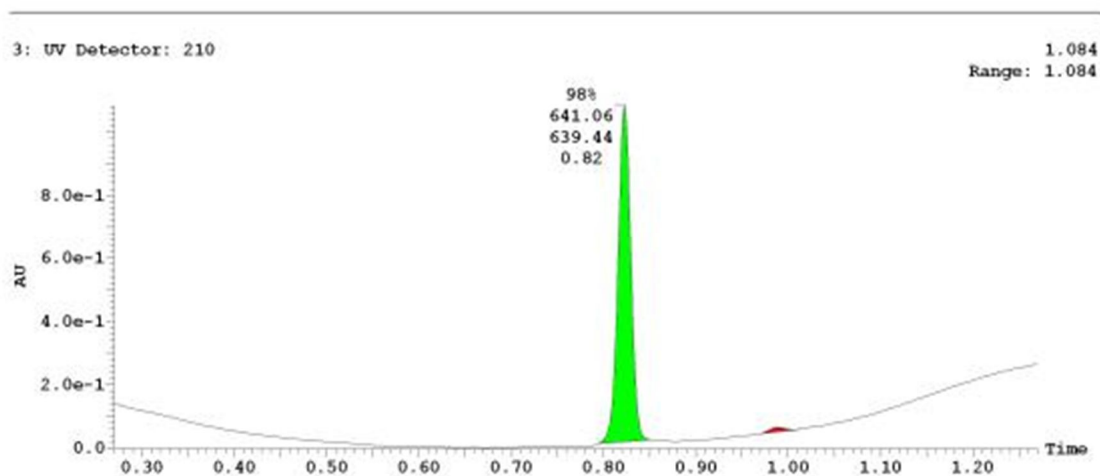
UPLC Chromatogram of Analog CID 49849937



<sup>1</sup>H NMR Spectrum (300 MHz, CDCl<sub>3</sub>) of Analog CID 49849927

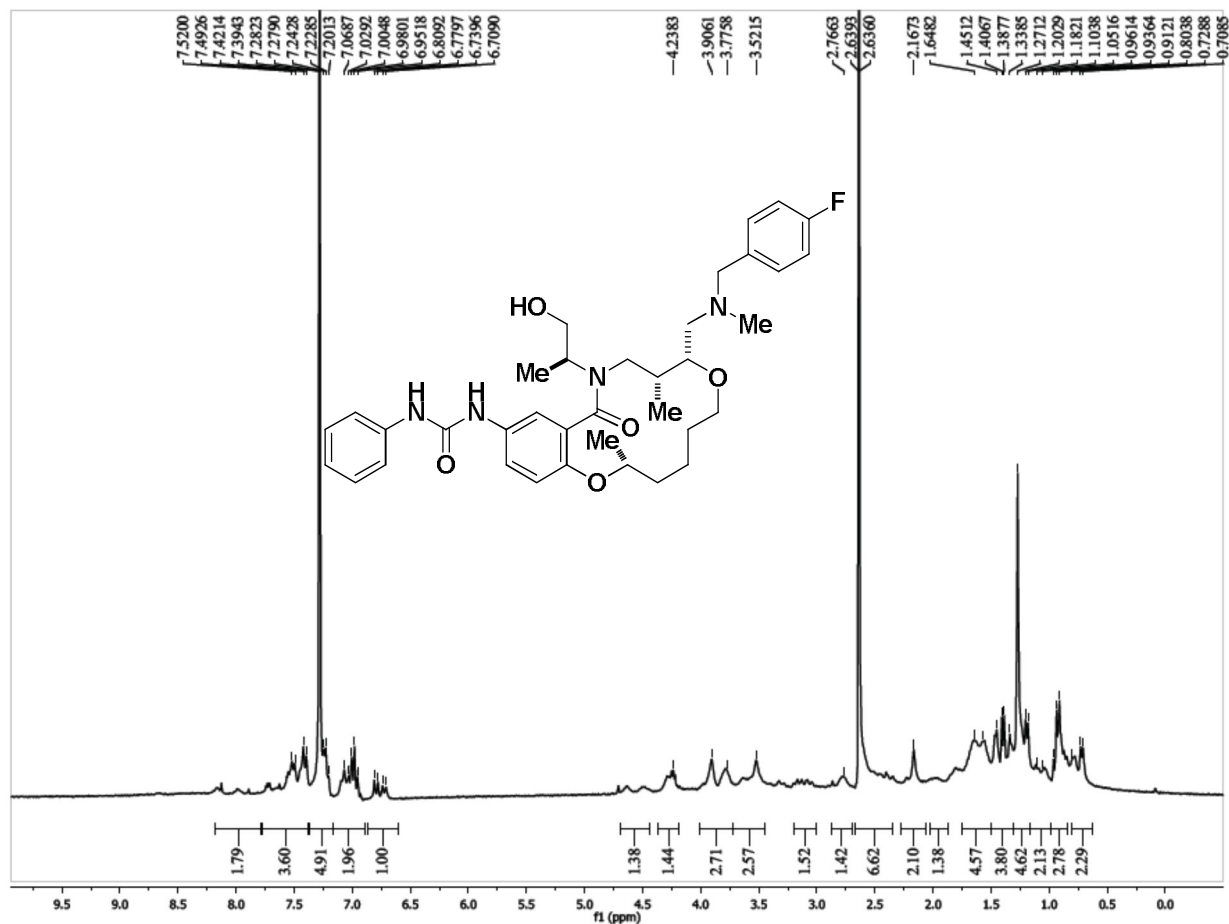


UPLC Chromatogram of Analog CID 49849927

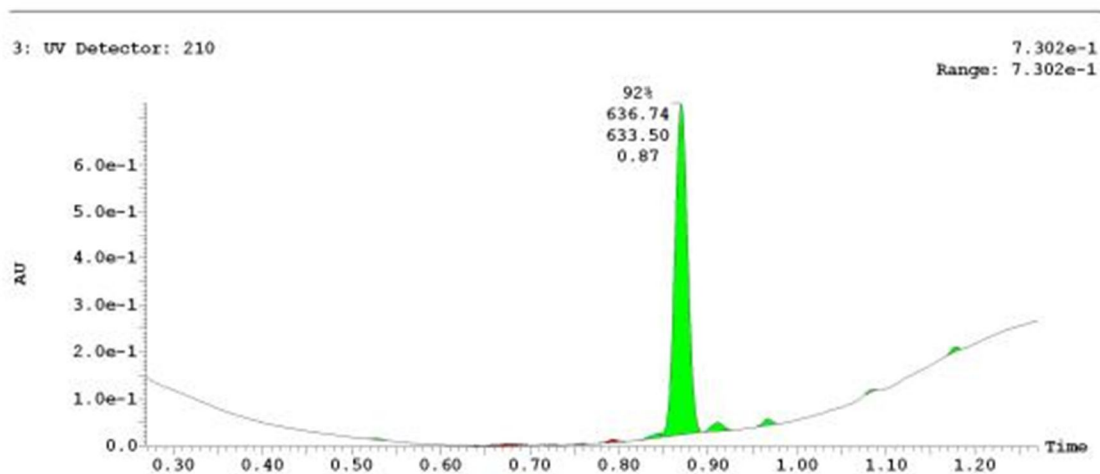




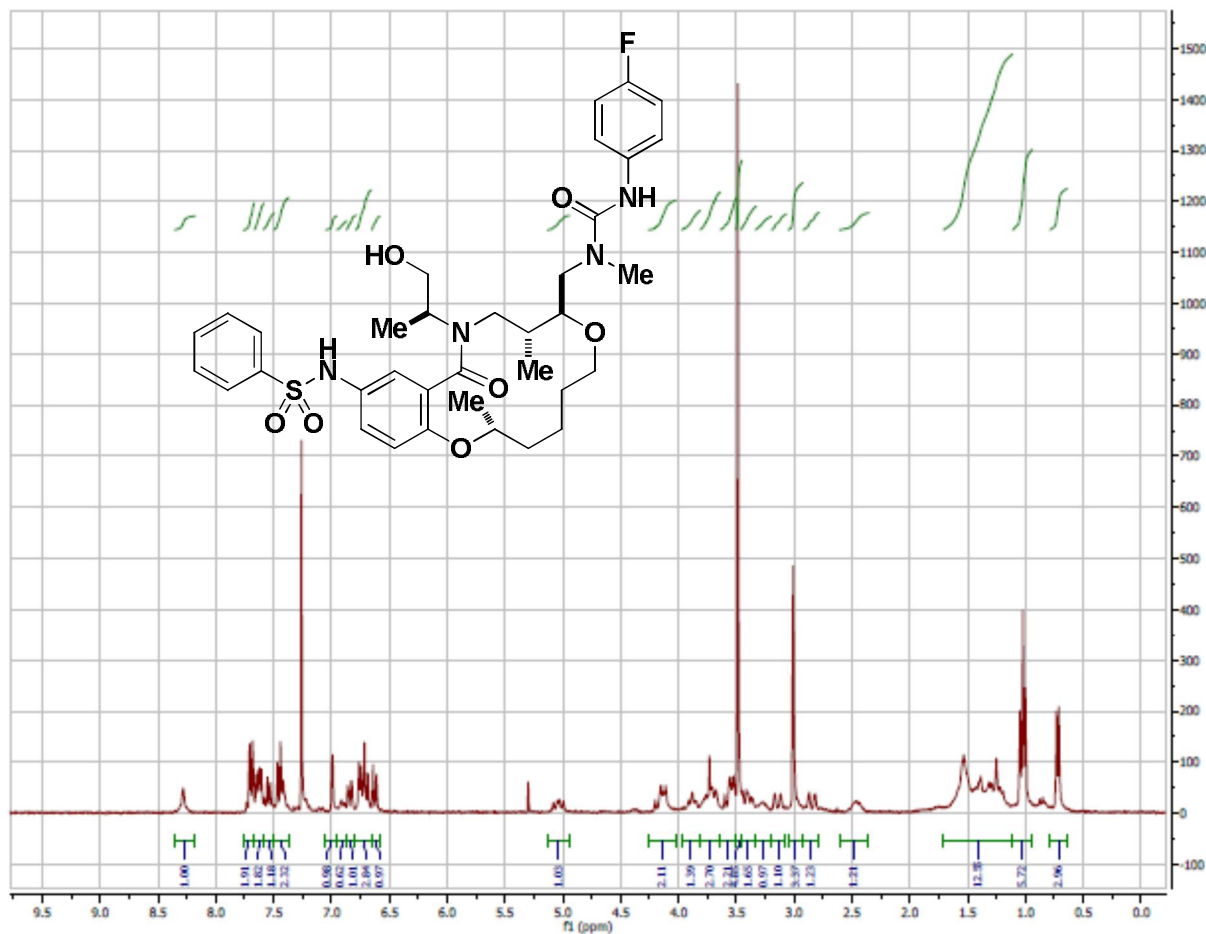
<sup>1</sup>H NMR Spectrum (300 MHz, CDCl<sub>3</sub>) of Analog CID 49849933



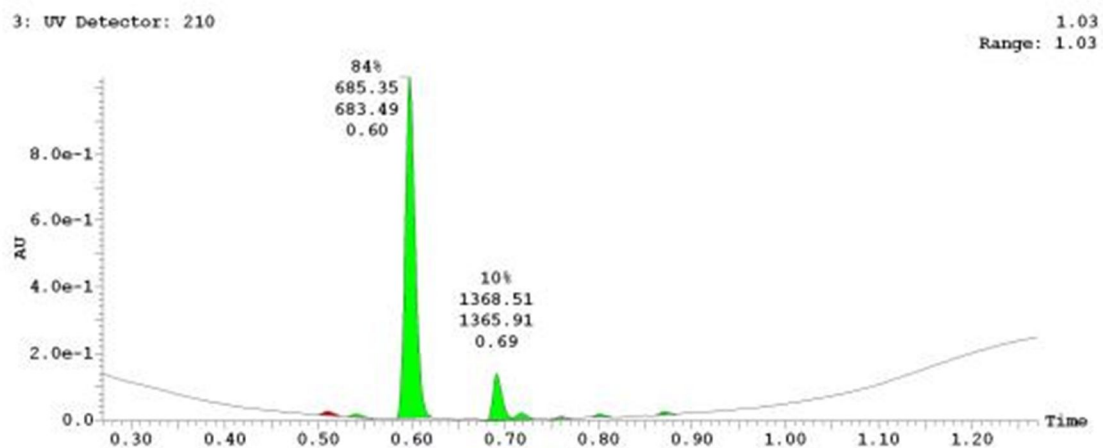
UPLC Chromatogram of Analog CID 49849933



<sup>1</sup>H NMR Spectrum (300 MHz, CDCl<sub>3</sub>) of Analog CID 44488207

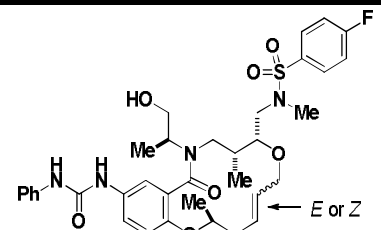
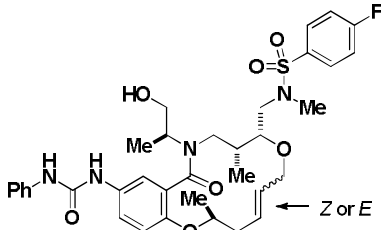


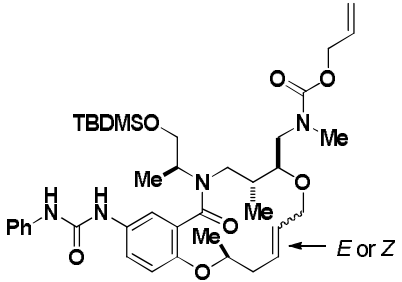
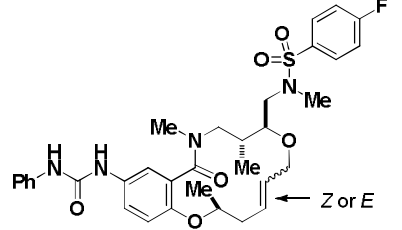
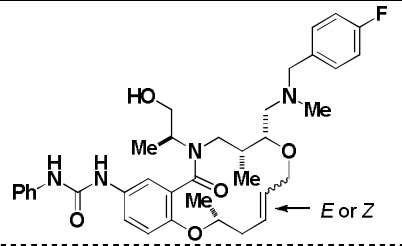
UPLC Chromatogram of Analog CID 44488207

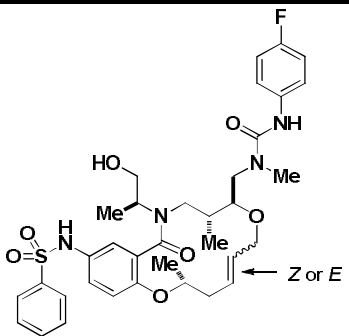


## Appendix E: Activity of Several Other Analogs Synthesized During the Optimization Phase

**Table E1.** Other Analogs Synthesized During the Course of SAR Study

Entry No.	CID	SID	Broad ID	Structure	Potency ( $\mu\text{M}$ ) Mean $\pm$ S.E.M.				Fold Selectivity HepG2/ Dd2
					3D7 48 h (n=1)	3D7 96 h (n=1)	Dd2 72 h (n=1)	HepG2 48 h (n=1)	
1	49849910	104179280	BRD-K15006730		0.15	0.12	0.67	IA	NA
				Solubility (PBS): <0.5 $\mu\text{M}$ , (water): <0.5 $\mu\text{M}$ ; Purity: 98%					
2	49849926	104179281	BRD-K08173135		0.36	0.30	1.32	11.79	8.9
				Solubility (PBS): <0.5 $\mu\text{M}$ , (water): <0.5 $\mu\text{M}$ ; Purity: 97%					

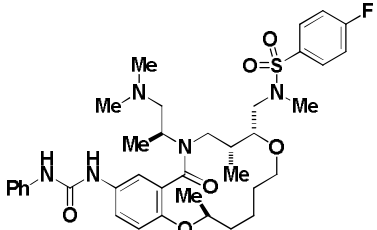
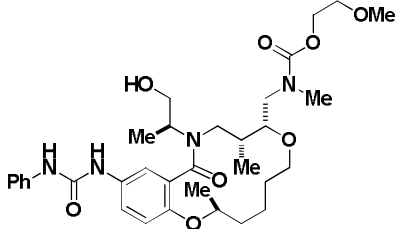
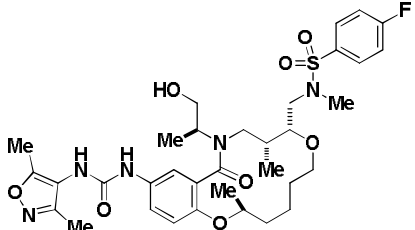
Entry No.	CID	SID	Broad ID	Structure	Potency ( $\mu\text{M}$ ) Mean $\pm$ S.E.M.				Fold Selectivity HepG2/ Dd2
					3D7 48 h (n=1)	3D7 96 h (n=1)	Dd2 72 h (n=1)	HepG2 48 h (n=1)	
3	49849937	104179264	BRD-K72547289		0.28	0.18	0.61	IA	NA
Solubility (PBS): <0.5 $\mu\text{M}$ , (water): <0.5 $\mu\text{M}$ ; Purity: 100%									
4	49849927	104179263	BRD-K95450288		1.37	1.09	3.71	IA	NA
Solubility (PBS): <0.5 $\mu\text{M}$ , (water): <0.5 $\mu\text{M}$ ; Purity: 98%									
5	49849933	104179285	BRD-K12861152		4.33	3.47	6.60	12.01	1.8
Solubility (PBS): <0.5 $\mu\text{M}$ , (water): 129.6 $\mu\text{M}$ ; Purity: 92%									

Entry No.	CID	SID	Broad ID	Structure	Potency ( $\mu\text{M}$ ) Mean $\pm$ S.E.M.				Fold Selectivity
					3D7 48 h (n=1)	3D7 96 h (n=1)	Dd2 72 h (n=1)	HepG2 48 h (n=1)	HepG2/ Dd2
6	44488207	104179261	BRD-K32582686		0.42	0.050	0.52	IA	NA
Solubility (PBS): <0.5 $\mu\text{M}$ ; (water): <0.5 $\mu\text{M}$ ; Purity: 94%									

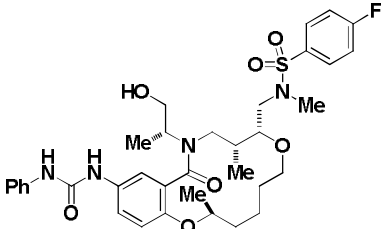
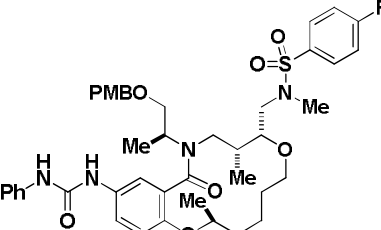
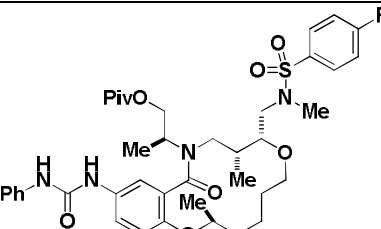
IA = Inactive; (m) = mouse; NA = Not applicable; ND = Not determined; PPB (h) = Plasma protein binding in human; PS (h) = Plasma stability in human

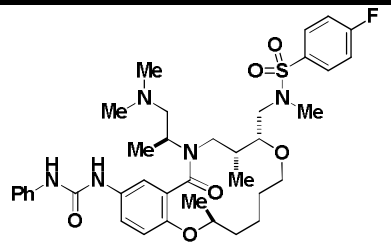
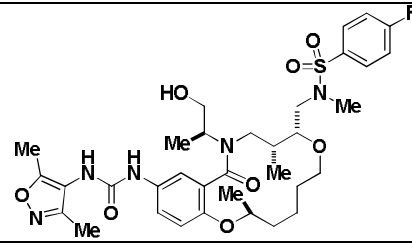
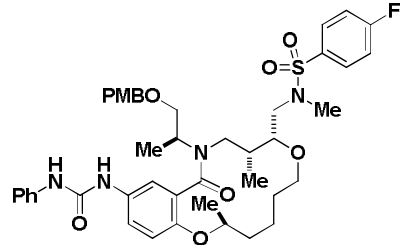
## Appendix F: Summary of Data Obtained by Assay Provider on 3D7 and Dd2 Cell Lines

**Table F1.** Summary of Data Obtained in the Flow Cyclometry Assay Against *P. falciparum*

Entry No.	CID	SID	Broad ID	Structure	Potency ( $\mu\text{M}$ ) Mean $\pm$ S.E.M.			
					3D7		Dd2	
					48 h (n=1)	96 h (n=1)	48 h (n=1)	96 h (n=1)
1	49849912	104179292	BRD-K45399554		0.00164	0.00214	0.00042	0.00057
2	49849932	104179275	BRD-K06180729		>16.7	>16.7	15.7	13.4
3	49843020	104179266	BRD-K05563014		1.15	1.53	0.70	0.70

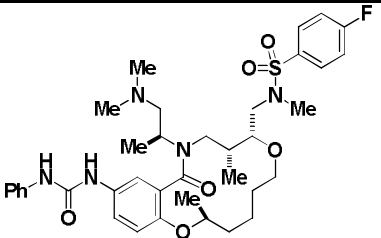
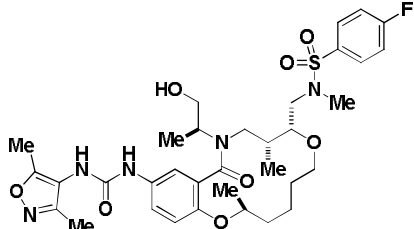


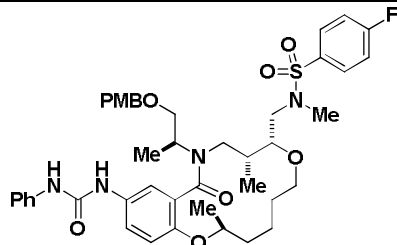
Entry No.	CID	SID	Broad ID	Structure	Potency ( $\mu\text{M}$ ) Mean $\pm$ S.E.M.			
					3D7		Dd2	
					48 h (n=1)	96 h (n=1)	48 h (n=1)	96 h (n=1)
4	44483977	104179269	BRD-K81592585		0.19	0.18	0.092	0.088
5	49849909	104179286	BRD-K95212245		0.0022	0.0027	0.0011	0.0011
6	49849931	104179288	BRD-K91442916		0.0081	0.0088	0.0044	0.0051

EntryNo.	CID	SID	Broad ID	Structure	Potency (μM)			
					Kidney Epithelial Cells	Dermal Fibroblasts	Lung Epithelial Cancer Cells (A549)	Erythrocyte Lysis
1	49849912	104179292	BRD-K45399554		2 4	27 63	2 >63	>40
2	49843020	104179266	BRD-K05563014		>63 >63	>63 >63	>63 >63	>40
3	49849909	104179286	BRD-K95212245		>63 >63	>63 >63	>63 >63	>40

## Appendix G: Summary of Other Cytotoxicity Data

**Table G1. Summary of Cytotoxicity Data in Kidney Epithelial Cells, Dermal Fibroblasts, Lung Epithelial Cancer Cells (A549) and Erythrocytes**

Entry No.	CID	SID	Broad ID	Structure	Potency ( $\mu\text{M}$ )			
					Kidney Epithelial Cells	Dermal Fibroblasts	Lung Epithelial Cancer Cells (A549)	Erythrocyte Lysis
1	49849912	104179292	BRD-K45399554		2 4	27 63	2 >63	>40
2	49843020	104179266	BRD-K05563014		>63 >63	>63 >63	>63 >63	>40

Entry No.	CID	SID	Broad ID	Structure	Potency ( $\mu\text{M}$ )			
					Kidney Epithelial Cells	Dermal Fibroblasts	Lung Epithelial Cancer Cells (A549)	Erythrocyte Lysis
3	49849909	104179286	BRD-K95212245		>63 >63	>63 >63	>63 >63	>40

## Appendix H: Compounds Provided to BioFocus

**Table H1.** Probe and Analogs Information

BRD	SID	CID	P/A	MLSID	ML
BRD-K45399554-001-02-4	113585210	49849912	P	MLS003448149	ML238
BRD-K91442916-001-02-8	113585212	49849931	A	MLS003448150	NA
BRD-K05563014-001-03-5	113585208	49843020	A	MLS003448151	NA
BRD-K06180729-001-02-5	113585209	49849932	A	MLS003448152	NA
BRD-K81592585-001-04-8	113585211	44483977	A	MLS003448153	NA
BRD-K95212245-001-02-3	113585213	49849909	A	MLS003448154	NA

A = Analog; NA = Not applicable; P = Probe